DOKUZ EYLÜL UNIVERSITY

GRADUATE SCHOOL OF NATURAL AND APPLIED SCIENCES

CORROSION FATIGUE CHARACTERISTICS OF TOTAL HIP PROSTHESIS IN SIMULATED BODY FLUID

by

Muhammer ERTEM

February, 2006

İZMİR

CORROSION FATIGUE CHARACTERISTICS
OF TOTAL HIP PROSTHESIS IN
SIMULATED BODY FLUID

A Thesis Submitted to the
Graduate School of Natural and Applied Sciences of
Dokuz Eylül University
In Partial Fulfillment of the Requirements for
the Degree of Master of Science in Metallurgical and Materials Engineering,
Material Sciences Program

by
Muhammer ERTEM

February, 2006
İZMİR

M.Sc THESIS EXAMINATION RESULT FORM

We have read the thesis entitled **"CORROSION FATIGUE CHARACTERISTICS OF TOTAL HIP PROSTHESIS IN SIMULATED BODY FLUID"** completed by Muhammer ERTEM under supervision of Prof. Dr. Ahmet ÇAKIR and we certify that in our opinion it is fully adequate, in scope and in quality, as a thesis for the degree of Master of Science.

Prof. Dr. Ahmet ÇAKIR
_____

Supervisor

Prof. Dr. Ramazan KARAKUZU   Yard. Doc. Dr. Bülent ÖNAY
_____   _____

(Jury Member)   (Jury Member)

_____

Prof.Dr. Cahit HELVACI
Director
Graduate School of Natural and Applied Sciences

ACKNOWLEDGMENTS

CORROSION FATIGUE CHARACTERISTICS OF TOTAL HIP PROSTHESIS IN SIMULATED BODY FLUID

ABSTRACT

Objective of this study is to perform fatigue testing of the total joint replacements made of 316L stainless steel to validate the safety of the component before the clinical use. Thompson hip prosthesis was tested by using double cantilever beams bending machine designed and manufactured at Department of Metallurgical and Materials Science Engineering. The physiological environment, namely the body fluid, can be very corrosive for implant materials. In order to ensure the safety of a hip prosthesis against corrosion fatigue failure, fatigue tests must be performed in a corrosive medium with low frequency load application. Component fatigue tests were therefore performed in Ringer's solution (0.9% NaCl) at a frequency of 10 Hz in accordance with ISO 7206/4 standard. At this rate, a single hip stem fatigue test requires 11.5 days of continuous testing without any failure for a numbers of 10^7 cycles.

The objective of this study was also to perform the fatigue test of the Thompson hip prosthesis in accordance with ISO 7206/4, evaluate the real stresses by using the strain gauge, and to determine the fatigue life of prosthesis. The purpose of this study was also to compare the real stresses measured at different location of prosthesis by means of strain gauges with the distributions of theoretical stresses calculated by CAD modelling.

Keywords :
Corrosion fatigue, Stainless steel 316L, Implant material.

TOTAL KALÇA PROTEZİNİN VÜCUT BENZERİ SIVIDA KOROZYONLU YORULMA ÖZELLİKLERİ

ÖZ

Bu çalışmanın amacı, klinik kullanımdan önceki yorulma hasarına karşı güvenilirliğini geçerli kılmak üzere, 316L paslanmaz çelikten imal edilmiş kalça protezlerinin yorulma deneylerinin yapılmasıdır. Metalurji ve Malzeme Mühendisliği bölümünde dizayn edilip imal edilen çift ankastre eğmeli yorulma makinası kullanılarak, Thompson kalça protezi test edilmiştir. Fiziksel çevre yani vücut sıvısı implant için korozif olabilmektedir. Korozyon yorulmasına karşı kalça protezinin güvenilirliği açısından, yorulma deneyleri bir korozyon ortamı içerisinde, düşük frekanslı yükleme uygulaması ile gerçekleştirilmelidir. Protezin yorulma deneyleri bu yüzden, % 0,9 NaCl Ringer solüsyonunda, 10 Hz yükleme frekansında, ISO 7206/4 standardına uygun olarak yapılmıştır. Bu frekansta, tek bir protezin yorulma testi için 10^7 çevrim sayısında herhangi bir hasar oluşmadan 11,5 gün gerekmektedir.

Strain gaugeler ile ölçülen gerçek gerilmelere bağlı olarak protezlerin yorulma ömürlerini tespit edilmiştir. Yükleme seviyesine bağlı olarak kalça protezinde ölçülen gerçek gerilme değerleri ile CAD'de yapılan teorik gerilme dağılımları karşılaştırılmıştır.

Anahtar sözcükler :
Yorulma korozyonu, Paslanmaz çelik 316L, İmplant malzemeler.

CONTENTS

CHAPTER ONE
INTRODUCTION

The human hip joint is subjected to high mechanical stress and undergoes considerable abuse. As a result of some osteological diseases such as osteitis, osteolysis, osteopenia and breakage of hip joint in consequence of a severe accident that forms unpredictable loads, total hip replacement (THR) may be required. THR has proven to be a successful procedure for the relief of pain and restoration of normal daily activities in elderly patients with hips disabled by disease or injury. Consequently, the general use of the total hip prosthesis has been extended to younger and more active patients (Gruen , 1979). This is the process of completely removing the existing hip and replacing it with an artificial one. Today, THR is performed more than 250,000 times a year in the United States, a sixty-four percent increase since 1982. The main goal of total hip replacement is to improve the quality of life of the patient by reducing the amount of pain in the hip and restoring its function. The major causes of failure in total hip arthroplasty are infection, dislocation of the joint, loosening of the stem and failure of the stem (Edmonson & Crensham, 1989). In every failure of an orthopaedic implant the patient is made to experience the trauma of repeated surgery besides severe pain experienced during the process of rejection of the device. The removal of the implant may cause great expense and hardship to patient. Therefore, it is highly desirable to keep the number of failures to a minimum. Hence, the determination of the mechanism that caused failure of an implant is important, but it is also necessary to explore the event or sequence of events, which caused that particular mechanism to become operative. Furthermore, failure investigation will help to improve the total performance of implant devices, besides revealing the details of the mode and origin of the failure mechanism.

The mechanism of failure appears to be caused by the resorption of the bone for uncertain reasons around the section where the head and neck are detached from the femur resulting in the reduction of strength. For whatever reason the resorption occurs, the result is that the implant is effectively not supported at its proximal end and the condition may arise where the implant is firmly fixed in a plug of cement at its distal end and loaded by the joint force. This gives a stress system, such as cantilever under bending, leading to fatigue failure at a section situated at between 1/3 and 2/3 of the stem length from its tip. The majority of these fatigue failures involve a fracture surface that is not perpendicular to the axis of the stem. This corresponds in fact to a combination of longitudinal bending and torsinal loading and for this reason the test procedure proposed currently by ISO 7206/4 standard involves the proximal femoral component being held in fixing medium, in such a way that load applied to the head of the femur causes such a combination stresses varying down the length of the stem (Azem, 1999).

In spite of the recent innovative metallurgical and technological advances and remarkable progress in the design of implants, failures of implants do occur. Although failures of implants have been reported to be due to fatigue, corrosion and/or other general mechanisms, the underlying causes for the initiation of these failure mechanisms are seldom determined. The causes of failures may also due to biomechanical reasons rather than to faults in the basic design and/or metallurgy of the implant (Sivakumar , 1995).

The objective of this study was to perform the fatigue test of the Thompson hip prosthesis in accordance with ISO 7206/4, evaluate the real stresses by using the strain gauge, and to determine the fatigue life of prosthesis. The purpose of this study was also to compare the real stresses measured at different location of prosthesis by

means of strain gauges with the distributions of theoretical stresses calculated by CAD modelling.

CHAPTER TWO
GENERAL OVERVİEW OF HIP JOINT

2.1. Biologic Properties of Hip Joint

Hip is composed of the head of the femur and the acetabulum of the pelvis. The hip joint is one of the most stable joints in body. The stability is provided by the rigid ball-and-socket configuration. In contrast to the knee, the hip joint has intrinsic stability, provided by its relatively rigid ball-and-socket configuration. It also has a great deal of mobility, which allows normal locomotion in the performance of daily activities such as sitting, walking, and squatting (Bronzino, 1995).

2.1.1. Acetabulum and Femur

The acetabulum is the concave component of the ball-and-socket configuration of the hip joint. The acetabular surface is covered with articular cartilage that thickens peripherally and predominantly laterally. The cavity of the acetabulum is located obliquely forward, outward, and downward.

The femur is the longest bone of skeleton and articulates with the hip bone above and the tibia below; it carries the patella in front of it. The femoral head is the convex component of the ball-and-socket configuration of the hip joint and forms two thirds of sphere. The articular cartilage covering the femoral head is thickest on the medial-central surface and thinnest toward the periphery. The variations in the cartilage thickness result in a different strength and stiffness in various regions of the femoral head. These differences in the mechanical properties from point to point on the femoral head cartilage may influence the transmission of stresses from the acetabulum through the femoral head to the femoral neck. Although it is known just

how stresses on the femoral head are distributed, the joint reaction force usually acts on the superior quadrant.
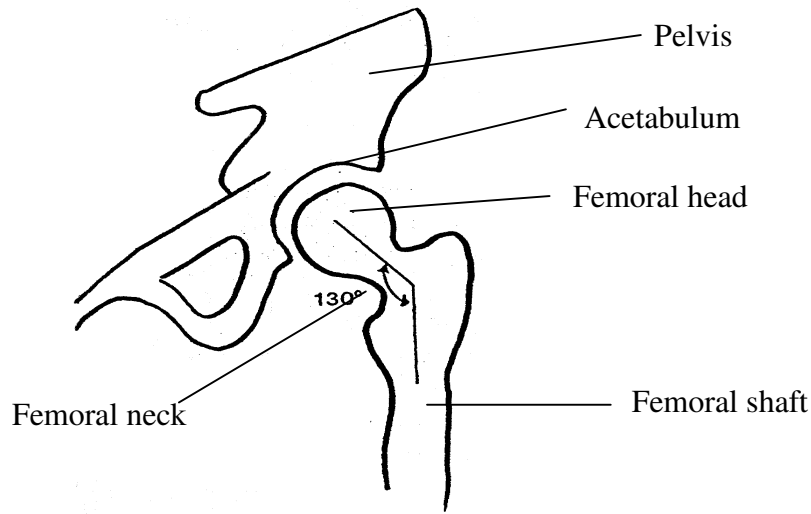
Figure 2.1. Acetabulum and upper femoral shaft (Bronzino, 1995).

2.1.2. Forces Acting on Hip

For the purpose of determining the forces acting on the hip joint, the body weight (BW) may be depicted as a load applied to a lever arm extended from the center of gravity of the body to the center of the femoral head.

The external and internal bony architecture of the proximal femur is exquisitely designed to withstand the enormous forces that act across the hip joint. These forces are generated by contraction of powerful muscles that move and stabilize the hip, by superincumbent body weight, and by inertial effects. The abductor musculature, acting on a lever arm extending from the lateral aspect of the greater trochanter to the center of the femoral head, must exert an equal moment to hold the pelvis level while one stands on one leg and a greater moment to tilt the pelvis to the same side while walking or running. Since the ratio of length of the lever

arm of the body weight to that of the abductor musculature is about 2.5:1, the force of the abductor muscles must approximate 2.5 times the body weight to maintain the pelvis level while standing on one leg. These forces can be resolved into a resultant compression load acting across the hip joint, which has been estimated to range from about the same as body weight during performance of a straight leg raise in a recumbent position, to three or four times body weight during normal level walking, to more than six times body weight during running. But the load during the jumping may be equivalent to 10 times the body weight. More importantly, these loads are repetitive and fluctuating depending on the activities such as standing, sitting, jogging, stretching, and climbing. The femoral neck is loaded in bending in cantilever mode, which creates large tensile forces in the superior portion of the neck and compression forces in the inferior neck. Internal linear thickenings of the trabecular bony architecture serve to resist these stresses. Tensile forces produced by contraction of the hip abductor muscles tend to reduce this bending load. Therefore excess body weight and increased physical activity add significantly to the forces that act to loosen, bend or break the stem of the femoral component which is used in place of hip joint that does not work properly any longer.

The forces on the joint act not only in the coronal plane, but because the center of gravity of the body (in the midline anterior to the second sacral body) is posterior to the axis of the joint, they also act to rotate and bend the hip posteriorly; these latter forces increase when the joint is flexed, as in getting up from a chair, ascending and descending stairs or incline, or lifting. It is this cycling loading with such forces acting in different planes and occurring more than a million times a year that tends to bend, rotate and loosen the stem of the femoral component and, to a lesser extends, loosen the acetabular cup. The durability of total hip components may well exceed that expected of some industrial machine parts.

The load which may occur during daily activities within 1 year according to body weight for active patients is given in Table 2.1. The annual occurrence is roughly separated into specific activities. The last column reports the maximum hip joint load corresponding to each activity.

2.2. History of THR

Total hip replacement (THR) is the process of completely removing the existing joint and replacing it with an artificial hip. When the hip joint is out of use because of disease or breakage, prosthesis is implanted in place of injured joint part to carry out function of hip joint.

Total joint replacements have improved the quality of life for thousands of people over the last quarter century. Clinical objective of joint replacement is pain relief and increased joint motion, the engineering objective is to provide a stress as physiological as possible to the remaining bone so that the integrity and functionality of the bone and prosthetic materials are maintained over a lengthy service-life.

Two English surgeons made outstanding contributions to the development of total hip replacements in the 1950s and 1960s. In 1951, G.K.McKee introduced metal-on-metal prostheses in which both the femoral and acetabular components were made of stainless steel. The acetabular cup was initially fixed into the pelvis by means of screws, but because these came loose within a year, no doubt due to the excessive friction associated with a stainless steel ball seated within a close-fitting acetabular cup, the material of construction was changed to Vitallium, a cobalt-chromium-molybdenum alloy. McKee then adopted a modified form of Thompson femoral component developed in the United States and a cloverleaf form of acetabular cup

Table 2.1. Load history assumed for implanted hip prosthesis (Baleani , 1999).

Activity	Cycles year^{-1}	Specific activity/speed	Supposed occurrence (%)	Max load (% BW)
Walking	2.5×10^{6}	Level walking / 1 km h^{-1}	20	282
		Level walking / 3 km h^{-1}	60	324
		Level walking / 5 km h^{-1}	20	429
Jogging	6.4×10^{5}	Level jogging / 5 km h^{-1}	50	484
		Level jogging / 7 km h^{-1}	30	496
		Jogging upstairs	10	515
		Jogging downstairs	10	384
Ascending Stairs	4.2×10^{4}	Walking upstairs / slow	20	333
		Walking upstairs / normal	70	356
		Walking upstairs / fast	10	386
Descending stairs	3.5×10^{4}	Walking upstairs / slow	20	374
		Walking upstairs / normal	70	387
		Walking upstairs / fast	10	432
Sitting/rising	7.2×10^{4}	Rising from a chair	100	123
Jolting	1.8×10^{3}	Stumbling	100	720

that was again fixed by a screw. A success rate about 50% was reported in the period of 1956 to 1960. In 1960, when McKee and his colleague Watson-Farrar introduced methyl methacrylate as a cement to hold the components in place, the success rate rose to an encouraging 90%. It was further recognized that the use of identical metals in the tribological pair, though necessary to avoid galvanic corrosion, was not an optimized tribology design. A high rate of loosening was encountered with early metal-on-metal artificial joints due to non-optimum fit between the articulating surfaces which produced high frictional moments and excessive wear of bearing surfaces. These early concerns limited to the application of metal-on-metal articulating devices, although follow-up examinations of metal-on-metal hip prostheses have shown very low wear rates for prostheses implanted for up to 20 years.

In the 1960s Sir John Charnley recognized that it was necessary to combat loosening of the components by reducing the frictional torque generated by the articulating surfaces. The outcome was his concept of a "low-friction arthroplasty" based upon a small-diameter metallic femoral head engaged in a polymeric acetabular cup. The philosophy prompted Charnley to introduce polytetrafluroethylene (PTFE, or Teflon) acetabular cups and stainless steel femoral stems in 1959. Attempts were made to improve the wear resistance of the polymer by introducing fillers into the PTFE, but the improvements noted in laboratory test were not reproduced in the body. In 1961, Charnley turned to ultrahigh molecular weight polyethylene (UHMWPE) as the cup material. This material exhibits a higher coefficient of friction than PTFE, but vastly enhanced resistance to wear. Its introduction was astonishingly successful, and today, some 30 years later, it is still the dominant polymeric material in total replacement joints (Dowson, 1992).

2.3. Parts of Hip Prosthesis

Artificial hips are composed of three main components. These components include the femoral head, the acetabular insert or component and a femoral stem. During the surgery, the insert replaces the deteriorated acetabulum or socket.   The femoral stem and femoral head replace the original femoral neck and head, respectively which are excised early in the procedure. Once these components are fixated or secured into place, the surgery is completed and the patient has a new hip.

2.3.1. Femoral Head

Femoral head is an articulating joint which transfers load from the femur to pelvis. Any articulating joint will involve the friction and wear of the two opposing members. Apart from the surface finish of the articulating portion of the prosthetic femoral head, the most mechanical feature is the head diameter. Charnley described the effect of head size and proposed a small head because it would create a lower frictional torque than a larger head and thus reduced the potential loosening. However, smaller heads imply greater contact stresses on the polyethylene cup. The size of the head and the geometry of the neck determine the range of the motion of the reconstruction. For a given neck geometry, a larger head size will permit a greater range of motion of the artificial joint. As wear progress, the head penetrates the acetabular cup, decreasing the range of the motion. For these reasons, head diameter is a crucial design variable for which a compromise is required (Cowin, 2001). For this reason the choice of femoral head size seems to have settled on 26 or 28 millimetres. The 32 millimetres head produces too much wear or creep. Less acetabular strain and lower revision rates are associated with used of a 26 or 28 millimetres head. Note also that the head may be removable from the tapered neck

(Modular prostheses) (Friedman, 1993).
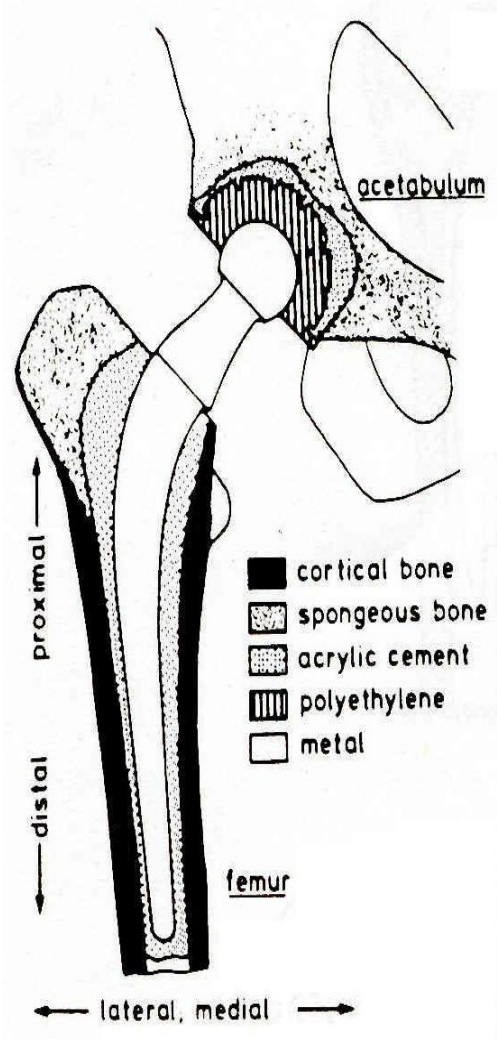
Figure 2.2. A schematic diagram of a hip replacement showing the metal prostheses inserted into the femur, and the cement layer surrounding the prostheses. The medial and lateral, and the distal and proximal sides are indicated.

2.3.2. Acetabular Cup

Acetabular cup is a counterpart articulating against femoral stem head. Orientation is critical for stability. In total hip arthroplasties the acetabular cups are made of UHMWPE, a viscoelastic material of limited flexibility under loading conditions. It also has the characteristic of creep or deformation under constant loads; this creep is minimized by

containing the cup within rigid boundaries, such as the bone of the acetabulum (Edmonson & Crensham, 1989).

2.3.3. Femoral Stem

Femoral stem transfers loads from head of the prostheses to femur by means of a medium such as polymethylmethacrylate (PMMA) or directly, that means cemented or uncemented fixation, respectively. The material properties, shape, and methods used for fixation of the implant to the patient determine the load transfer characteristics. Stresses on the femur can be defined in terms of three unique loads:

Axial Loads: The loads transmitted straight down the canal.

Bending Loads: The "tipping" loads seen in the A-P (Anterior-Posterior) and M-L (Medial-Lateral) planes.

Torsional Loads: The loads twisting around the long axis of the bone.

Prior to reconstruction, all three of these loads are transmitted directly to the host bone. Once a femoral component is introduced into the canal, it now shares the responsibility of taking up these loads while allowing less of the load to be transmitted to the bone. If the three loads are looked at independently, axial and torsional loads can essentially be addressed with tapered or cylindrical stems distally.

An implant design that transmits axial load distally seems to be the most damaging. It has been reported that a cylindrical, distal-fit prosthesis has shown as much as 64 to 78% bone demineralization and stress shielding at five year follow-up.

Torsional load transfer is also vitally important to prevent loosening. Designs, which depend heavily on distal fit within the femur to achieve torsional stability, run the risk of stress shielding and bone resorption. Such a trade-off may create future clinical problems. A well designed prosthesis will transmit the majority of these loads.
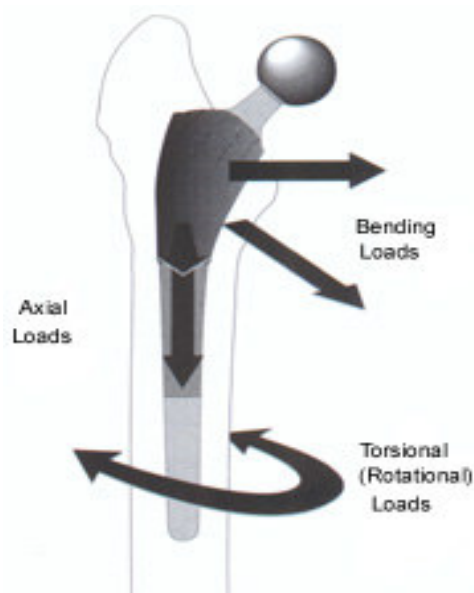
Figure 2.3. Stresses on the femur.

Some prostheses have collar placed between neck and stem, which was observed to assure a permanent contact with the calcar bone in the analysis of the hip stem. This is a paramount importance to achieve physiological loading of the proximal femur. The neck part assures a proper load transfer to the proximal femur, whilst the stem has to assure the stability of the stem in the bone (Sloten , 1998). There are three potential functions of the collar. First is the transfer of load directly to the cut surface of the femoral neck by collar-calcar contact. This requires a large collar. Second is the transfer of load to the proximal end of the cement column, rather than directly to the cut surface of the femoral neck. Such collars are often

small and may be flanged. Finally, for many surgeons, the primary function of the collar is as form of "stop" to indicate when they should cease pushing the stem distally into the cement column during insertion (Ling , 1992). Several experimental and computer studies have indicated a higher (more nearly normal) transmission of compressive stress from the prosthesis into the medial calcar femoral bone with a collar. This effect is beneficial in that it may reduce adaptive bone resorption in the proximal femur (stress shielding), reduce the bending stress in the component stem, and reduce the stress in the distal cement.

The most important design properties of stem are cross section, length, stiffness and surface properties of stem, each of which is handled in the following sections.

2.3.3.1. Cross-section of Stem

Cross-sectional geometry of a femoral component is conception of the volume and distribution of material of the stem. Certain sectional shapes produce a more favourable mechanical environment than others. Sharp corners in the stem should be avoided as they produce marked stress concentrations and may cause cement or bone failure. The area moment of inertia is a term that describes the distribution of mass of an object in regard to its neutral axis. The larger the area moment of inertia, the greater the resistance of the object to bending. The cross-sectional shape of a diamond and I-beam represent the extremes of a small and large area moment of inertia for a given mass. Those stems with a large volume of material along the lateral border are more resistant to bending and produce less tensile stress in the cement mantle. Those stems that have a relatively thick medial side also produce less compressive stress in the cement. Since bone cement is about three times stronger in compression than in tension, compression loading may be the only safe mode (i.e.,

the less tensile stress, the less likely that cement will fracture, resulting in component loosening).

Changes in cross-section geometry had only a limited effect on the magnitude of the proximal cement stresses. In general, the use of a smaller medial radius of the stem resulted in increased proximal cement stresses. Clinically, stem geometries with a small medial radius have performed poorly when compared to stems with broad medial radius. The choice of A-P width of the stem cross-section had a minimal effect on the proximal cement mantle stresses. Although cement stresses may not be affected by use of a stem with a large A-P dimension, there may be other mechanical effects at the cement-bone interface (Mann , 1995).

Crowninshield found that increasing the cross section of the stem decreased the stress in both the stem and the cement. Viceconti lessened the stiffness of the stem by using transverse holes (Gross & Abel, 2001).

2.3.3.2. Length of Stem

Mathematical modelling studies have shown that either very short or very long stems have stress concentrations at some point in the component for example; very long stems produce increased stress on the stem and distal stress transfer with shielding proximal bone. Very short stems produce very high stress proximally that may exceed the ultimate strength of cement or bone. A stem length of between 100-130 millimeters seems optimum.

2.3.3.3. Stiffness of Stem

The physical properties of a prosthetic femoral device are defined by its response to loading and determined by its size and shape and also by the properties of the material from which it is manufactured. Obviously, the higher the yield stress and ultimate stress of a device the greater the safety margin and the less likely is the device to fail (i.e., to bend or break). Repeated or cyclic loading of the device below the point of yield stress will eventually result in fatigue fracture. The number of loading cycles possible before fracture occurs is termed the fatigue strength. This property is of critical importance in the performance of a prosthetic femoral device.

The lower the elastic modulus, the more stress the device will transfer to cement and bone. Stainless steel was used to manufacture many of the early prosthetic femoral devices. However, stainless steels are relatively stiff (i.e. high elastic modulus) material but have low fatigue and yield strength characteristics. Cobalt-chromium alloys have better fatigue and yield stress but have slightly greater elastic modulus than stainless steels. Titanium alloys have been increasingly used recent years because of their favourable strength characteristic and lesser stiffness.

The elastic modulus of the materials, however, does not fully describe the properties of the prosthetic component. The stiffness of a given device depends on its cross-sectional geometry as well. If one designs a stem of a rather elastic material but makes it large and massive to resist fracture and to improve fit into the proximal femur, the overall stiffness would likely be greater than that of a smaller stem made of a stiffer material. Smaller, more flexible stems carry less internal stress but transmit more compression stress to the proximal bone and cement. Large, stiff stems reduce the thickness of the cement mantle and produce high tensile

stress in the cement distally. Either situation may produce cement failure and component loosening. Titanium alloys thus have physical properties that appear advantageous for femoral components used without cement. However, with cemented devices, the vulnerability of the bone cement appears to override the theoretically advantageous material properties of titanium alloy.

Femoral components with a stiffer (higher elastic modulus) stem have been shown to decrease the stress in the proximal bone and cement for cases where there is a perfect bond between the materials (Mann , 1995).

2.3.3.4. Surface Properties of Stem

Surface finish is another design feature that has generated considerable discussion and controversy. Some recent prostheses, intended for use with cement fixation, have been manufactured with stem surfaces that are sandblasted, hobnailed, porous, or pre-coated with methyl methacrylate. The rational is that these rough surfaces provide increased adhesion of cement to the stem and thus resist distal migration and micromotion of the stem within the cement. This may reduce the radial compressive forces (hoop stress) acting at the interface between stem and bond cement that may be an important cause of cracking or failure of the cement mantle. However, again there are compromises to be considered. It no longer is obvious that surfaces of total hip arthroplasty stems, to provide better grip on cement and prevent debonding, should be roughened. Roughness reduces slip, but it enhances abrasion if slip occurs. Clinically it was shown that particular designs have better endurance with smooth (or polished) surfaces, as opposed to rough (or matte) surfaces. The idea that a polished stem reduces the amount of abrasion particles when rubbing against cement, thus preventing bone Osteolysis to develop, was suggested as an explanation for this improvement. Surface texture

or roughness, or prosthetic collars, would hamper such a requirement. Finally, it was hypothesized that a polished stem, able to subside within the cement mantle, would reduce stress transfer at the cement-bone interface, thus protecting the bond against mechanical failure. (Huiskes , 1998)

The rough surfaces may introduce stress concentrations that weaken the stem and reduce the fracture toughness of the cement. They also may increase the technical difficulty in removing the prosthesis, should revision become necessary.

Axial load applied to the stem forces the wedge into the cement. The smooth surface of the stem and its tapered design minimize friction, such that the axial forces are converted into radial compressive forces, which favorably load the bone through the cement mantle.

2.4. Materials Used in Total Joint Replacements

A definition of biomaterials is any substance or combination of substance synthetic or natural in origin, which can be used for any period of time, as whole or as a part of a system, which treats, arguments, or replaces any tissue, organ, or function of the body (Bronzino, 1995).

Implant materials may corrode and/or wear, leading to the generation of particulate debris, which may, in turn, elicit both local and systemic biological responses. Although metals exhibit high strength and toughness, properties needed in joint replacement, they are more susceptible to electrochemical degradation, than ceramics or polymers. Therefore, a fundamental criterion for choosing a metallic implant material is that the biological response it elicits is minimal. Because of the combined mechanical and environmental demands, the

metals used in bone and joint reconstruction have been limited to three classes: stainless steel (iron based), cobalt-based alloys and titanium-based materials. Each of these materials is well tolerated by the body because of its passive oxide layer. The body in trace amounts can usually tolerate the main elemental constituents, as well as the minor alloying constituents of these metals, since most materials have specific biological roles and are therefore essential. However, larger amounts of metals usually cannot be tolerated. Minimizing mechanical and chemical breakdown of implant materials is therefore a primary object.

The "ideal" material or material combination for TJR (Total Joint Replacement) prostheses should therefore exhibit the following properties: a "biocompatible" chemical composition to avoid adverse tissue reactions, an excellent resistance to degradation (corrosion) in the human body environment, acceptable strength to sustain the cycling loading endured by the joint, a low modulus to minimize bone resorption, and a higher-wear resistance to minimize debris generation(Long & Rack, 1998).

Over the 30 years considerable progress has been made in understanding the interactions between the tissues and the materials. Researchers have coined the words "biomaterial" and "biocompatibility" to indicate the biological performance of materials. Materials that are called biomaterials and biocompatibility are a descriptive term, which indicates the ability of a material to perform with an appropriate host response, in a specific application. In simple terms it implies compatibility or harmony of the biomaterial with the living system. Wintermantel and Mayer extended this definition and distinguished between surface and structural compatibility of an implant. Surface compatibility meanings the chemical,

biological and physical (including surface morphology) suitability of implant surface host tissues. Structural compatibility is optimal adaptation to the mechanical behavior of the host tissues. Therefore, structural biocompatibility refers to the mechanical properties of the implant material, such as elastic modulus and strength; implant design (stiffness, which is product of elastic modulus, E and second moment of area, I) and optimal load transmission (minimum interfacial strain mismatch) at the implant tissue interface. Optimal interaction between biomaterial and host is reached when both the surface and the structural compatibility are met. Further more it should be noted that the success of a biomaterial in the body also depends on many factors such as surgical technique (degree of trauma imposed during implantation, sterilization methods, etc), health condition and activities of the patient (Ramakrishna , 2001).

2.4.1 Stainless Steel

The first stainless steel utilized for implant fabrication was the 18-8 (type 302 in modern classification), which is stronger and more resistant to corrosion than the vanadium steel. Vanadium steel is no longer used in implants since its corrosion resistance is inadequate in vivo. Later 18-8s Mo stainless steel was introduced that contains a small percentage of molybdenum to improve the corrosion resistance in chloride solution (salt water). This alloy became known as type 316 stainless steel. In the 1950s the carbon content of 316 stainless steel was reduced from 0.08 to a maximum amount of 0.03% for better corrosion resistance to chloride solution and to minimize the sensitization and hence, became known as type 316L stainless steel (Bronzino, 2000). Today, stainless steel is one of the most frequently used biomaterials for internal fixation devices because of a favorable combination of mechanical properties, corrosion resistance and cost effectiveness when compared to other metallic

implants (Disegi & Eschbach, 2000). The most important alloying constituent in stainless steel is chromium, which should have a concentration of at least 12% for the steel to develop a passive chromium oxide layer necessary for corrosion resistant. Elemental compositions outside of the specified bounds can lead to less than optimal microstructures and compromise the physical and mechanical properties. For example, chromium content above approximately 28% leads to the precipitation of grain boundary chromium carbide ($Cr_{23}C_{26}$) and a localized zone of depleted chromium to the carbides. This depleted zone is anodic relative to the remainder of the alloy and, as a result, localized intergranular corrosion occurs, in a process known as sensitization. Since carbide formation occurs at 450-900 ^{o}C, stainless steels are heat treated above 950 ^{o}C to avoid carbon diffusion and formation of carbides.

The austenitic stainless steels, especially type 316 and 316L, are most widely used for implant fabrication. These cannot be hardened by heat treatment but can be hardened by cold-working. The inclusion of molybdenum enhances resistance to pitting corrosion in salt water. The American Society of Testing and Materials (ASTM) recommends type 316L rather than 316 for implant fabrication. The specifications for 316L stainless steel are given in Table 2.2. The only difference in composition between the 316L and 316 stainless steel is the maximum content of carbon, i.e., 0.03% and 0.08%, respectively, as noted earlier.

The nickel stabilizes the austenitic phase [γ, face centered cubic crystal (fcc) structure], at room temperature and enhances corrosion resistance.

The 316L stainless steels may corrode inside the body under certain circumstances in a highly stressed and oxygen-depleted region, such as the contacts under the screws of the bone

fracture plate. Thus, these stainless steels are suitable to use only in temporary implant devices such as fracture plates, screws, and hip nails. Surface modification methods such as anodization, passivation, and glow-discharge nitrogen-implantation, are widely used in order to improve corrosion resistance, wear resistance, and fatigue strength of 316L stainless steel (Bronzino, 2000), (Disegi & Eschbach, 2000).

Table 2.2 Compositions of 316L Stainless Steel (American Society for testing and Materials, F139-86, 1992)

Element	Composition (weight %)
Carbon	0.03 max
Manganese	2.00 max
Phosphorus	0.03 max
Sulfur	0. 03 max
Silicon	0.75 max
Chromium	17.00-20.00
Nickel	12.00-14.00
Molybdenum	2.00-4.00

2.4.2. Cobalt-Based Alloys

By the early 1930s, a cobalt-chromium alloy called Vitallium was introduced to dentistry as an alternative to gold alloys. Cobalt-chromium alloy soon found application in orthopaedic surgery for fabrication of hip prostheses and internal fixation plates and has become one of the three major biomedical metallic materials (Greco, 1994). There are basically two types of cobalt-chromium alloys: (1) the castable CoCrMo alloy and (2) the CoNiCrMo alloy which is usually wrought by (hot) forging. The castable CoCrMo alloy has been used for many decades

in dentistry and, relatively recently, in making artificial joints. The wrought CoNiCrMo alloy is relatively new, now used for making the stems of prostheses for heavily loaded joints such as the knee and hip.

The ASTM lists four types of CoCr alloys, which are recommended for surgical implant applications: (1) cast CoCrMo alloy (F 75), (2) wrought CoCrWNi alloy (F90), (3) wrought CoNiCrMo alloy (F562), and (4) wrought CoNiCrMoWFe alloy (F563). The chemical compositions of each are summarized in Table 2.3. At the present only two of four alloys are used extensively in implant applications, the castable CoCrMo and the wrought CoNiCrMo alloy. As can be noticed from Table 2.3, the compositions are quite different from each other.

The two basic elements of the CoCr alloys form a solid solution of up to 65% Co. The molybdenum is added to produce finer grains, which results in higher strengths after casting or forging. The chromium enhances corrosion resistance as well as solid solution strengthening of the alloy.

The CoNiCrMo alloy originally called MP35N (Standard Pressed Steel Co.) contains approximately 35% Co and Ni each. The alloy is highly corrosion resistant to seawater (under chloride ions) under stress. Cold working can increase the strength of the alloy considerably but there is a considerable difficulty of cold working on this alloy, especially when making large devices such as hip joint stems. Only hot forging can be used to fabricate a large implant with the alloy.

The superior fatigue and ultimate tensile strength of the wrought CoNiCrMo alloy make it suitable for the applications, which require long service life without fracture or stress fatigue. Such is the case for the stems of the hip joint prostheses. This advantage is better appreciated

when the implant has to be replaced, since it is quite difficult to remove the failed piece of implant embedded deep in the femoral medullary canal.

2.4.3. Ti Alloys

Experiments on the surgical use of this metal began more than 50 years ago and it has been used in orthopaedic since the mid-1960s (Williams, 1994). Titanium and some Titanium-based alloys seem to have been well established for heavy load-bearing skeletal implants, such as artificial tooth roots or joint endoprostheses. Stainless Steel or cobalt-based alloys for implants exhibit corrosion pitting when subjected to cyclic loading and thus are unsatisfactory corrosion fatigue properties. The corrosion products are correlated to biocompatibity-problems. Titanium is known for its high corrosion resistant due to instant formation of an inert oxide surface layer. This is given Titanium a reputation of being a biocompatible implant material. However, the low wear resistance and poor tribological properties of Titanium and its alloys have resulted in the release of significant amounts of metal into the adjacent tissues. This can induce immunological responses and influence negatively the long-term biocompatibility of Titanium implants (Papakyriacou , 2000), (Pohler, 2000). There are four grades of unalloyed commercially pure titanium for surgical implant application as given in Table 2.4.

One titanium alloy (Ti6Al4V) is widely used to manufacture implants and its chemical requirements. The main alloying elements of the alloy are aluminum (5.5~6.5%) and vanadium (3.5~4.5%). The Ti6Al4V alloy has approximately the same fatigue strength (550 MPa) of CoCr alloy after rotary bending fatigue tests.

Table 2.5 summarizes some characteristics of orthopaedic metallic implant materials.

Table 2.3. Chemical compositions of Co-Cr Alloys (American Society For Testing and Materials, F 75-87, F 90-87, F562-84, 1992).

Element	CoCrMo (F75)		CoCrWNi (F90)		CoNiCrMo (F562)		CoNiCrMoWFe	
	Min	Max	Min	Max	Min	Max	Min	Max
Cr	2.7	30.0	19.0	21.0	19.0	21.0	18.0	22.0
Mo	5.0	7.0	-	-	9.0	10.5	3.0	4.0
Ni	-	2.5	9.0	11.0	33.0	37.0	15.0	25.0
Fe	-	0.75	-	3.0	-	1.0	4.0	6.0
C	-	0.35	0.05	0.15	-	0.025	-	0.05
Si	-	1.00	-	1.00	-	0.15	-	0.50
Mn	-	1.00	-	2.00	-	0.15	-	1.00
W	-	-	14.0	16.0	-	-	3.00	4.00
P	-	-	-	-	-	0.015	-	-
S	-	-	-	-	-	0.010	-	0.010
Ti	-	-	-	-	-	1.0	0.50	3.50
Co	Balance							

Table 2.4. Chemical Compositions of Titanium and its Alloy (American Society for Testing and Materials, F67-89, F136-84, 1992).

Element	Grade 1	Grade 2	Grade 3	Grade 4	Ti6Al4V
Nitrogen	0.03	0.03	0.05	0.05	0.05
Carbon	0.10	0.10	0.10	0.10	0.08
Hydrogen	0.015	0.015	0.015	0.015	0.0125
Iron	0.20	0.30	0.30	0.50	0.25
Oxygen	0.18	0.25	0.35	0.40	0.13
Titanium	Balance				

2.4.4. Ceramics

There are three categories of ceramics used to replace bone. The first is structural ceramics (alumina, Al_2O_3, and zirconia, ZrO_2). These have higher stiffness and hardness than the metals and much better wear resistance. Pure zirconia can undergo phase transitions on cooling and, to avoid this, it is alloyed with CaO, MgO, or Y_2O_3, forming partially stabilized zircona or tetragonal zircona. Both alumina and zirconia are used for heads of hip prostheses.

The second category of ceramic used to replace bone is calcium phosphate. Hydroxyapatite (HA), is a form of calcium phosphate that is found naturally in bone. Another calcium phosphate is tricalcium phosphate (TCP). TCP biodegrades more quickly than HA, indicating that the amount of TCP shold be minimized to slow the dissolution rate of an HA/TCP mix. Calcium phosphates have useful osteoconductive properties and are used to coat metallic implants that aim to bond to the bone by osteointegration. They are also used for synthetic bone graft materials.

The third category of ceramic is bioactive glass. Ceramics in this category have excellent biocompatibility. Glasses are amorphous materials have no long-range atomic order. This results when the cooling from the liquid phase is sufficiently rapid to prevent crystallization. Glass bioceramics have large amounts of SiO_2, with amounts of the following compounds: P_2O_5, CaO, $Ca(PO_3)_2$, CaF_2, MgO, MgF_2, Na_2O, K_2O, Al_2O_3, B_2O_3, and Ta_2O_5/TiO_2. Glass-ceramics used for implantation undergo surface dissolution in physiological environment, resulting in the formation of a chemical bond with bone. This results in high interfacial strength. However, the toughness of the underlying glass can be low, leading to failure within the bulk material.

Table 2.5. Some characteristics of orthopaedic metallic implant materials (Long, 1998).

	Stainless Steels	Cobalt-base allovs	Ti&Ti-base allovs
Designation	ASTM F-138	ASTM F-75 ASTM F-799 ASTM F-1537 (Cast and wrought)	ASTM F-67 (ISO 5832/II) ASTMF-136(ISO 5832/II) ASTM F-1295 (Cast and wrought)
Principal Alloying Elements (wt%)	Fe(bal.) Cr (17-20) Ni(12-14) Mo(2-4)	Co (bal.) Cr (19-30) Mo(0-10) Ni(0-37)	Ti (bal.) Al(6) V(4) Nb(7)
Advantages	•cost, availability •processing	•wear resistance •corrosion resistance •fatigue strength	•biocompatibility •corrosion •minimum modulus •fatigue strength
Disadvantages	•long term behavior •high modulus	•high modulus •biocompatibility	•power wear resistance •low shear strength
Primary Utilizations	Temporary devices (fracture plates, screws, hip nails) Used for THRs stems in UK (high Nitrogen)	Dentistry castings Prostheses stems Load-bearing components in TJR (wrought alloys)	Used in THRs with modular (CoCrMo or ceramic) femoral heads Long-term, permanent devices (nails, pacemakers)

Table 2.6. Physical and mechanical properties of implant metals and alloys used in orthopedic surgery applications (Doewson, 1992).

	Materials	316 SS (wrought)	Co-Cr-Mo alloy (cast)	Titanium (wrought)	Ti-Al-V alloy (wrought)
Physical properties	Density (g/cm^3)	7.90	7.80	4.50	4.40
Mechanical properties	Young's modulus (GPa)	200	200	127	111
	Tensile strength (MPa)	465	665	575	900
	0.2% proof stress (MPa)	170	455	465	830
	Fracture strain, %	40	10	15	8
	Fatigue stress (MPa), 10^8 cycles — Air	241	290	250	380
	Fatigue stress (MPa), 10^8 cycles — Saline	103	140	120	140

2.4.5. Polymers

A wide range of polymers is used for implantable devices. The first category is polymers with no crosslinking of polymers chains-called thermoplastics. Well-known examples are polyethylene (PE) and polymethylmethacrylate (PMMA). Ultra-high-molecular-weight polyethylene (UHMWPE), so-called because it has a very long molecular chain, is very wear resistant and is used as a bearing material for the articulating surfaces of many artificial joints.

PMMA is used as an orthopaedic component to the bone. The material serves to interlock the prosthetic component to the bone. Polymerization takes place during the mixing of powder and liquid components, which is carried out in the operating theatre. Mixing is critical to the removal of pores and increasing the strength. As the polymerization reaction progresses, the material solidifies and the prosthesis is fixated into its final position. Cement must endure considerable stresses in vivo applications, thus strength characteristics are more important for its clinical success. The main function of the bone cement is to transfer load from the prostheses to the bone or increase the load carrying capacity of the surgical construction.

PMMA cement has many advantages, but there are also negative attributes such as thermal necrosis of bone due to the exothermic reaction associated with polymerization process. Another issue is the deterioration of cement/implant or cement/bone interface with time, leading to problems of mechanical failure and instability. PMMA undergoes damage accumulation as the cyclic load is applied over the lifetime of the patient (Cowin, 2001).

PMMA is currently the only material used for anchoring cemented arthroplasties to the contiguous bones. In this application the main functions of the cement are to transfer body weight and service loads from the prosthesis to the bone and/or increase the load carrying capacity of the prostheses-bone cement-bone system. The cement performs these functions admirably because of the array of properties it possesses. It is well recognized, however, that bone cement is beset with a number of drawbacks, of which there are six main ones. First, it is postulated to have a role in the thermal necrosis of the bone, impaired local blood circulation, and predisposition to membrane formation at the cement-bone interface. All of these phenomena have been attributed to the high exothermic temperature of the cement, amounting to between 67 and 124 $^{\circ}$C at the centre of the cement mantle in vivo (depending on the cement formulation). The second drawback is the part that the cement is said to play in the chemical necrosis of the bone, this being postulated to be due to the release or leakage of unreacted

monomer (MMA) liquid before polymerization of the cement in the bone bed. The third problem is the shrinkage of the cement during polymerization. The large stiffness mismatch between the cement and the contiguous bone is the fourth drawback. The fifth disadvantage is the identification of the cement mantle, the implant-cement interface, and the cement-bone interface to be the three "weak-link zones" in the construct. The sixth drawback is that the cement particles, however produced, can interact with the surrounding tissues, evoking inflammatory periprosthetic tissue responses and increasing bone destruction.

In spite of the many drawbacks of the bone cement, the survival probabilities of recently implanted cemented arthroplasties, especially those of the hip and knee in patients aged over 50 years, are very high, averaging at least 90% after 15 years (Lewis, 1997).

The PMMA does not chemically bond to either the prosthesis or the bone; instead fixation depends on the formation of a secure mechanical interlock. Cyclic loads of several times body weight are commonly experienced leaving the PMMA cement susceptible to fatigue failure (McCormack , 1998).

2.5. Fixation Methods

The hip prostheses have been the most active of joint replacement research. A dramatic improvement in the efficacy of the hip implant occurred with the introduction by orthopaedic surgeon John Charnley (later knighted for this innovation) of his total hip arthroplasty consisting of a metal femoral prostheses that was held in place by PMMA, with the acetabulum component made of UHMWPE, also cemented in place with PMMA. This system has seen many variations over the years, but is still a significant factor in modern joint

replacement surgery (Ratner, 1996). In addition to the prostheses design and material, the fixation method is also important for the success of THRs. It is purpose of implant fixation to produce a composite structure of the implant and skeleton that minimizes relative motion at the prostheses-tissue interface and provides a long-lasting, useful joint reconstruction.

Effective long-term implant fixation requires a durable interface between the prostheses and the surrounding tissue. Interface durability can be characterized as having both mechanical and chemical components.

Mechanical interface durability is required to transfer high hip loads across the implant interface to the surrounding skeletal structure. Implant size, shape, surface area, and flexural characteristics all affect stress development at the interface. The fixation method needs to account for the magnitude of stress developed at the interface. A mechanically durable interface will occur when the stresses developed at the interface are consistent with the interface's ability to withstand those stresses. Mechanical interface strength in tension, compression, and shear are relevant measures of interface strength.

Chemical interface durability is also a relevant consideration in the overall durability of the implant. Chemical and electrochemical processes at the interface of both metallic and polymeric implants can change the character of the interface and may affect the longevity of implant fixation. It is well established that all metal implants are subjected to corrosion at some level. Contemporary hip implant metals have extremely low levels of corrosion. However, early attempts to use porous stainless steel for bone ingrowths applications failed due to excessive metal corrosion (Crowninshield, 1988).

The fixation of the stem is largely divided into two categories, i.e., cemented and uncemented. The uncemented can be classified into interface fit and porous-coated for tissue ingrowth fixation. The porous-coated type can be further coated with a hydroxyapatite layer to aid tissue ingrowth.

2.5.1. Cemented Fixation

The first total hip replacement was performed in 1938 by Wiles. These early prostheses were press fit into the medullary canal, or fixed to the bone with screws or nails. The lack of interfacial rigidity, along with stress concentration in bone caused by mechanical fixation, ultimately led to loosening. Some twenty years later, Charnley (1960) used PMMA as a grouting agent to fix prostheses to bone. The introduction of PMMA, or bone cement, enabled joint replacement surgery to advance. When the bone cement sets or hardens, it mechanically interlocks with the roughened bone surface and the prostheses. The main function of the bone cement is to transfer load from the prostheses to the bone or increase the load carrying capacity of the surgical construct. PMMA was chosen for being relatively inert, rapidly setting, and biocompatible (Greco, 1994). Bone cement fixation creates two interfaces: cement-bone and cement-implant. The incidences of loosening for the femoral prostheses were evenly divided at about 10 and 11% for cement-bone and cement-implant interfaces, respectively.

Loosening led to biomechanical failure at the bone-cement and/or cement-implant interface, component fracture, and excessive wear of prostheses. Failure can also occur due to the brittleness and low fatigue strength of the bone cement. Pre-coating with bone cement or polymethylmethacrylate polymer can minimize the cement-implant interface loosening. Pre-coating can achieve a good bonding between the cement and prostheses (Park, 2000).

The deterioration of cement-implant or cement-bone interface with time remains to be still an important issue, leading to problems of mechanical failure and instability. Fatigue failure has been found to be a predominant in vivo failure mode of bone cement. Researchers have tried to improve bone cement mechanical properties by reinforcing with stainless steel and Ti alloy wires, and polymer fibres such as UHMWPE. Use of such fibres reinforcement also reduces the peak temperature during polymerization of the cement, and thus reducing the tissue necrosis.

In cemented THR, the cement layer cannot integrate micromechanically or chemically with bone. Impact loading forces of up to eight times the body weight on the bone-cement-implant interfaces results in cracks. This disruption of proper stress transfer from the prostheses to bone results in bone resorption, preventing bone integration and increasing chances for long-term loosening, recurrence of pain, and functional disability. The many disadvantages associated with PMMA fixation led in investigators to pursue uncemented fixation of femoral stems.

2.5.2. Uncemented Fixation

Cemented fixation is achieved by establishing an interface fit between the implant and the surrounding tissue. The inherent difference between cemented and cementless implant systems lies in the time necessary to achieve stability of the prostheses. With a cemented implant system, fixation is achieved almost immediately post-operatively, whereas with a cementless implant system, tissue integration must occur before the prostheses may be loaded. Thus cementless implant systems are conceived in such a way that the time necessary for tissue integration is minimized and interfacial stability maximized.

The introduction of uncemented arthroplasty offered three types of fixation: press fit, macro-interlock and micro-interlock. Press fitting of smooth-surfaced metals has been abandoned because of excessive postoperative pain, due to a lack of mechanical fixation, resulting in increased revision rates. The macro-interlock type of fixation has shown disappointing results with osteolysis at the implant-bone interface and is not recommended in osteoporotic patients undergoing THA revision. In micro-interlock devices, the implant surfaces are rough or porous so bone can ingrow and provide rigid "bioinert" fixation. Surface porosities, grooves, threads, or beads theoretically provide long-term stability by direct bone integration. Surface texture, corrosion resistance, mechanical properties, and biocompatibility influence bone ingrowth.

CHAPTER THREE
COMPLICATIONS OF THR

Orthopaedic implants regarded as artificial mechanical devices fixed in human body are considered to have failed when they are prematurely removed from the body as the implant does not accomplish its intended function and hence has to be removed due to the implant failure. The mechanical and chemical stability of implanted materials in body fluids are of fundamental importance in the successful treatment of bone fractures and replacement.

The common failures encountered in metallic implants are wear, loosening, pitting corrosion, crevice corrosion, fretting corrosion, corrosion fatigue and fatigue (Sivakumar , 1995).

3.1. Wear

As the fixation of total joint implants has become more reliable and durable and as the technology of total joint replacement has been applied to younger and more active patients, the current limitations of total joint arthroplasty are related to the wear of the components. Wear is the removal of material, with the generation of wear particles that occurs as a result of the relative motion between the articulating surfaces under load. In complex mechanical-biological systems such as total hip and knee replacements, there can be many types of wear. Although the mechanical consequences of wear, such as progressive thinning of polyethylene components, can limit the functional life of a joint replacement, the clinical problems from wear more frequently are due to the release of an excessive number of wear particles into a biological environment (Schmalzried & Callaghan, 1999). Wear particulate is produced primarily trough three mechanisms: abrasion, adhesion, and fatigue. Wear

debris can also act as a stress concentrator, producing secondary three-body wear (Friedman, 1993). Adhesive wear mode involves bonding of the surfaces when they are pressed together under load. Sufficient relative motion results in material being pulled away from one or more surfaces, usually from the weaker material. Another aspect of adhesive wear is the adhesion of passivated layer of oxide on the opposing implant surface to the ultra-high molecular weight polyethylene, resulting in transfer of the passivated layer to polymer. Thus, three-body wear develops, with oxide or cobalt-chromium oxide-instead of cement-as the third body. Implant-derived wear particles may potentially arise from all interfaces created in an artificial joint where there is movement between two surfaces. The main source is the articulating joint surfaces, and the presence of foreign material, such as cement particles and metal beads or hydroxyapatite particles derived from coatings on uncemented implants, exacerbate this production of wear particles by the process of three-body wear. The prostheses-bone, or the prosthesis-cement and cement-bone interfaces will all produce wear particles, as there is inevitably some movement between the surfaces, mostly due to the mismatch of the rigidity of the materials involved. Furthermore, increased surface roughness of implant surfaces have been shown to increase loosening rates (McGee, 2000).

Abrasion is a mechanical process wherein asperities on the harder surface cut and plow through the softer surface, resulting in removal of material. When stresses generated exceed the fatigue strength of material, that material fails after a certain number of loading cycles, releasing material from the surface. High contact stress in ultra-high molecular weight polyethylene, resulting from low conformation of the articulating surfaces, high loads, or both, can cause subsurface stress than exceeds the fatigue strength of the polyethylene. One or more of the classic mechanisms of wear may be operating on the prostheses in a particular

wear mode, and a prostheses may function in several wear modes over its in vivo service life.

Friction is the resistance to movement between two surfaces in contact. The degree of resistance is proportional to the load. The ratio between frictional force and load vertically applied on the articulating surfaces is the coefficient of friction. Frictional torque is the force created as a result of the friction of bearing. Charnley initially selected a stainless steel-on-PTFE bearing couple because of a low coefficient of friction. The small, 22.2 milimeters diameter head was selected to minimize the moment arm of the frictional forces and, thus, to minimize the frictional torque. Unfortunately, Charnley hip components with the polytetrafluoroethylene bearing uniformly failed because of rapid wear with the release of polytetrafluoroethylene wear particles, formation of granulomas, and loosening of the component (Schmalzried & Callaghan, 1999).

Saikko has also studied 14 metallic head and UHMWPE cup combinations. It was concluded that the 22-mm joints produced the lowest frictional torques as well as the lowest friction factor. The frictional torque was dependent not just on the head diameter but on the surface finish, material combination, clearence ratio, thickness of the cup and stiffness of the backing (Hall & Unsworth, 1997).

UHWPE has been commonly used as a counterpart material in artificial joints because of its superior properties such as ductility and impact load damping. Polyethylene wear particles generated at the articular surface, however, have been recognized as a long-term cause of loosening and failure of the artificial hip joint due to osteolysis. It is thought that the majority of polyethylene wear debris travels distally into the fibrous tissue surrounding the implant via the peri-prosthetic fluid and body fluid. These particles are then phagocytosed mainly by

macrophages (type of white blood cell that functions as a patrol cell and engulfs and kills foreign infectious invaders), osteocytes (bone cell) and giant cells in the surrounding bone. The release of different cytokines (a small protein released by cells that has specific effect on the interactions between cells, on communications between cells or on the behaviour of cells) and enzymes from macrphages and giant cells has been shown in many cases to induce the formation of osteoclasts (a cell that nibble at and breaks down bone and is responsible for bone resorption), thus resulting in local bone loss (osteolysis) and aseptic loosening of artificial femoral stem. The occurrence of Osteolysis in association with both well-fixed and loose cemented total hip prostheses has given rise to the term cement disease. Histologically, cement disease is characterized by the presence of variable amounts of cement, ultra-high molecular weight polyethylene, and metal debris in tissue infiltrated with macrophages, giant cells, and vascular granulation tissue.

Therefore, it is essential to quantitatively minimize the polyethylene wear particles in hip joints. For the acetabular cup, metal or ceramic bearing surfaces, improvement UHWPE and various carbon-fibre reinforced synthetic materials are under investigation (Raimondi & Pietrabissa, 2000). It is generally accepted that ion implantation treatment can modify the mechanical wear properties of metals. In particular, nitrogen ion implantation is an excellent candidate to enhance the wear resistance of a wide range of ferrous materials and titanium based alloys.

Titanium alloys have many interesting properties for orthopaedic implants. The most important is their high corrosion-fatigue resistance. However, they have very poor friction and wear behavior, even when rubbing against a soft material such as polyethylene and cannot be used without a surface treatment for orthopaedic implant.

On the other hand, 316L stainless steel has been applied for many years for permanent or temporary implants. Its mechanical properties are lower than those of the titanium alloy, but its friction and wear characteristics are far better. In some cases, crevice corrosion has been observed. It is often associated with wear (Rieu, 1991).

Several researchers have utilized the ion beam applications in the medical area, such as for orthopaedic prostheses that require high wear properties, excellent corrosion resistance and biocompatibility. In a 3-year follow-up with the nitrogen – ion implanted cobalt-chromium (Co-Cr) femoral head using ion beam process, Maruyama et. al. reported a significant reduction in polyethylene wear (Ikeda, 2002).

3.2. Loosening

The number of total hip replacement operations being performed is growing, with over 800,000 being carried out each year. The increase is particularly noticeable in younger people, who are on average more active and therefore impose larger and more frequent loads on the joint than do the more traditional elderly population. Prostheses are therefore more prone to failure, leading to an increased incidence of early revision operations (Gross & Abel, 2001).

Failure is generally due to aseptic loosening of the implant. Four main causes have been identified. The presence of wear particles triggers cell processes that cause osteolysis. Relative movement of the prostheses leads to the development of a soft tissue interface. Mechanical failure of the implant or cement and stress shielding of bone surrounding the

prostheses due to mismatch in structural behavior can lead to bone resorption (Sloten , 1998).

3.2.1. Effect of Wear Particles

Implants usually fail by a combination of mechanisms, but different basic designs tend to show different dominant mechanisms of failure. There are several different mechanisms and modes of implant wear, and perhaps the most important cause of aseptic loosening is an inflammatory reaction to particles of wear debris. Abrasive, adhesive, and fatigue wear of polyethylene; metal and bone cement produces debris particles that induce bone resorption and implant loosening. Charnley found that reaction to excessive wear particles might result in bone resorption while a further biological response is the development of a soft tissue layer at the cement-bone interface, which may compromise fixation. A number of factors can stimulate bone resorption, including the inflammatory reaction associated with infection, the inflammatory reaction stimulated by particles of wear debris, insufficient mechanical load, implant motion, and, probably, high fluid pressures (Bauer & Schils, 1999).

3.2.2. Micromotion

Micromotion of implants that did not achieve adequate initial fixation is another important mechanism of loosening. Fatigue failure at the bone/cement and bone/implant interface may cause aseptic loosening, and may be especially important for implants with relatively smooth surfaces. Based on clinical, radiological, and histological observations, it is believed that micromotion between cement and bone is the cause of failure of cement fixation. The amplitude of such motion need not exceed 30 μm of displacement since this is the smallest acrylic "spherule" displaced from its bed and incorporated into the shape of modified bone.

These spherules are the small particles recognisable from a mass of acrylic. In this theory the structure of the acetabulum is the cause of initiation of micromotion. The weight-bearing portion of the bone of the acetabulum after exposure of bony trabeculae by removal of the subchondral plates is responsible for the deformation of bone and micromotion at the interface. If the stiffness of the acetabulum is reduced by removal of the subchondral bone, plastic deformation of the bone may occur. Stress may than be concentrated at the exposed trebaculae which, in turn, results in bone necrosis. Necrotic bone, in time, is replaced by a fibrous membrane that may or may not turn into a strong fibrocartilaginous metaplastic weight-bearing structure. If this fibrous interface results in significantly decreased stiffness, further motion will break down the acrylic and causes more looseness (micromotion) (Azem, 1999).

3.2.3. Effect of Mechanical Factors

Loosening may be attributed to a combination of mechanical and biological factors as well. Moreland et. al. reported an increase in loosening detected radiologically in young, heavy males. Increased body weight requires the implant system to sustain increased loads. Since the patients were young their activity levels were also high, which may hasten loosening of femoral component. Willert et.al. found that varus positioning of the stem, which is the inclination of the femoral component stem in the coronal plane, may cause the implant fixation to experience higher stresses. It has been shown by experiment that considerable reductions in tensile and shear strengths of the bone cement are caused by the infiltration of blood prior to curing. Failure of the mantle is believed to start at the cement-stem interface, which is significantly weaker than the bulk of the cement under static and fatigue loading. A number of studies have indicated that once the cement-stem interface has become loose the

stresses become significantly higher in the cement mantle (Bishop , 1996). Other mechanical factors, which have been stated to cause loosening of the femoral component, include poor cement technique and inferior hip replacement design. The high strains or stresses on the cement at the tip of the prostheses are strong indications that this location is a likely site for the initial event of failure. High strains at the proximal and distal tip of the prostheses are appeared to cause debonding between the stem and cement and were associated with radial crack initiation at the debonded surface of the pores in the cement surrounding the areas of debonding (Humpreys, 1991).

3.2.4. Stress Shielding

The natural femur carries its external load by itself. When a femoral component is introduced into the canal, it shares the load and the carrying capacity with the bone. Where one structure, the bone, originally carried the load, the two stem and the bone now carry it. As a result, the bone is subjected to reduced stresses, and hence stress shielded. Wolff's Law suggests that the coupling of an implant with a previously load bearing natural structure may result in tissue loss. Indeed, it has been shown that when the tension/compression load or bending moment to which living bone is exposed is reduced, decreased bone thickness, bone mass loss, and increased osteoporosis ensue. This phenomenon, termed "stress shielding", has been related to the difference in flexibility or stiffness, dependent, in part on elastic moduli, between natural bone and the implant material.

The bone resorption resulting from stress shielding can lead to excessive stresses in the bone cement and the interfaces with the bone and the prostheses stem. This effect is a consequence of the mechanism of load transfer from the prostheses to the femur. Whereas the

physiological mechanism of the proximal to distal load transfer is by direct long axis loading, in the prostheses shear forces transfer the load across the material interfaces at the proximal and distal ends of the stem. The more rigid stem, the less load it transfers proximally so the greater stress shielding of the proximal femur. A stem of a lower stiffness material will transfer more of the load to the femur proximally, is expected to enhance stress redistribution to the adjacent bone tissues, therefore reducing stress shielding, however, this is achieved at the expense of higher load transfer stresses at the cement interfaces with the bone and implant and the risk of cement failure. At the same time, there is no means of reaching a totally satisfactory compromise between low stress shielding and low interface shear stresses in this type of implant (Gross & Abel, 2001).

Although THRs are used widely; one of the major unsolved problems in this important application has been the mismatch of the stiffness of the femur bone and the prostheses. Commercial hip joint stems are made from metal alloys, which are isotropic and at least five to six times stiffer than the bone. It has been acknowledged that the metallic stems due to stiffness mismatch induce unphysiological stresses in the bone, thereby affecting its remodeling process. It is discussed that this leads to bone resorption and eventual aseptic loosening of the prostheses. Gese demonstrated that Ti alloy stems result in a 50% reduction in the femur peak stress compared to the Co-Cr alloy stem. It has been acknowledged that the implant loosening and eventual failure could be reduced through improvements in the prostheses design and using a less stiff material with mechanical properties close to the properties of bone (i.e. isoelastic materials). However, because of the high strength requirement for hip prostheses design, materials suitable for these implants are very limited.

3.2.5. Factor of PMMA Loosening

The causes of loosening itself are multifactorial, with both biological and mechanical processes operating simultaneously. In the case of the femoral side, fatigue fracture of the metal stem is sometimes reported, but fatigue damage accumulation in the polymethylmethacrylate (PMMA) cement is the most common cause of loosening. Damage accumulation can be accelerated by stress increases caused by biological adaptations, e.g. bone resorption or fibrous tissue formation at the cement/bone interface.

Several structural analyses of hip replacements have been carried out to establish the relationship between prostheses design and joint lifetime. Despite its widespread use, PMMA is not an ideal fixation material because it cannot sustain cyclic loading over an extended period; mechanical failure of the cement can occur leading to implant loosening and need for a revision operation. For this reason, cementless or "cement-free" fixation is sometimes preferred for younger patients who will need the implant to survive for longer and who are also likely to subject the fixation to higher
loads. To improve the performance of PMMA under cyclic loading, a clear understanding of the mechanism of PMMA failure in vivo is required.

One framework for understanding the biomechanics of failure of orthopaedic implants was proposed by Huiskes. In particular the bone cement can undergo failure
by microcrack growth in the bulk cement and on the cement-prostheses and cement- bone interfaces. This can lead to loosening by itself, or it can lead to the generation of particles as the crack surfaces abrade each other causing the particulate reaction failure scenario. The result is mechanical loosening of the implant fixation and pain for the patient (Prendergast, 2001).

Table 3.1. Young modulus of cancellous bone and cortical bone compared to the metallic
biomaterials.

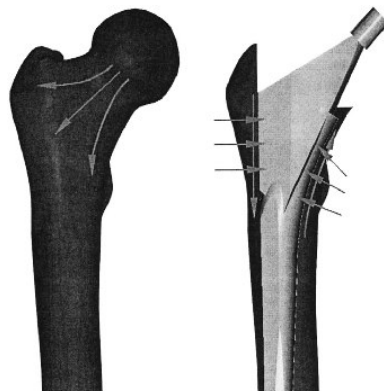| Material	E (GPa)
316L Stainless Steel	196
Co-Cr alloy	210
Ti alloy	116
Cancellous Bone	0.4
Cortical Bone	15-25
PMMA	2.5
UHMWPE	1

Figure 3.1. Schematic representation of
the load transfer before and after THA
(Gross & Abel, 2001).

Experimental investigation has proved to be very difficult, mainly for the following
reasons: (i) the weakest structural component (the PMMA) is encased between the prostheses
and the bone, and hence quantification of fatigue crack propagation is difficult; (ii) the fatigue

failure is multifactorial, possibly involving crack propagation along and out from both the PMMA-metal and PMMA-bone interfaces accompanied by crack kinking into the bulk cement, and the crack propagation from defects (pores, cold shuts, etc.) within the bulk cement; and (iii) the loading conditions are complex and vary considerably during daily activities.

In an attempt to overcome the complexity of the loading, the authors have investigated the bending and torsional aspects of the load separately. McCormack et. al. described an experimental model used to investigate damage accumulation due to bending, and showed that damage accumulation under bending is by crack growth from pores with very little interface crack propagation. This result is not in agreement with autopsy-retrieved implants, where crack propagation from interfaces is observed as dominant cracking pattern. This suggests that bending is not the critical loading mode for implants in vivo, but rather that torsion may be the loading mode generating critical interface damage under cyclic loading. Torsional loading plays a significant role in creating damage in cemented hip replacements by causing crack propagation from pores and the PMMA cement-implant interface, and should not be neglected in theoretical or experimental analyses. Because of this designers of joint hip replacements should attempt: minimize the torsional component of the load; and design cross sectional geometries, which are optimized to reduce damage accumulation due to torsion (McCormack , 1999).

3.3. Corrosion

3.3.1. General Aspects of Corrosion

Corrosion may be regarded as the usually unwanted interaction of a metallic component with the environment in which it exists. During the process, metal ions may be lost from the metal surface to form either a solid corrosion product or one that is soluble in its environment. The corrosion environment may in general be liquid or gaseous. Corrosion of metallic materials in implants may affect the body tissue by cell reaction to electrical current, change of pH and release of metallic ions from the implant. For stainless steel the biological environment reacts by formation of connective tissue between metal surface and body tissue; besides that, allergic reactions to nickel and chromium are also reported. Surface modifications of stainless steel implants by application of ceramic coatings, such as TiN or diamond-like carbon films, have been investigated as a means to reduce friction and increase corrosion resistance. However, ceramic thin films are very brittle and cannot normally withstand plastic deformation of the substrate without cracking and/or delamination (Macionczyk , 2001). In dealing with the corrosion of orthopedic implants, emphasis will be given to aqueous corrosion. Tissue fluid in the human body contains water, dissolved oxygen, proteins, and various ions such as chloride and hydroxide. As a result, the human body presents a very aggressive environment for metals used for implantation. Corrosion resistance of a metallic implant material is consequently an important aspect of its biocompatibility. For this reason the biocompatibility of a metallic implant is usually equated with its corrosion resistance. Thus, the biocompatibility of metallic materials is controlled by the chemical, or more precisely the electrochemical interaction that results in the release of metallic ions into

the tissue, and the toxicology of these released substances (Zitter & Plenk, 1987).
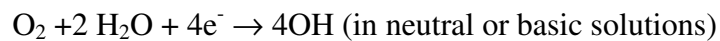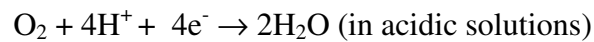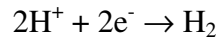
Corrosion reactions are chemical process that take place at the surface of the metal and obey well-established laws. It has been established that corrosion in aqueous media is an electrochemical process.

Corrosion can be viewed as the tendency of a metal to revert back to its natural and more stable state as an ore. Certain environments offer opportunities for these metals to combine chemically with elements to form compounds and return to their lower energy levels. The lowest free energy state of many metals in an oxygenated and hydrated environment is that of the oxide. Corrosion occurs when metal atoms become ionized and go into solution, or combine with oxygen or other species in solution to form a compound, which flakes off or dissolves. The body environment is very aggressive in terms of corrosion it is not only aqueous but also contains chloride ions and proteins. A variety of chemical reactions occur when a metal is exposed to an aqueous environment. Electrolyte, which contains ions in solutions, serves to complete the electric circuit. In human body, the required ions are plentiful in body fluids.

Anions are negative ions, which migrate toward the anode, and cations are positive ions, which migrate toward the cathode. At the anode, or positive electrode, the metal atoms are oxidized by losing valence electrons as in following. Two kinds of chemical reactions usually occur on a metal surface exposed to an aqueous solution. There is an oxidation or anodic reaction, which procedures a supply of electrons of the type:

$$Me \quad \rightarrow \quad Me^{n+} \quad + \quad ne^-$$
$$\text{(metal)} \quad \text{(metal ion)} \quad \text{(electrons)}$$
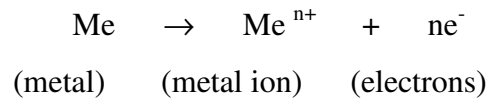
And a reduction or cathodic reaction consumes electrons produced by the anodic reaction. The reduction of dissolved oxygen and the production of hydrogen ions are the two principle cathodic reactions, represented as:

$$2H^+ + 2e^- \rightarrow H_2$$
$$O_2 + 4H^+ + 4e^- \rightarrow 2H_2O \text{ (in acidic solutions)}$$
$$O_2 + 2 H_2O + 4e^- \rightarrow 4OH \text{ (in neutral or basic solutions)}$$

As with any electrochemical cell, both the anodic and cathodic reactions must occur simultaneously, to preserve electrical neutrality and, must proceed at the same rate. The sites of these reactions, i.e., the anode and the cathode, need not be adjacent, but can be widely separated, providing that they remain in electrical contact.

3.3.2. Types of Corrosion

Under conditions where the anodic and cathodic sites are mobile or randomly distributed, the resulting attack may be general over the whole surface. In many instances, however, the attack is concentrated at specific sites, resulting in many different forms of localized corrosive attack, the most common of which are described below.

3.3.2.1. Galvanic Corrosion

If two dissimilar metals placed in contact with each other are subsequently exposed to a conductive solution, an electrical potential will exist between them. This will serve as the driving force for the flow of current, with subsequent corrosion, referred to as galvanic corrosion, of one of the metals in the couple. The larger the potential difference between the two, the greater is the probability of corrosion of the less noble metal (galvanic attack). Galvanic corrosion only causes accelerated deterioration of the less noble material, which would have undergone attack even if placed in the solution in isolation.

Reference may be made to the electrochemical series to determine which component of a galvanic couple will be protected and which will be attacked. The phenomenon is clearly of importance in multicomponent devices, for example, bone plates and screws, where use of items of dissimilar materials may induce galvanic attack.

Whenever stainless steel is coupled with another alloy, it will suffer from galvanic corrosion. If both alloys remain within their passive region when coupled in this way, the additional corrosion may be minimal. Some modular orthopedic systems are made of titanium alloys and cobalt-based alloys on the basis that both should remain passive.

3.3.2.2. Pitting Corrosion

Stainless steels, as is the case with many other metals, depend on the presence of a closely adherent oxide surface layer for their resistance to corrosion. The austenitic chromium-nickel-molybdenum steel achieves its "stainless" characteristics through the formation of a 1-5 nm

thin and adherent chromium rich oxide film. Molybdenum is typically added to stainless steels to increase corrosion resistance-particularly in chloride containing environments. The chromium oxide that forms on the surface passivates the stainless steels (Ratner, 1996). When continuous, this thin layer of oxide protects the metal from any further oxidation. Due to the mechanism of this type of protection the corrosion resistance of the metal and the ability to maintain the integrity of the oxide film depend on the continuous presence of oxygen in the environment. Thus, the stainless steels are passive in corrosive salt solutions such as the body fluids as long as the oxygen retention remains relatively high and is uniform over the entire surface (Bement, 1971).

In surface defects like fissures or pits the local corrosion rate may be drastically increased, due to incomplete repassivation of the surface caused by the lack of oxygen. For implants made of stainless steel in vivo pitting corrosion has been observed. When differential oxygenetion is present over the surface of stainless steel several means are available for corrosion to occur. Where the surface is in contact with low oxygen environmental the equilibrium of the reaction on metal with environmental oxygen is shifted in favor of the breakdown of the protective oxide film and producing small areas in which the protective surface is removed. The localized spots will actively corrode and pits will form in the surface of the material. The resulting exposed metal acts as an anode to the surrounding protected areas, which are cathodic. The shape of the pits varies from hemispherical to a wide variety of irregular shapes caused by undercutting with the result that the surface diameter may be less than the diameter below the surface (Ducheyne & Hastings, 1984).

Work on pitting propensity in simulated physiological saline solutions has shown that for titanium and chromium cobalt alloys, the probability of pit formation is very small. With the

stainless steel, however, there is a significant probability of pit formation. This is borne out in practice where the observation of pitting is confined to stainless steel components.

Both chromium and nickel as the major elements of austenitic stainless steels increase resistance to pitting. Other important alloying elements that increase resistance to pitting are molybdenum and nitrogen (Sedriks, 1996). Pitting attack on the prostheses would probably have been initiated owing to the low molybdenum content and excess of sulphide inclusion, which is known to play an important role in initiating pitting attack in stainless steel. The presence of pits in the implant at such a critical site had resulted in a decrease of pH in the vicinity of implant at the fractures site. The pits could have acted as stress raisers, and hence the cracks would have been initiated from these pits. Therefore, the failure of the prostheses was due to the microcracks formed on the prostheses. The cracks were aggravated by the high inclusion content and large grain size of the implant material (Sivakumar, 1992).

3.3.2.3. Crevice Corrosion

As the principal cathode reaction in aqueous solutions is the reduction of oxygen to hydroxyl ions, it follows therefore that regions of highest oxygen concentration and easy oxygen access will be principally cathodic, whereas those regions with restricted oxygen access will become anodic. A circuit will flow between a well-aerated electrode and a less-aerated one with the latter suffering preferential attack. This phenomenon is known as differential aeration and is important in many corrosion phenomena, noticeably crevice attack.

Because the electrolyte in a crevice has only limited access to the surrounding

saline fluid, corrosion leads to a build-up of hydrogen and metal ions in the solution, together with a decrease in oxygen. The highly mobile chloride ion migrates into the crevice, and by a similar mechanism to that observed with pitting, the attack becomes accelerated. Titanium is generally considered to be biocompatible and highly corrosion resistant. On the other hand, titanium is also prone to crevice corrosion if fixed with PMMA. This is why titanium is recommended to be used in cementless implants (Tiainen, 2001).

As crevice attack occurs at interfaces, multicomponent devices, notably bone plates and screws, suffer from this type of attack.

3.3.2.4. Grain Boundary Attack (Intergranular Corrosion)

All metals crystallize from the molten state to form thousands of grains (regions of regular atomic arrangements). Where grains meet there is a region of mismatch, the grain boundary.

These regions are less ordered and possess higher energy than the body of the grains and may suffer preferential attack, resulting in intergranular corrosion. The attack may be due to the higher energy of the boundaries or to alloy segregation, resulting in a potential drop between the boundary and the body of the grain sufficient to lead to the development of corrosion currents of considerable magnitude.

Stainless steels made of 18Cr-8Ni are susceptible to intergranular corrosion when heat treated in the temperature range 500 to 800°C, as can occur, for example, in regions adjacent to welds or as a result of insufficient thermal control during forging.

In this temperature range, chromium carbides $Cr_{23}C_6$ are precipitated at the grain boundaries and the immediately adjacent areas become depleted in chromium, as shown in Figure 3.2. These chromium-depleted regions become active with respect to the body of the grain, and in the presence of an electrolyte can lead to the formation of an electrochemical cell. The low anode/cathode area ratio leads to corrosion under anodic control and the possibility of very severe attack.

This phenomenon can be remedied by the addition of strong carbide formers to the steel, for example, niobium or titanium. These will then form carbides preferentially to $Cr_{23}C_6$, thus preventing the formation of the chromium-depleted region. Steel in this condition is said to be stabilized. Low carbon grades of steel, for example, AISI 316L also reduce the problem by limiting the carbon available to form carbide. Phosphorous and sulfur segregation have also been proposed as being responsible for weld decay, i.e., attack close to welds.
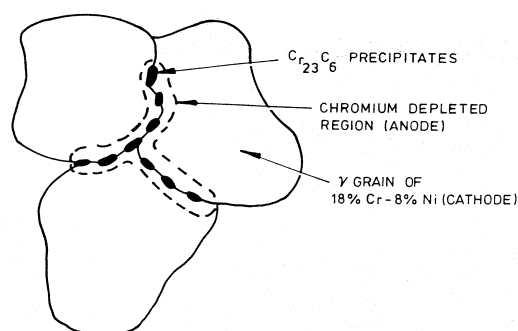

Figure 3.2. Carbide particles at grain boundaries leading to the setting up of electrochemical cell and grain boundary dissolution. (Ducheyne & Hastings, 1984).

3.3.3. Role of Corrosion on Mechanical Failure

Many alloys when subjected to the conjoint action of tensile stress and a corrosive solution will suffer cracking and premature failure. The process is a synergistic action since in

many cases both the stress level and the solution themselves are relatively harmless and only induce premature failure when acting together. Three basic examples of the phenomenon will be considered here, stress corrosion cracking (SCC), corrosion fatigue, and fretting corrosion.

3.3.3.1. Stress Corrosion Cracking

Stress corrosion cracking (SCC) is a general term describing stressed alloy failures that occur by the propagation of cracks in corrosive environments. SCC has the appearance of brittle fracture, yet it can occur in highly ductile materials. SCC requires the presence of a tensile stress, either residual, applied, or a combination of both, and the presence of specific corrosive entities (corrodent). The cracks form and propagate roughly at right angles to the direction of the tensile stress at stress levels much lower than those required to fracture the material in the absence of the corrodent. On a microscopic scale, the cracks that run across grain called "transgranular" and those that follow grain boundaries are termed "intergranular" (Sedriks, 1996).

The typical sequence of events in stress corrosion cracking of steel aptly depicted by Brown as consisting of the following stages: localized breakdown of the oxide film, crack nucleation from the pit, stress corrosion crack propagation and termination of crack by mechanical rupturing

Therefore, the failure of the intramedullary nail was a result of stress corrosion cracking due to the propagation of cracks radiating from a corrosion pit or pits. The crack was aggravated by the high inclusion content and large grain size of the implant (Sivakumar, 1992).

In 18Cr-8Ni stainless steel, failure can be either transgranular or intergranular, the latter frequently being associated with sensitized material. Transgranular cracks can, however, be initiated, by intergranular cracks. Elevated temperatures favor transgranular cracking in stainless steel so that care must be taken during sterilization procedures to avoid critical combinations of stress, temperature, and environment.

In titanium alloys, failure is transgranular and is due either to hydrogen embrittlement or a dissolution mechanism. Although chromium cobalt alloys are most unlikely to suffer from SCC in the body, premature failure can result due to the chemical sharpening of notches, which may already be present in the design of the component, cast chromium cobalt alloys in particular having very low resistance to notch impact failure.

SCC of stainless steels is dealt with in an attempt to understand the mechanism of failure. The suggested mechanisms can be categorized according to the following unit process thought to be responsible for the propagation of the stress corrosion crack.

There is basically two different unic process: (a) the removal of material at the crack tip and (b) the separation of the material at the crack tip. These unit processes provide the basis for the classification of the SCC mechanisms shown in the following list:

(a) Removal of Material by Dissolution or by Film Formation

Stress-Accelerated Dissolution: The crack propagates by dissolution of the metal along an active path. The role of plastic deformation is to accelerate the dissolution mechanism.

Brittle Film Rupture: The crack propagates by the repeated formation and rupture of a brittle film that grows into the metal at the crack tip. The crack is confined to the brittle film and does not extend into the metal.

Film Rupture Plus Dissolution: The crack propagates by repeated formation and rupture of a brittle film at the crack tip and by some dissolution of the adjacent metal before the film re-forms.

(b) Separation of Material

Hydrogen Embrittlement: The crack propagates by the mechanical fracture of a region weakened by hydrogen accumulation.

Adsorption: The crack propagates due to species absorbing and reducing bond strength at the crack tip.

Film Rupture Plus Mechanical Fracture: The crack propagates by the repeated formation and the rupture of a brittle film at the crack tip and by some mechanical fracture of the adjacent metal before the crack is arrested by the plastic deformation and the film re-forms.

3.3.3.2. Fretting Corrosion

Fretting corrosion is most probably a combination of abrasive and corrosive wear acting conjointly, and abrasion, caused by the entrapment of the worn off oxide film and oxidized wear particles between the surfaces, ruptures the oxide film, thus allowing further corrosion to occur.

Fretting is a small amplitude oscillatory movement that may occur between contacting surfaces and may cause surface damages. If a relative movement is the consequence of a cyclic loading of one or both the contacting components, fretting will act conjointly with the cyclic stress, and the fatigue strength of the component will be much reduced. This phenomenon is referred to as fretting fatigue. Since fretting fatigue is a surface phenomenon, engineering the surface to produce a hard and wear resistant layer is believed to be an effective palliative. Attempts have been made in the past to modify the contact surfaces so as to improve the fretting fatigue strength of materials. These investigations have ranged from traditional surface techniques such as electroplating, thermochemical treatments and cold working, to the modern surface coating and surface modification techniques such as PVD, CVD and ion implantation (Li , 2000). Fretting Corrosion is the combination of the surface degradation occurring due to relative oscillatory tangential slip of small amplitude between components and the action of a corrosive environment. The relative amplitude is low (< 75 µm) and relative velocities are much lower than in wear, giving rise to the trapping of fretting debris between the surfaces.

Mechanism of fretting corrosion:

Three mechanisms are thought to occur in fretting corrosion, the relative importance of each depending on the nature of the two surfaces and the circumstances:

Removals of metal particles from the cold welds, which are formed at the relatively few points of intimate metallic contact, are ruptured. This mechanism is similar to the process occurring when two metals slide in contact with each other,

which has been demonstrated by Bowden and Tabor. The subsequent oxidation of the metal powder to the oxide is assumed to play no part in the process.

The metal particles initially produced by the first mechanism are oxidized to a hard abrasive oxide, and the action is further intensified by this abrasive.

The continual rupturing of oxide films on the surface, which, in the absence of any mechanical disturbance, would be protective. The clean metal, which is continually being exposed, is highly deformed and therefore more chemically active.

Corrosion fatigue and fretting corrosion are both to some extent the result of increased chemically activity brought about (a) by the rupture of oxides films on the surface, and (b) the altered electrode potential, and possibly chemical potential, of plastically deformed metal (Fuchs, 1980).

In stainless steel implants, fretting corrosion produces scars with a pitted or granular appearance as distinct from the more polished wear traces. Angular corrosion pits are found at the periphery of the fretting scars. Deep corrosion tunnel-pits are observed in some scars, and chemical attack occurs along selected crystallographic planes leading to etch pitting,

By contrast, chromium-cobalt-molybdenum alloys show evidence of polished scars, cor-rosive activity varying from intense local attack to more general corrosion. The scars possess a rippled appearance possibly caused by grooves worn in the material by an abrasive wear process. Some grooves may contain fine rounded particles, possibly the result of a breakup of brittle carbide particles exposed to the fretting surface.

Titanium alloys possess poor wear properties and finely divided metallic titanium is believed to be a product of the wear process. Fretting scars have a plowed appearance rather than polished or pitted, and cratering may also be observed.

3.3.3.3 Corrosion Fatigue

A material subjected to repeated stress cycle may be susceptible to fatigue cracking, depending on the amplitude and the number of the stress cycles. If the material is also exposed to a corrosive environment, then the fatigue cracking may be accelerated as a result of a process termed corrosion fatigue.

The process of failure by corrosion fatigue comprises two stages. During the first stage the combined action of corrosion and cyclic stresses damages the steel by pitting and crack formation to such a degree that fracture by cyclic stressing would occur ultimately even if the corrosive environment were removed altogether. The second stage is essentially a fatigue stage in which failure proceeds by propagation of the crack and is controlled primarily by stress concentration effects and physical properties of the steel (Uhlig, 1955). General aspects of corrosion fatigue of 316L are dealt with in details in Chapter 3.4.4.

Factors Influencing Corrosion Fatigue:

The corrosion fatigue properties of a material are naturally closely linked with its corrosion resistance. In general it is found that pure metals and solid solutions are superior to compositions containing two or more phases. The fatigue curves for the first two are almost identical in corrosive and non-corrosive environments.

The extent of the damage depends on the corrosive nature of the environment. Ordinary dry fatigue in air may be regarded as corrosion fatigue under rather mild conditions. Tests carried out on various materials in a partial vacuum showed that the fatigue properties were improved, a fact which has been confirmed in tests performed with the test piece immersed in a oil, covered with grease, and painted with rubber solution.

A mean compressive stress applied to the specimen during test results an endurance limit similar to the normal fatigue strength. The pressure tends to heal up cracks, which develop in the oxide film, and so to limit electrochemical corrosion. A compressive stress can therefore be regarded as making the metals and/or alloys nobler.

Corrosion is a chemical process and the amount of material removed depends on the length of time that the specimen is in contact with the corrosive. Since corrosion fatigue endurance limits are quoted for a given number of cycles, it is obvious that the lower the frequency of the applied stress the longer the specimen is in contact with the corrosive. Endurance limits are, therefore, very dependent on frequency, in contrast to normal fatigue where frequency effects are slight.

3.3.4. Contribution Factors on the Corrosion Process

The following features are frequently contributory factors in the initiation or acceleration of the corrosion process:

3.3.4.1. Effect of Metallurgical Variables

As type AISI 316L, the principal austenitic stainless steel used for surgical implant applications, is susceptible to corrosion in aqueous environments, it is of paramount importance that the chemical composition is maintained within the specifications laid down by the various standards organizations. The amounts of chromium, molybdenum, carbon, and nickel present in the steel are all important if the material is to have adequate corrosion resistance. The presence of molybdenum within the limits of 2.0 to 4.0% is of the greatest significance.

Variations in the nickel content affect both mechanical properties and the corrosion resistance. Reducing the concentration of nickel increases the possibility of galvanic corrosion in multicomponent devices. As discussed earlier, this phenomenon is not restricted to different materials, but may occur when components, made from different compositions or with different microstructures, are in electrical contact. This frequently occurs in bone plates and screws, where manufacturing techniques involving cold deformation can lead to martensitic transformations in screws which may then corrode preferentially when in contact with the austenitic plate. This process would be reduced if the nickel content were kept above 11% as it retards the martensitic transformation. High nickel contents, however, may result in .screws of inferior mechanical properties due to the associated decrease in work hardening rate. These two effects of nickel concentration may imply that the range of concentrations allowed should be reduced. Concern for the corrosion properties of the steel has been shown by the increase in recent years in the minimum concentration of nickel allowed in the steel by BSI from 8 to 10%, although this may still be "top low" as 11% is felt by some workers to be a critical concentration. Very few cases of steel depleted in chromium have been reported possibly

because this element is standard to all stainless steels.

3.3.4.2. Incorrect Metallurgical Condition

When considering incorrect metallurgical condition, sensitization, which has been discussed previously, is of paramount importance. A continuous network of grain boundary precipitates provides a path for corrosion and a means of deep penetration of the implant. Removal of whole grains may occur, resulting in serious weakening or fracture.

3.3.4.3. Poor Design and Use of Implants

Poor design or the incorrect use of implants is principally apparent in multicomponent devices, leading to the formation of crevices and notches which then promote corrosive attack. Bone and nail plates present particular problems in this area due to the multiplicity of design combinations available for plates and screws.

Although the design of the threadform would appear to have little effect upon corrosion behavior, the surface finish is of paramount importance, with electropolishing being necessary, especially if a thread rolling technique has been used, which may lead to a highly work hardened surface containing inclusions, folds, and rakes.

Many design problems relate to interfaces which can result in crevice formation, pitting attack, or fretting corrosion. Components which have many points of contact frequently exhibit evidence of corrosive attack. Reducing the amount of corrosion could be achieved either by redesigning the component, minimizing the number of

points of contact, or by manufacturing it from a material less susceptible to pitting corrosion.

3.3.4.4. Effects of Surface Finish

There are two aspects of surface finish which are of importance to corrosion studies. These are the effects of surface treatments or blemishes upon the propensity for corrosive attack and the probability of initiating corrosion-stress interrelated phenomena.

One of the most important surface treatments applied to stainless steel implants is passivation in nitric acid which has long been recognized as giving improved corrosion treatment. The process which is also applied to titanium alloys and which has the additional advantage of removing any iron particles which may have become embedded in the implant surface during polishing consists of immersion in a 30% nitric acid solution at 40 to 60°C for approximately 15 min. More recently, it has been proposed that passivating in oxygenated isotonic saline solutions can give enhanced corrosion resistance.

Polishing either by mechanical or electrochemical methods is frequently used to improve the surface finish. The latter gives a superior corrosion resistant surface, possibly due to the method and nature of the treatment. Mechanical polishing leaves a slightly work hardened layer on the surface, while electropolishing (which may be regarded as a controlled electrochemical corrosion process) preferentially removes high energy atoms, for example, kink sites or ledges, which might be expected to undergo accelerated attack.

After polishing, the effects of isolated scratches incurred, for example, during handling or insertion, depend significantly upon their position on the implant and the ability of the damaged area to repassivate. Where repassivation is possible, only a short-term increase in the corrosion rate would be expected. If, however, the damage were in a crevice a permanent site of attack might result. A further factor to be considered is how the scratch was formed; contact with a harder material, for example, leads to the possibility of fretting corrosion, metal transfer, and galvanic attack.

Surface finish is also of considerable importance when considering resistance to corrosion fatigue or SCC. Fatigue crack initiation is a surface phenomenon and usually occurs in a region of maximum stress. Once a crack has initiated it will, in most circumstances, continue to propagate until complete failure of the device occurs. Any surface defect, for example, polishing or grinding marks, may be sufficient to promote cracking if it occurs in a region of high stresses. The effect of the defect may be to act as a pre-crack or stress concentrator, increasing the stress intensity at that point. Examples have been noted of surface defects which have initiated fatigue cracks, notably in stems of artificial hip joint prostheses.

Lack of appreciation of the above has led to occasional examples of cracks starting at defects deliberately introduced into the implant in highly stressed regions. Two cases have been reported of failed artificial hip joint prostheses which have broken on the stem due to cracks initiated at spark-etched trade marks on the lateral surface of the stem in the region of the maximum stress. Marks induced by this method produce very sharp notches which consequently have large stress-raising effects. These examples together with other design features such as sharply notched serrated edges, sharp corners, and sharply curved edges, may all serve as suitable stress concentrations to damage the oxide film and so help initiate corrosion fatigue or SCC.

The incidence of failures is low, but what emerges from many of the examples of components that have failed due to excessive corrosion is that in many cases the factor or combination of factors which contributed to the attack could have been avoided. Failure to produce steel to the required compositional standards or in the required metallurgical condition implies insufficient control over the manufacturing processes and ineffective quality control which allows such implants to be passed as satisfactory. Quality control can also be questioned when surface defects in highly stressed regions remain undetected. Improvements in the quality of implants are being achieved as realistic standards are being produced and as a result of the cooperation and understanding being achieved between surgeons and materials engineers.

Marking of implants in highly stressed regions and in such a manner as to produce sharp notches indicates a deep-rooted lack of understanding of the problems involved which can only be overcome by increased awareness by all involved with surgical implants of the principles governing the mechanical properties and corrosion behavior of the product when in service. Where failure is the result of poor component design or incorrect material selection, the remedy lies with ion product and improvement or use of a different alloy. In this area, new designs are continually being adopted frequently using computer aided designs. A detailed program of standardized testing may be required to prevent the large-scale production of implants containing fundamental design faults or which utilize unsatisfactory material. The frequency of failed devices due to excessive corrosion can be reduced, but only by greater vigilance and effort by all associated with surgical implants (Ducheyne & Hastings, 1984).

3.4. Fatigue

Fatigue is the progressive, localized; permanent structural change that occurs in materials subjected to fluctuating stresses and strains that may result in cracks or fracture after a sufficient number of fluctuations. Fatigue fractures are caused by the simultaneous action of cyclic stress, tensile stress and plastic strain. If any one of these is not present, fatigue cracking will not initiate and propagate. The cyclic stress starts the crack; the tensile stress produces crack growth (propagation).

The process of fatigue consist s of three stages:

1. Initial fatigue damage leading to crack nucleation and crack initiation,
2. Progressive cyclic growth of a crack (crack propagation) until the remaining cross section of a part becomes too weak to sustain the loads imposed,
3. Finally, sudden fractures of the remaining cross section.

Fatigue cracking normally results from cyclic stresses that are well below the static yield strength of the material. (In low cycle fatigue, however, or if the material has an appreciable work-hardening rate, the stress may also be above the static yield strength).

It would seem, therefore, that surface cracking could occur in any of three ways, namely, as a continuation of surface roughening in broad slip bands, as a result of severe strain incompatibilities across grain boundaries, or because of the presence of inclusions or inhomogeneities in the surface. The type of cracking that occurs will depend on material, stress level, and environment, if the grain boundaries or

inclusion-matrix interfaces can sustain the imposed strain incompatibilities across them without cracking, microcracks will develop from slip bands.

Fatigue cracks initiate and propagate in regions where the strain is most severe. Minimizing these strain concentrations must be the first rule for avoiding fatigue failure. Real structures contain discontinuities, which may develop into cracks with applications of stress, progressive crack extension following up to final failure. Because most engineering materials contain defects and thus regions of stress concentration that intensify strain, most fatigue cracks initiate and growth from structural defects. Under the action of cyclic loading, a plastic zone (or region of deformation) develops at the defect tip. This zone of high deformation becomes an initiation side for a fatigue crack. The crack propagates under the applied stress through the material until complete fracture results. On the microscopic scale, the most important future of the fatigue process is nucleation of one or more cracks under the influences of reversed stresses that exceed the flow stress, followed by development of cracks at persistent slip bands or at grain boundaries (Boyer, 1986).

Final catastrophic failure occurs when a crack has grown to a critical length such that the next application of load produces static failure of the remaining net section. Under service conditions of variable amplitude loading, the critical crack length must be defined of course, in terms of the highest expected load and the total load spectrum. Redundant structures, i.e. structures designed with "crack arrestors" stopping the rapid growth of critical cracks before they weaken the integrity of the total structure, represent an important advance in fatigue design based on the previously described crack growth mechanisms (Dieter, 1988).

In the presence of stress concentration, enhanced fatigue hardening will occur in proportion to the stress or strain concentration factor. One can expect this enhancement in the vicinity of notches, fasteners, welds, and most importantly, near the tip of a fatigue crack.

3.4.1. Initiation of Fatigue Cracks

The general and basic features of fatigue failure are the initiation of surface microcracks and their subsequent extension across and penetration into the body of the metal. The onset of damage and cracking is associated with the surface grains, only those grains in the body of a specimen through which a crack, formed in a surface grain, passes as it grows across the specimen being damaged (Frost, 1974). Defining a crack in terms of the highest resolving power instrument available (the electron microscope for instance) it is possible to establish a number of load cycles N_I, to generate an observable fatigue crack. It is usual to express the result in terms of the fraction of total life, N_I/N_T. It has been shown that this ratio is normally a small number in unnotched members, about 0.1, so that fatigue crack propagation occupies a large percentage of total life.

Fatigue cracks always begin at concentrations of plastic strain. Consequently if no other manufacturing imperfections are present fatigue cracks have their origins at the surface. The so-called slip band formation, extrusions and intrusions on the surface of an otherwise uncracked material form fatigue crack initiation sites.

An important structural feature which appears to be unique to fatigue deformation is the formation on the surface of ridges and grooves called slip-band

extrusions and slip-band intrusions. Wood, who made many basic contributions to the understanding of the mechanism of fatigue, suggested a mechanism for producing slip-band extrusions and intrusions. Figure 3.4 illustrates Wood's concept of how continued deformation by fine slip might lead to a fatigue crack. Slip produced by static deformation would produce a contour at the metal surface similar to that shown in Figure. 3.3. In contrast, the back-and-fro fine slip movements of fatigue could build up notches or ridges at the surface. The notch would be a stress raiser with a notch root of atomic dimensions. Such a situation might well be the start of a fatigue crack. This mechanism or the initiation of a fatigue crack is in agreement with the facts that fatigue cracks start at surfaces and that cracks have been found to initiate at slip-band intrusions and extrusions.
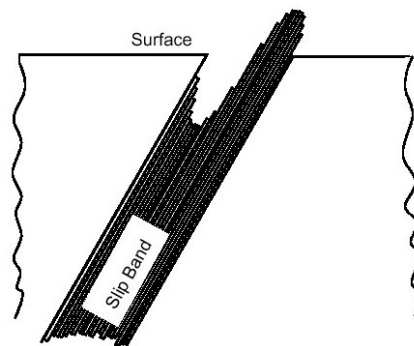
Figure 3.3. Notch-Peak geometry of slip
bands at a free surface.

In general, slip lines formed under static loading appear, under low and moderate magnifications, as sharp, straight lines and are distributed evenly over each grain. Under high magnification, the individual lines appear as bands of parallel lines of various heights. The slip lines produced under cyclic stressing form in bands, which do not necessarily extend right across a grain, new slip lines forming beside old ones as test proceeds, the intervening regions between the bands being apparently free from slip.

The increased life resulting from the removal of a surface layer at frequent intervals throughout a test, respective of whether the life is many millions or only a few thousand cycles demonstrates that crack initiation is confined to the surface grains. Electropolishing removed the roughness associated with a slip band, and most of them became visible. A few, however, became accentuated and were termed "persistent slip bands"; fatigue cracks grew eventually from these bands. If the polishing was continued until the persistent bands were removed, it was found that, on retesting, the slip bands reformed and became persistent. These persistent slip bands are embryonic fatigue cracks, since they open into wide cracks tend to propagate initially along the slip planes.

The fact that the initiation and development of microcracks are a consequence of cyclic plastic strain means that whether or not they form is dependent on the magnitude of the resolved maximum cyclic shear stresses in the loading cycle. Thus, the addition of a mean stress does not have a marked effect on the cyclic shear stress necessary to initiate a microcrack, and therefore they are able to form under a wholly compressive loading cycle. A compressive mean stress, however, tends to prevent a microcrack opening and so retards its development to the macrocrack stage. Of course, if the loading cycle is such that the crack faces are never opened, cracks can only keep developing as microcracks (provided the cyclic stress level is sufficiently high); they cannot grow as macrocracks. The introduction of surface compressive stresses of sufficient magnitude and depth therefore increases the fatigue strength of a specimen as a whole. On the other hand, a tensile mean stress tends to open in crack and so enhances its development to the macrocrack stage.

Under high amplitude loading fatigue cracks start at grain boundaries. In many commercial alloys the existence of large second phase particles, inclusions, play a

predominant role in crack generation. They cause localised plastic deformation leading to cracking usually at the inclusion matrix interface. Other flaws such as internal voids or large surface scratches may be the sites of fatigue crack generation. Such flaws need only the application of cyclic load to begin their growth as real fatigue cracks.

The combination of fatigue stresses and even a mildly corrosive environment accelerates the time for crack generation. The effects on later crack growth are even more pronounced. Previous load history can have two effects. First, if the material has been hardened, the yield stress is increased, and under constant stress conditions, the time to generate a crack would be increased. Secondly, prior loading can produce significant residual stresses at the root of a notch. For example prior tensile stress will leave a compressive residual stress, and cracks at the notch root will be very slow in developing compared to the annealed state. A similar situation may arise by superimposed stress conditions such as mean stresses due to external loads or to residual stresses. Treatments such as shot peening are used to induce compressive residual stresses on surfaces, so that N_I can be significantly increased.

There is indication that cracks must reach a minimum critical size before they can begin propagating. Nonpropagating microcracks, which have been observed at very low stress amplitudes, may be examples of cracks, for which the generation mechanism ceased to operate before they reached critical size. The value of N_I/N_T is dependent of the load amplitude, specimen geometry, material properties, the temperature, previous loading history, and the environment. The value of N_I/N_T decreases with increasing load amplitude, so that in the extreme low cycle range the entire life is consumed in crack propagation and in the extreme high cycle range a substantial portion of the entire life is consumed in crack initiation.

3.4.2. Growth of Fatigue Cracks

The direction of crack growth is now that which allows the maximum crack opening and closing during the fatigue cycle. Ideally, this approximately perpendicular to the nominal maximum cyclic tensile stress and is independent of any crystallographic plane close to the ideal direction. The crack can now be termed a macrocrack; its growth rate is much faster than that of the initial microcrack, and it now spreads rapidly through the metal. The brittle appearance of a fatigue fracture follows from the fact that, during the macrocrack growth stage, the cyclic plastic strain occurring at any instant (at stress levels less than those causing general yielding) is confined to the small volume of material just ahead of the crack front.

Crack propagation occupies a major portion of fatigue life, especially at high load amplitudes. Final failure may be the result of the growth of one crack, or of many small cracks coalescing into a final crack. The higher the load amplitude, the more likely the production of multiple cracks. Corrosive environment also produces multiple cracking and accelerates failure.

There are two main stages of fatigue crack growth. The stage I crack propagates initially along the persistent slip bands. In a polycrystalline metal the crack may extend for only a few grain diameters before the crack propagation changes to stage II. Cracks forming in slip bands propagate along the active slip planes, which are inclined at ±45° with respect to the tensile stress axis. This shear mode propagation, Stage I growth, tends to continue more deeply into the specimen the lower the amplitude of loading. The crack soon begins to turn and follow a course perpendicular to the tensile axis. This tensile mode propagation as called Stage II

growth, characterizing crack growth up to the critical length for which the next load peak produces tensile failure of the specimen.

Actually, the Stage I growth in a polycrystalline material involves hundreds of individual slip band cracks linking up to form a dominant crack at about the time when stage II growth begins. Stage II crack growth life increases with increasing load amplitude. Cracks formed at inclusions grow only a few micrometers in Stage I before changing to the Stage II mode. At low stress or strain amplitudes, very few inclusion cracks are generated and one such crack may grow all the way into the final failure crack. At higher amplitudes several inclusion cracks may joint together to form the final crack.

Examination of fracture surfaces tells us a lot about the mechanism by which the crack advances. For all practical purposes the entire fracture surface formed is governed by the Stage II mode. Very near the crack nucleus, while the crack length is still small, conditions of plane strain hold at the crack tip. The fracture surface is microscopically flat and oriented perpendicular to the tensile axis. As the crack grows in length a shear lip begins to develop where the fracture surface intersects the specimen surface. This reorientation of the fracture surface to a 45° position with respect to the tensile axis is caused by the plane stress conditions at the crack tip intersecting the surface. As the plastic zone in front of the crack tip increases in dimension to become comparable to that of the specimen thickness, plane stress conditions hold everywhere at the crack tip and the fracture surface is one continuous shear lip or double shear lips. The flat, plane strain surface is especially rich in detail, exhibiting regularly spaced striations, even visible at optical magnification. Each striation represents the crack advance for one cycle of load and this was verified experimentally.
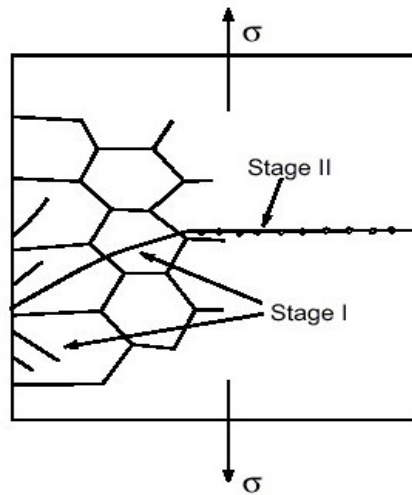
Figure 3.4. Stage I and II fatigue crack growth

By marked contrast the fracture surface of stage II crack propagation frequency shows a pattern of ripples or fatigue fracture striations. Each striation represents the successive position of an advancing crack front that is normal to the greatest tensile stress. Each striation was produce by a single cycle of stress (Figure 3.5).
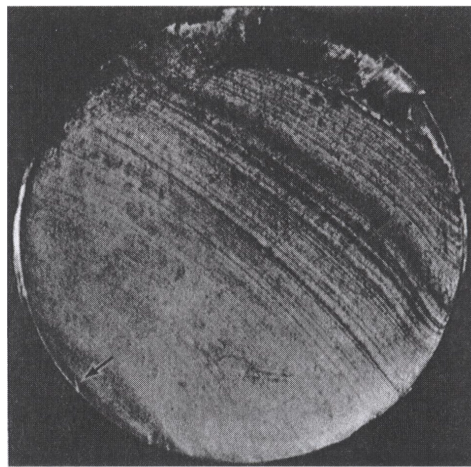

Figure 3.5. Beach marks on fatigue surface.

Stage II crack propagation occurs by a plastic blunting process that is illustrated in Figure 3.6. At the start of the loading cycle the crack tip is sharp (a). As the tensile load is applied the small double notch at the crack tip concentrates the slip along planes 45° to the

plane of the crack (b). As the crack widens to its maximum extension (c) it grows longer by plastic shearing and at the same time its tip becomes blunted. When the load is changed to compression the slip direction in the end zones is reversed (d). The crack faces are crushed together and the new crack surface created in tension is forced into the plane of the crack (e) where it partly folds by buckling to form a resharpened crack tip. The resharpened crack is than ready to advance and be blunted in the next stress cycle. Cross sections comprising the crack

tip formed at various parts of a load cycle have established that Stage II growth occurs by repetitive blunting and re sharpening of the crack tip (Colange & Heiser, 1987).

The effects of multiple load amplitude can be best understood in terms of crack tip plastic deformation. The two important concepts are localized work hardening and localized residual stresses at the crack tip.
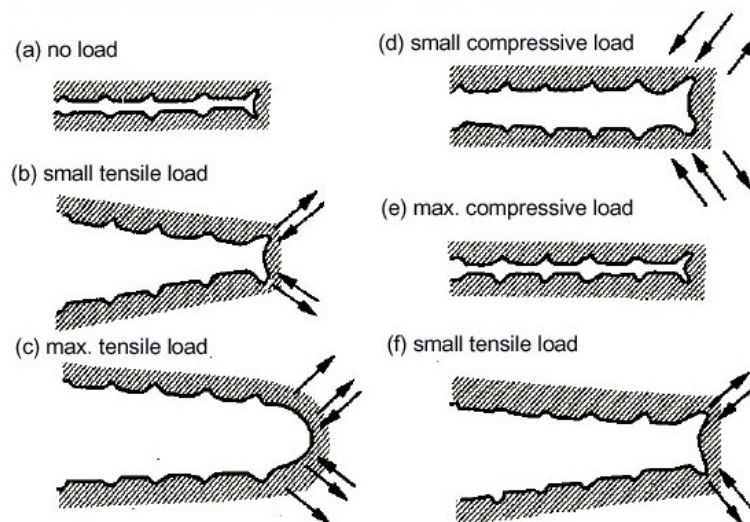
Figure 3.6. Fatigue crack growth by the plastic blunting mechanism.

Intermittent overloads can delay the subsequent growth of cracks at lower loads. On the other hand, such overloads are capable of generating new cracks, which can

then grow on the lower amplitudes. The overall effect would be to shorten the effective service life of the member by linking together many individual cracks generated in this manner. An opposite case is the so called "coaxing", in which fatigue at low amplitudes followed by high amplitudes leads to longer, overall lives, even though such a sequence can produce growth rates larger than normal crack. In this case nucleation of cracks is suppressed by the coaxing procedure, which hardens the surface layers.

3.4.3. Fatigue Failure of Stem

Although successful, total joint replacements do also fail. One of the reasons of clinical failure is fatigue fracture of the metal stem (Ducheyne , 1983). A common precursory mechanism to fatigue failure is loosening of the femoral component. The problems of loosening and fatigue failure of the stem are closely interrelated.

While several methods are presently being worked out to improve the long-term fixation of permanent implants, it is obvious that attention should still be focused on the availability of hip prostheses with sufficient mechanical properties. Most manufacturers realized this aspect soon enough and came up with solutions which basically can be divided into three groups:

a) use a prostheses material with a high fatigue limit
b) use a prostheses design with a large cross section and thus a higher bending moment of inertia; and
c) use a prostheses material with a lower modulus of elasticity.

Stem fracture usually occurs after proximal loosening with loss of medial support of the stem (Desmond , 1993). Fatigue failure of the stem is the product of repetitive cyclic load, which is normally initiated at a site of high tensile stress that usually resides at the lateral surface of the stem. Cracks usually start at places where the stress is concentrated, that is, at a defect such as a scratch, notch, or void.

Fracture is the result of "excessive tensile stress" at the lateral surface of the prosthesis owing to the bending moment and the load (patient's weight and activities), it is important to consider the geometrical factors that may contribute to its appearance. They are as follows:

1.The neck shaft angle of the prosthesis; that is, the smaller the neck shaft angle, the greater the stress.

2.The neck length; that is, the longer the neck the greater the stress.

3.The orientation of the stem in the canal; that is, the greater the angle of varus, the greater the stress (Eftekhar, 1990).

In a two-dimensional stress analysis, the effect of some of the factors leading to early fatigue failure of the femoral stem in total hip arthroplasty was studied. This led to a similar conclusion: loss of proximal stem support at the level of the calcar femoral resulted in a level of stress on the stem that led to fatigue failure. The load (body weight) and the range of cyclic stress played an important part in fatigue life under test conditions. Increasing the stem dimension at the middle-third level of the stem (the critical level, where maximum tensile forces are found) was suggested, although it should be emphasised that static testing in laboratories might oversimplify the three-dimensional geometry of the stem and the forces

applied to it as they occur in the body. So this model would only partially explain the early failure of the metal.

Consequently, based on the clinical analysis of stem failures today, one may search for the cause of failure in the following categories: excessive load, failure of support by the bone, loss of fixation at the cement-bone-metal interface, uneven stress distribution throughout the cement column, metallurgical causes, and failure of surgery.

3.4.3.1. Failure Modes of Hip Stem

Classification of the modes of failure cemented stem-type femoral components is as follows;

3.4.3.1.1. Mode I: Pistoning Behaviour. This mode is characterized by pistoning of one material with respect to another, i.e. metal stem pistoning within the acrylic cement embedded stem pistoning within the bone (mode Ib). Mode Ia occurs as a result of incomplete cement encapsulation or subsequent loss of proximal-medial acrylic support from axial loading which tends to result in the stem being displaced distally. Close examination of the acrylic sheath indicates sufficient encapsulation everywhere except in the lateral midstem region allowed mode Ia to occur.

In mode Ib the applied stresses tend to disrupt the mechanical bond at the cement-bone interface with subsequent slip. This may be enhanced by inadequate interdigitation of acrylic cement into cancellous bone. This mode is the most familiar to orthopedic surgeons of loose total hip replacements.

3.4.3.1.2. Mode II: Medial Midstem Pivot. This mode is characterized by medial migration of the proximal stem coupled with lateral migration of the distal stem tip. It is caused by combined weak proximal-medial "calcar" support and lack of distal acrylic support. The loss of distal support may also occur following the distal punch-out of acrylic cement in cases of mode Ia failure. The progression continues with simultaneous proximal-medial migration and distal stem toggling followed by subsequent fracture, in some cases, of acrylic cement in the midstem region.

3.4.3.1.3. Mode III: Calcar Pivot. The action of this mode is a medial-lateral toggle of the distal end of the embedded stem due to lack of distal acrylic support with subsequent bone reaction. The prosthesis may have adequate proximal support or "hang up" on the medial femoral neck cortical rim upon which its pivot. This mode is analogous to the "windshield type" loosening of uncemented Austin-Moore or F.R. Thompson femoral head prostheses, where the large stage of these prostheses pivoted upon the transected femoral neck cortical rim and the distal part of the stem toggled within the intramedullary cavity.

3.4.3.1.4. Mode IV: Bending Cantilever Fatigue. This mode is characterized by partial or complete loss of proximal support with subsequent stem while the distal end remains rigidly fixed in acrylic cement encasement or from proximal cement-bone interface, the load transfer to the proximal femur is lost and the stem is then, consequently, transformed into a cantilever which must resist increased cyclic bending stresses (Jones, 1992).

3.4.3.2. Contributing Factors on Fatigue Failure of the Stem

There are five factors considered that contributed to the fatigue failure of the stem: cementing technique yielding inferior cement properties; varus position of the femoral component; the prostheses material; the weight of the patient, and the lack of support at the level of the calcar femoralis (Ducheyne, 1983).

3.4.3.2.1. Loss of Fixation. As indicated earlier, the most important cause of stem failure is initiation of the loosening of the prosthesis in the shaft, especially in the upper region (with the medial side of the prosthesis at the calcar region). Although most loosening may not terminate in failure by stem fracture, retrospective examination of most cases reveals early loosening before stem fracture. Improper cementing, that is, varus orientation of the stem and lack of support by the cement at the concave side of the prosthesis (in the compression side), increases stresses on the metal and the cement as well as the bone, leading to failure of fixation in this region.

Experimental studies coupled with studies of clinically failed prostheses can help determine the area of high-stress concentration and the location of the fracture. In both clinical and laboratory situations, loss of fixation by the cement precedes failure of metals; therefore it seems reasonable to assume that paying attention to the technical details of insertion and producing adequate support for the prosthesis at the calcar region to eliminate loosening are the first lines of defence against fatigue fracture.

If both proximal and distal fixation were poor, the femoral component would be expected to fail by subsiding. However, if the component is firmly fixed distally, so
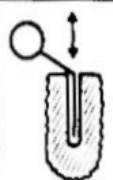
I	Ia	Pistoning: Stem within Cement	
	Ib	Pistoning: Stem within Bone	
II		Medial Midstem Pivot	
III		Calcar Pivot	
IV		Bending Cantilever (Fatigue)	

Figure 3.7. Schematic diagram of the 4 modes of failure characterizing the various mechanisms of hip stem**.**

that it is not free to subside, but there is poor fixation which allows movement proximally, it would be liable to bend under the influence of excessive load. Jones concluded that their results are consistent with the accepted mechanism that stem fracture of proximal fixation, while distal fixation is maintained suggesting that stem fracture can be avoided by careful fixation and the selection of appropriately sized prostheses.

3.4.3.2.2. Varus Position. Only few anatomical differences were founds between the fracture and loose groups. Patients with fractured stems were reported to be

significantly heavier than those with loose stems by an average of 10 kg. Features, which were determined by surgical technique, showed greater differences between the two groups. A significant difference in stem alignment was indicated such that; the fracture group tended to be inserted varus while loose group was in valgus. Valgus and varus were used to describe the inclination of the femoral component stem in the coronal plane, relative to the femur and are defined in Figure 3.8. Previous studies indicated that, the fractured stems were significantly more medial at the proximal, mid-stem and distal levels, but not at the stem tip. In keeping with the valgus inclination, the loose stems had significantly thicker medial cement at the proximal level. In the fracture group, the lateral cement thickness was found to be greater at the mid-stem and distal levels (Jones , 1992).
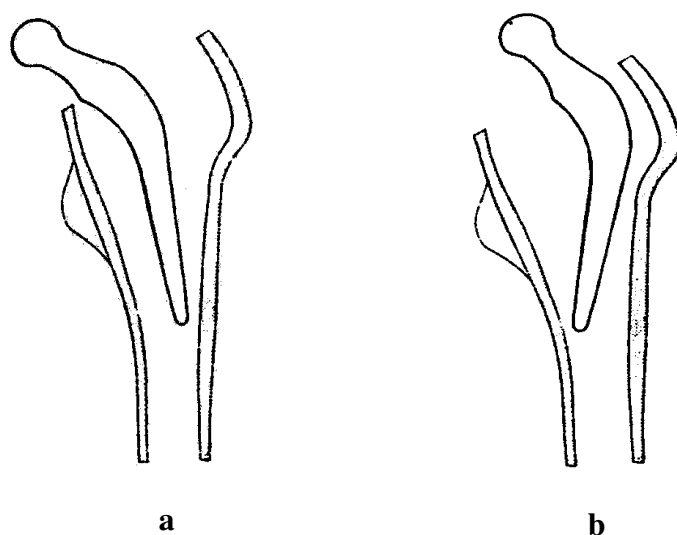
Figure 3.8. Schematic diagram showing; (a) a stem in varus,
 (b) a stem in valgus.

3.4.3.2.3. Metallurgical Causes. Fatigue is an engineering term used to describe the failure of material by a fluctuating stress, which if applied a sufficient number of times, produces failure in the material. The stress required to produce failure is often much lower than that required to fracture the same material on a single application.

While this principle is applicable to most machine elements and laboratory tests may produce the basic information regarding fatigue properties of the materials, the stress cycles that cause fatigue failure in biological situations are usually extremely complex. The gross appearance of a fatigue-fractured surface of a metallic component such as the stem of a total hip prosthesis shows two distinct regions: (1) a relatively smooth surface area with concentric markings described as clamshell, beach, or ripple markings, and (2) a surface area of rough granular appearance with the appearance of a cross-section of a multifilament cord. The smooth area indicates slow propagation of the fatigue cracks, and the rough zone indicates the brittle, ruptured final fracture zone.

A new alloy used in Europe and the United States is a combination of cobalt, nickel, chromium, and molybdenum known as Protosul10 or MP36N. This alloy is made in a "multiphase" state. The mechanical properties of this alloy are outstanding with yield strength of 400 MPa when fully annealed with elongation of 70%. With work hardening, and heat treatment, the yield strengths rise to 2000 MPa with only 10% elongation. These characteristics make MP36N an ideal alloy, combining the good properties of stainless steel and chromium-cobalt.

A study of 35 stainless-steel and chromium-cobalt-molybdenum alloy devices showed that a very large numbers were defective or deficient; the effects were caused by the presence of delta-ferrite in 316L stainless steel, porosity in the cast-chromium alloy, and the presence of cracks and pits and in some instances a low molybdenum content in the steel. A number of other mechanical explanations have been proffered for the failure of metal in orthopaedic surgery. A brittle fracture owing to stresses exceeding the ultimate strength of the material, the use of an alloy not resistant to corrosion, brittle fractures as the result of combined mechanical and electrochemical

defects, impact loading, fatigue crack propagation of 316L stainless steel, and weakness of the bone in the region of the femoral calcar. The effect of grain size on the fatigue life of 316L stainless steel has not been established, but it may be a significant factor in determining the strength of the stainless steel used for the stem of the femoral component. It is possible that a fine grain size is preferable and that a fine and uniform grain size could be maintained by manufacturers, Galante (1975) feel that strings of shrinkage porosity in cast chromium and cobalt alloy should be considered flaws. When string length approaches an appreciable fraction of a millimetre, it must be considered as a progenitor of early failure, and large amounts of shrinkage porosity could impair the strength of the metal. Obviously maintaining the highest standards of microstructural quality in the metal used in the stem of the prosthesis is imperative.

In regard to metallurgical studies, the main morphological characteristic of most of these fractures is obviously fatigue. Failure, but in most of the cases examined so far, a premature fatigue failure was largely observed, probably because of a combination of circumstances. These include inadequate quality controls in manufacture and flaws in the metallic structures; for example 316 annealed stainless steel is unsuitable for a femoral stem, since this material can be expected to weaken under loading conditions; wrought cold-worked 316 stainless steel should be the material of choice when stainless steel is used.

3.4.3.2.4. Excessive Load. Fatigue fracture of the femoral prosthesis was reportedly assumed to be the product of a "successful arthroplasty" in a heavy, athletic, active patient in which the dimensions of a standard prosthesis have been used. The valgus position of the prosthesis, while important in reducing bending stresses, is assumed inadequate to eliminate the fracture. The support of the prosthesis by the cement on

the medial aspect is most important; use of an extremely heavy stem in the upper portion automatically reduces the amount of cement used, inviting further loosening problems that can initiate fatigue fractures. The anatomical advantages of a 130-degree shaft-neck angle are great enough to warrant its sole use in patients with a huge bony structure, to allow clearance between the neck and rim of the acetabulum. Obviously, heavier prostheses have now been designed for people who anticipate excess load from their weight or excess stress from the degree of their activities.

3.4.3.2.5. Failure of Support by Bone. The loss of support by the bone is now assumed to provide a substantial evidence for a fundamental cause of the failure of cement fixation in the calcar region, leading to eventual failure of fixation at the concave side of the stem. Therefore from histological evaluation of the calcar region, it seems reasonable to suggest that the cystic erosion of bone in this region is caused by slight movement between the cement and the bone. With the stress concentration at the calcar region and cement fragmentation causing tissue reaction such as bone resorption and necrosis, further varus subsidence of the prosthesis follows; the similarity between the periodontal disease and bone necrosis with the loosened cemented prosthesis is striking. In both in-stances, once loosening begins a vicious cycle is created. The cement loses support and permits increased motion in the upper end of the prosthesis between the bone and the calcar at the concave side of the prosthesis, while the remainder of the prosthesis (the distal portion) may remain fixed in the bone. To solve the problem, surgical technique was suggested as such that should include, in addition to a slight valgus orientation for the prosthesis, removal of the loose cancellous bone of the calcar region to provide strong support by the cement. Poor support by the bone, despite a valgus orientation of the stem, has been occasionally observed (Azem, 1999).

3.4.4. Corrosion Fatigue of 316L Stainless Steel

When metallic materials are placed in the body two points of view may be considered. One is the effect of the corrosive environment upon the metal and its corrosion products upon the fluids and tissues of the surrounding environment (Bement, 1971). The environment of the body may not appear at first sight to be particularly aggressive. It is an aqueous environment, extremely well buffered so that the pH is maintained around 7.4 and it is held at a constant temperature of 37 ^{o}C. Two features control the corrosivity of this environment. Firstly, the saline solution is an excellent electrolyte and facilitates electrochemical mechanisms of corrosion and hydrolysis. Secondly, there are many molecular and cellular species in the tissues, which have the ability to catalyze certain chemical reactions or rapidly destroy certain components identified as foreign. Corrosion of metals within the body occurs by conventional and largely predictable mechanisms.

One of the main reasons for concern about fatigue of biomaterials arises from the adverse host-tissue response to wear debris generated by fatigue process. This appears to be a natural defence mechanism of the body. The wear debris often invokes an inflammatory and immunological response. This in turn cases blood clotting processes, leukocytes, macrophages and, for severe cases, giant cells to move in on the foreign particles resulting in interfacial problems between the implant and the host tissue. Numerous biochemical activities occur at this stage. These include a change in the local environment to highly acidic one (pH less than 3). In general, assuming that the wear debris is nontoxic, there are three scenarios: (i) the cells will try to digest the foreign debris by releasing chemicals and enzymes to dissolve and later absorb them so that the by-products can be eliminated through the blood circulation and lymphatic system into the various organs such the kidney and liver; if this fails then (ii) the body

will try to excrete them out of the body system; however, if (i) and (ii) cannot be achieved, then (iii) cellular fibrous linings will engulf the foreign bodies so as to keep them away (isolate) from the surrounding host tissue.

In order to understand the fatigue failure of biomaterials it will be essential to have some understanding of the surface substructure of biomaterials. Figure 3.9 shows a schematic picture of the cross-section of a deformed metallic biomaterial surface, surrounded in a physiological environment. Illustrated here are three distinguishable layers, namely (1) the molecular absorbed layer, (2) the passive oxide film, and (3) the deformed layer. How these layers interact with the physiological environment during the fatigue-wear process is of paramount importance to the behavior of the biomaterial and the long term fatigue performance of the medical device. Figure 3.9 exhibits this type of behavior under repeated impact loading.

However, the molecular absorbed layer is dependent on the underlying passive oxide layer, which protects the base material from corrosion. If the deformed layer has a high compressive stress field (for instance, in the case of forged stainless steel), the incident of crack initiation is reduced and hence the fatigue strength of the material is increased.

One can readily see that the process of removal of these layers (by wear) can greatly affect the fatigue of biomaterials.

In general, cracks initiate under tensile stresses. It is well known that the anterior and lateral surfaces of femoral prostheses are subjected to high tensile stresses during

walking and stair climbing. These stresses are additive and generally peak at or near the anterolateral corner of the stem. Historically, analysis has shown that fractures most commonly emanates from the anterolateral corner in the middle third of the stem (Woolson, 1997). Fracture waves are similar to tide marks. As one might expect, they occur during different fatigue phases of the metals.
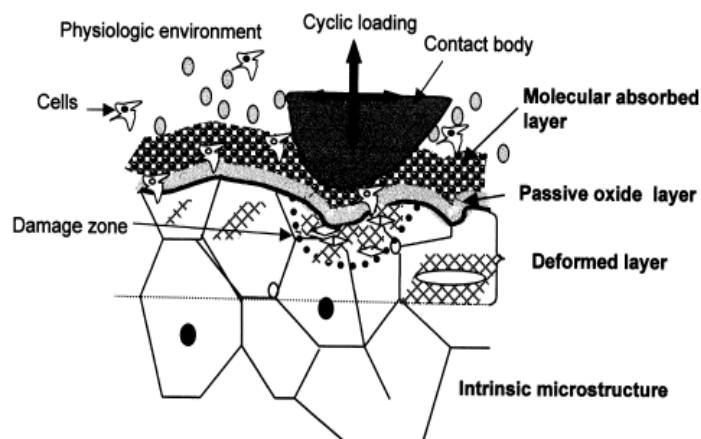

Figure 3.9. The cross-section of a deformed metallic biomaterial surface showing the complex interactions between the material's surface and the physiologic environment is schematically illustrated (Teoh, 2000).

Corrosion of retrieved stainless-steel hip stems has received little attention since early 1970s. Any subsequent reports of corrosion involving retrieved stainless-steel fracture fixation devices were not reported. Corrosion of these implants was investigated as the corrosion products of this alloy have been implicated in the generation of sensitivity reactions, the risk of local tumors, particulate debris leading to osteolytic implant failure and mechanical failure of the implant.

Austenitic stainless steel which has been used in the manufacture of hip prostheses since the earliest Charnley implants consists mainly of gamma-iron (austenite) as a

solution with less than 2% carbon, stabilized by the presence of nickel. The surface was treated to from a passivation layer of chromium oxide that imparts much of the corrosion resistance. Changes were initially made in response to reports of corrosion of retrieved fracture fixation plates and screws, and subsequently due to reports of hip arthroplasty stem fractures and reports of mechanical failure of 316L in vitro. Fracture of the stem of the early stainless steel hip arthoroplasties was a major concern, but has only rarely been reported in association with corrosion. Refinements in manufacture, in particular, double-vacuum malting and cold working appear to have led to a satisfactory solution to stem failure, although corrosion fatigue leading to mechanical failure of fracture fixation devices is still reported.

The location of corrosion was specific to each design in their study. The proximal corrosion of the Charnley stems being contrasted with the distal corrosion of the grooves of the Müller stems. The area of the Charnley stems that was corroded is an area of high stress. This may weaken the passivation layer and also promote corrosion fatigue. This area is prone to fretting, which along with crevice corrosion, has been implicated as a major cause of corrosion of retrieved implants. Localized pitting corrosion, which could be attributed to implant surface defects, was only demonstrated in one implant series of Walczak , where the corroded area corresponded with the area of electro-etched serial numbers. This process is recognized to be a risk factor for pitting corrosion and has been superseded by laser-marking. The distal location of the corrosion in the Müller stems may reflect the different stresses in the surface layers on a straight stem with increased valgus neck geometry. This results in relative reduction of stress and fretting at the proximal third and increased stress distally and medially. The most consistent site for corrosion in the Müller implants is at the distal end of the grooves that exist on the anterior and posterior surface of the prostheses. This may well

be secondary to stem-cement debonding, which may, in addition, permit crevice corrosion.

Corrosion Products

The lamellar nature of corrosion plaques or scales on variety of alloys in industrial environments was well documented. Such compounds formed are insoluble and are relatively adherent to the alloy surface. There is also a lamellar structure to the corrosion scales in austenitic stainless steel.

EDX analysis of the elemental composition of corrosion plaques has been previously reported for stainless steels in industrial and dental environments. Plaques consisting of iron, calcium, chromium, sulfur, chloride and potassium were demonstrated following in vitro aqueous corrosion of 18-8 stainless steel and of chromium and oxygen following corrosion of 316L in seawater.

The change in appearance of the metal surface following black scale removal indicates disturbance of the passivation layer during the process of corrosion. It is possible that accumulation of chromium in the black corrosion plaques may be resulted in a local depletion of chromium. This may result in repassivation occurring with a less protective oxide such as FeO. Occasional areas of high iron and oxygen content between the chromium-rich plaques and the pitted alloy may represent such a process. This may well lead to a self-perpetuating increase in the rate of corrosion and possibility the acceleration of any fatigue failure of the implant.

The sulfur, chloride, calcium and phosphorus in the plaques is assumed to arise from the interaction of the prostheses with the body, as these elements are present in microscopic amounts in the alloy.

When corrosion products were present on the stem-cement interface they had a similar composition to the plaques found on the stem. Of particular interest is the corrosion plaques found in the substance of one cement mantle. Their composition is similar to the chromium-rich stem plaques.

The biological significance of the corrosion plaques is at present unknown. Although the toxicity of certain of their elemental components is well established, their effect as a whole has yet to be identified. The clinical success of stainless steels hip implants has resulted in the implantation of such devices into a younger population with a longer life expectancy (Walczak, 1998).

3.5. Coating Applications Against Failures of Metallic Materials

In general, components used in engineering applications must possess the appropriate structural characteristics to provide stiffness or flexibility and to carry applied loads without macroscopic failure. Such properties are associated with the bulk material of the component. However, the majority of engineering failures are surface initiated and occur through such phenomena as friction, wear, corrosion, fatigue, or a combination of these factors as mentioned former sections. Surface related failures arise from two specific causes; in the first place, stress levels are often highest at the surface, and secondly, the surface is usually the only part, which is subjected to the external environment. An increasingly common way of coping with such a situation is to provide different surface material properties from those of

the bulk material. Surface treatment technology has advanced rapidly over the last few decades and has greatly assisted in meeting the ever-increasing demands placed on materials.

Since the early 1980s there has been a continuing and rapid development of advanced surface engineering practices for the optimisation of corrosion and wear resistance. It is now possible to produce coatings of novel composition and microstructure by a variety of sophisticated physical and chemical processes such as PVD (Physical Vapour Deposition), CVD (Chemical Vapour Deposition), Ion Implantation and Laser surface treatment methods.

Process, which deposits thin films and coatings of physically generated atoms or molecules from the vapour phase onto a substrate in a vacuum environment, is called PVD processes. This method of surface modification does not chemically alter bonding arrangements. PVD systems all incorporate a means of evaporating coating material from a solid source under a partial vacuum (Hübler, 2001).

In the basic CVD process gases containing volatile compounds of the elements or elements to be deposited are introduced into a reaction chamber, and condensed onto the substrate to form a coating. Most chemical reactions in CVD are endothermic, so that thermal energy must be supplied by heating the substrate or by the environment in the neighbourhood of the substrate. So, only systems, which do not undergo phase transformations within the temperature range required for deposition, can be employed by this coating method (Kuo, D. & Huang, K., 2001).

Ion implantation involves the bombardment of a target material with energetic ions (electrically charged particles). These ions penetrate the target to a depth dependent on the energy of the ion and the nature of the ion and the target. In a metallic substrate the neutralised ions come to rest in the lattice in interstitial and substitutional positions and remain there in a metastable solid-solution. The nature of the process allows any element to be introduced into the near-surface region of a solid in a controlled and reproducible manner that is independent of most equilibrium constraints. Due to the non-equilibrium nature of this process, composition and structures unattainable through conventional methods may be produced. The chosen atomic species are first ionised and them accelerated in an electric field to level of energies, which lie in the range from a few tens to a few hundred kiloelectronvolts in a moderately high vacuum. These ions arrive at the work piece (target) with velocities around that of a rifle bullet and can does penetrate the surface. The energetic ion comes to rest by displacing atoms from their normal lattice sites by ionising target atoms, thus producing a large number of point defects. Most defects are annihilated by recombination shortly after the passage of the bombarding ion, but some survive. The resultant structure consists of the host (target) material with an impurity (alloying) addition and a defect structure characteristic of radiation damage. Such a process does not require a high temperature, the penetration being achieved by high kinetic energy.

Laser processing utilises a laser to produce a source of energy which, when in contact with materials, can produce a large amount of heat in a very small volume of material. The amount of heat generated depends on the power density absorbed from the laser and the time of interaction with the surface. Laser-induced surface alterations include annealing, etching, deposition, welding, cutting, surface transformation and polymerisation.

Transition metal nitrides such as TiN, ZrN, VN, BN, and Ti0.5Al0.5N are generally utilised as a protective coatings because of their complex bonding structure exhibiting characteristics of covalent, ionic and metallic bonds. The metallic character of these compounds is shown in their high thermal and electrical conductivities while the covalent nature give rise to high mechanical microhardness, typically in the range 20-30 GPa.

Protective properties of these films come especially from their hardness properties. The hardness of a material is determined both by its intrinsic hardness (the hardness characteristic of the material in the single-crystal form) and by microstructural features that affect the deformation mechanisms. The intrinsic hardness of a material is determined both by the strength of the interatomic forces and the crystal structure. Materials exhibiting a high intrinsic hardness can be characterised as having high cohesive energy, short bond length and a high degree of covalent bonding (Sundgren, 1986). The strength of the interatomic forces and the bonding length plays an important role in determining the elastic properties of the material and thus also the hardness. A high resistance to dislocation propagation and multiplication is found in materials with high bond strength and thus a high Peierls stress (intrinsic lattice resistance to dislocation motion). Also highly directional bonds, such as covalent will restrict dislocation propagation. In general, the hardness decreases as the proportion of covalent bonding decreases. Some typical microstructural features that influences dislocation movement, are grain boundaries, precipitates, and impurity atoms. Since thin films often have different microstructures compared to bulk materials, e.g., a much smaller grain size and a higher concentration of other defects it is understandable that thin films often show much higher hardness values compared to bulk materials (Rieu, 1991).

CHAPTER FOUR
EXPERIMENTAL STUDY

4.1. Purpose

The successful long term functioning of a hip replacement is influenced by many factors. Among all the others fatigue fracture and wear have been identified as the major problems associated with implant failure in forms of loosening, stress shielding and ultimate implant failure. The stem failure by fatigue is the consequence of several concurrent causes such as the surface or bulk material defects induced by technological processes, the high local stress concentration due to the stem design, the patient weight and activity, the stability of the stem-bone mechanical interface, the material properties, and corrosion (Raimondi & Pietrabissa, 1999). An important mechanical factor is the ability of the implant to withstand the continual application of load, which may exceed the body weight of the patient by several folds (Humphreys, 1990).

The development of THR combines three areas of investigation: theoretical, experimental and clinical. Component fatigue testing, the final step in the development of total joint replacements, is performed to validate the safety of these components against fatigue failure before clinical use, as part of the design approval. The fatigue test is one of the most common laboratory tests to evaluate the reliability of prostheses. In this manner, designs are tested to ensure that the minimum fatigue strength requirements are fulfilled. The first component fatigue test to be standardized was in response to the unacceptably high rate of in vivo hip stem fractures of the first generation hip stem designs. The fatigue test is usually performed according to the ISO 7206 standard. The international standard specified

vertical load application to the head of the stem and fixation of the distal stem in bone cement to a height of 80 mm below the center of the head.

The objective of this study was to perform the fatigue test of the Thompson hip prosthesis in accordance to ISO 7206/4 by using the strain gauge and to determine the fatigue life of prosthesis. Also, the purpose of this study was to compare the values of real stresses measured on the hip prosthesis by means of strain gauges and compare these with the theoretical stresses calculated by CAD modeling.

4.2. Materials and Methods

4.2.1. The Component

Implant quality 316L stainless steel is used in the field of implant surgery because of its relatively low costs, high machinability, and reasonable corrosion resistance but since it has some poor properties it requires applying some coatings to withstand dynamic loads and aggressive body fluids in human body. Chemical and mechanical properties of an implant quality 316L stainless steel used in this study are given in Table 4.1 and Table 4.2 respectively.

Table 4.1. Chemical properties of 316L stainless steel (Higo & Tomita, 1994).

% Element	Cr	Ni	M o	C	M n	P	S	Si	N	Cu	N b	Fe
	17- 20	14- 17	2-4	0.0 3	2.0 0	0.0 3	0.0 3	0.7 5	0.1 0	0.5 0	-	Balance

Table 4.2. Mechanical properties of 316L stainless steel (Higo & Tomita, 1994).

Property	Wrought (ASTM F55 and F56)	Cast (ASTM A269)	Cold worked	Annealed
Elastic modulus (MPa)	$1.9\text{-}2.1 \times 10^5$	1.93×10^5	2.0×10^5	2.0×10^5
Shear modulus (MPa)	8.4×10^4	-	-	-
Yield strength (0.2%) (MPa)	$2.05\text{-}2.41 \times 10^2$	2.06×10^2	$7.5\text{-}7.9 \times 10^2$	2.8×10^2
Ultimate tensile strength (MPa)	$5.1\text{-}5.5 \times 10^2$	4.82×10^2	$9.6\text{-}10.0 \times 10^2$	5.5×10^2
% Elongation	55	30	9-22	50

In this study 316L stainless steel Thompson hip prosthesis supplied by HIPOKRAT A.Ş. was tested by double cantilever beams bending fatigue machine (DCBBM) designed and manufactured at the Department of Metallurgy and Materials Engineering at Dokuz Eylül University. Dimensions of the original Thompson hip prosthesis are given in Figure 4.1.

4.2.2. The Apparatus and Set-up for Fatigue Test

The main aim of ISO 7206/4 standard for the fatigue testing of hip prosthesis is to specify test conditions, which, if satisfied, will give confidence that the prostheses will not break or fail under any expected circumstances during its service life. In order to satisfy this requirement, the test conditions should be similar to those, which are likely to be encountered in service (Humphreys, 1990).
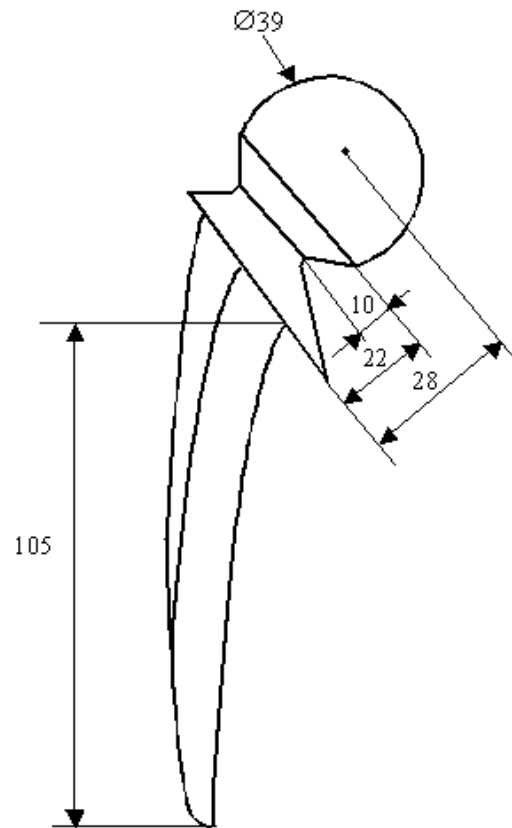
Figure 4.1. Dimensions of Thompson hip prosthesis.

Double cantilever beams bending fatigue machine used to investigate the fatigue properties of hip prosthesis in this work is shown in Figure 4.2. This machine consists of two main units; mechanical components that produce fluctuating forces and electronic parts that consist of amplification data acquisition system by which the load-cell generated data signals are pre-amplified and transferred to a PC where they are processed. The details of this machine can be found elsewhere (Ak, 2002).

Figure 4.2. Front and back view of the double cantilever beams bending fatigue machine.

4.3. Experimental Procedure of ISO 7206/4

The ISO 7206 standard describes the test apparatus and procedure to assess the fatigue resistance of femoral stems without and with torque. Test procedure adopted in this study was executed in accordance with the ISO 7206/4, which includes determination of endurance properties of stemmed femoral components with application of torsion.

This part of ISO 7206/4 describes a test method for determining the fatigue endurance properties, under specified laboratory conditions, of stemmed femoral components of total hip joint prosthesis subjected to a loading system which includes the combination of compression, bending and torsion. It is generally felt that the important factors are the application of cyclic stress, the value of the mean stress, the environment and the orientation of the femoral component in relation to the applied load. It also defines the conditions of testing as such that the important parameters affecting the components are taken into account, and describes how to set up the specimen for testing.

Preparation of the prosthesis for the test is given as follows:

The anatomical axis of the femur has been assumed to be at an angle of 10° (in adduction) to the load line, when viewed perpendicular to the plane that includes the stem and neck. The offset angle (which introduces the torsional component of force) has been set at 9° ± 1° (in flexion). This orientation process was arranged by means of a gripping device (Figure 4.3). Furthermore, the test conditions are fixed on the assumption that the stem becomes unsupported proximally, remaining restrained at 80 mm from the centre of the head of the prostheses. This assumption is consistent

with the clinical observations that failures generally occur in the middle third of the stem (Baleani, 1999).
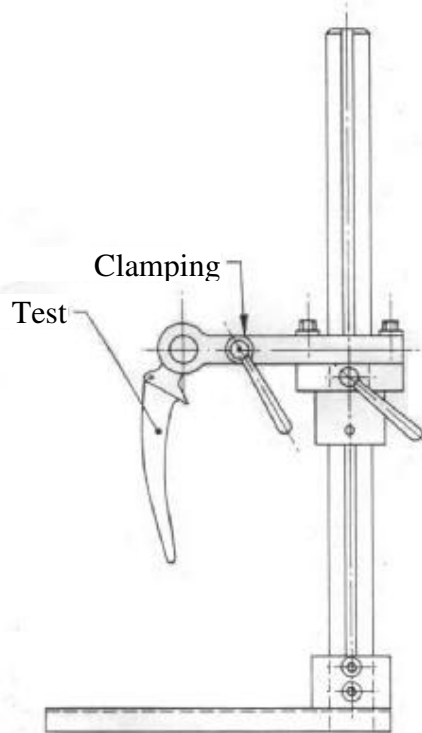
Figure 4.3. The gripping device.

Two strain gauges were fixed on the prosthesis. The locations of the strain gauges on the prosthesis were at 10 mm above and below the level of bone cement as shown in Figure 4.4. The strain gauges and their wiring were insulated against the test environment by spreading the silicon on the related surfaces.

The head of the prosthesis was loosely clamped by a gripping device, before the final fixation of the stem was obtained by changing its position.

Then the stem of the prosthesis was aligned according to the orientation angles that mentioned above.
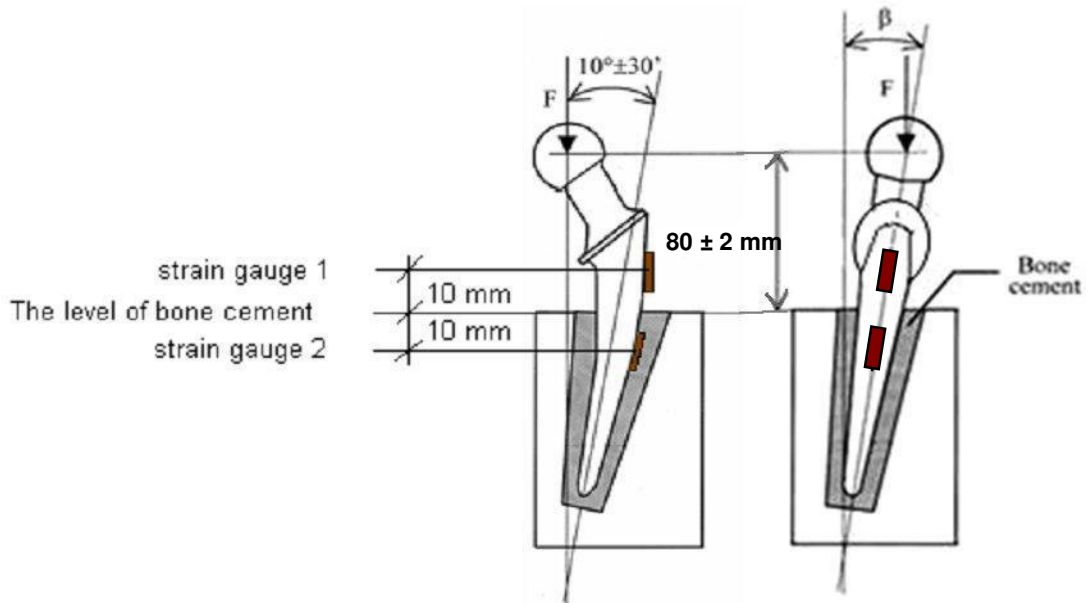
Figure 4.4. The locations of the strain gauges on the prosthesis.

The specimen was embedded in the self-curing medium. PMMA cement was used as embedding medium. To obtain final embedding medium, 50 g of self-curing acrylic powder and 33 ml methyl methacrylate liquid were mixed rapidly in a pot and poured in the cavity of the specimen holder before polymerization was due to start. The prosthesis vertically plunged into specimen holder until the distance, between the centre of the head and cement surface, of 80 ± 2 mm is reached (Figure 4.5). Prosthesis was left for 24 hours whilst the embedding medium hardened.

The femoral component set in a test rig as described above was subjected to compression test with an electro mechanic tensile test machine, Shimadzu, with a loading capacity of 5 tons, in order to determine the linear load-displacement curve of the fixed prosthesis together with the test rig.
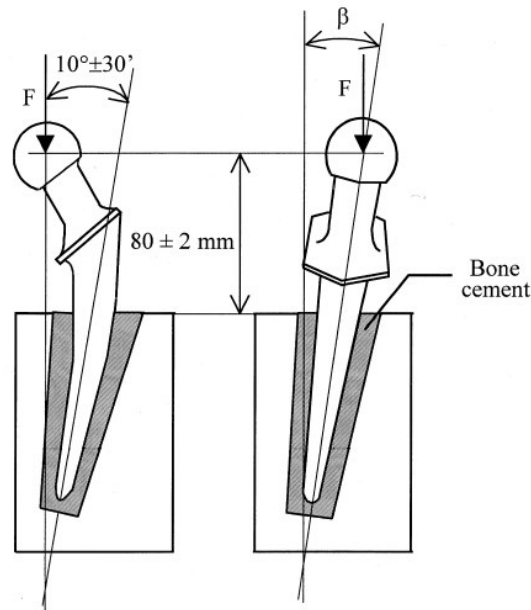
Figure 4.5. The position of the stem for the fatigue test an indicated in the ISO 7206/4. The flexion angle β is 9° for the set without torque and 9±1° for the test with torque.

Aim of this compression test was to obtain an initial load-displacement curve of the system comprising the stainless steel sample holder, PMMA cement and the prosthesis fixed in PMMA hold by the sample holder was in the loading, prior to the test. The purpose of this test was of twofold: firstly to ensure that the prosthesis was firmly reset by eliminating the presence of possible cavities in the acrylic bone cement. Secondly it provided a means at first sight to fully appreciate the range of loads that could be applied without causing any plastic deformation on the prosthesis. The load-displacement curve of the system as such is given in Figure 4.6.

LOAD-DISPLACEMENT CURVE
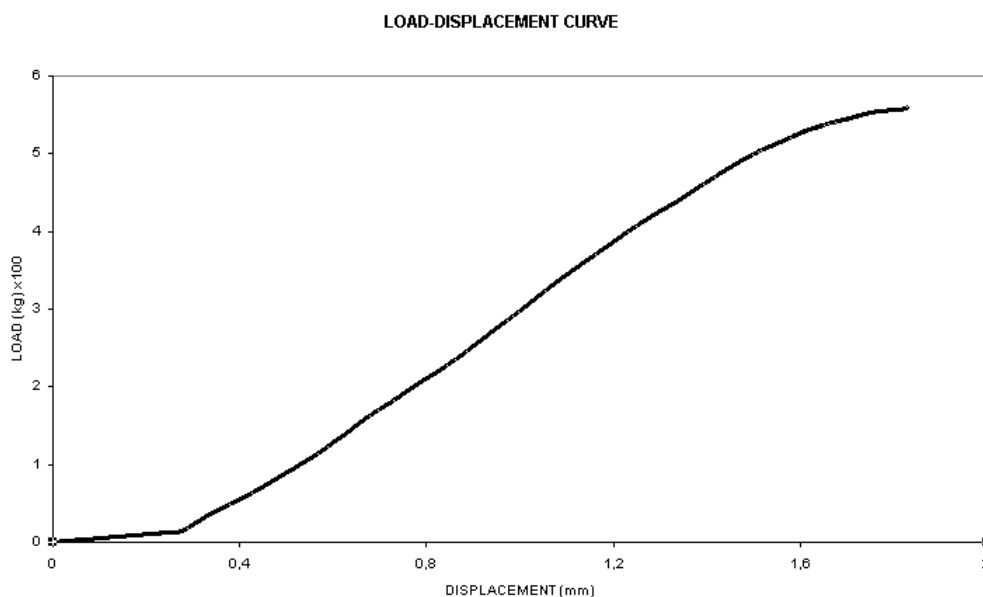
Figure 4.6. The load-displacement curve of the system.

The specimen with test rig (Figure 4.7) was located in the testing machine with squeezing clamps and the specimen was exposed to the saline test environment of 0.9 % NaCl up to the level of the stem neck. The sample of the prosthesis immersed in plexiglas liquid chamber is seen in Figure 4.7. The temperature of the test environment was maintained at $37 \pm 1\ ^{0}C$ during testing by means of a thermostat. The test environment was circulated constantly at a fixed flow rate by a peristaltic pump between a 3 litres glass container held in thermostat controlled bath and the test chamber. The desired load ranges for fatigue tests were adjusted with reference to the linear portion of the load-displacement curve. Thus a fixed ratio of the maximum load on the linear portion of the load-displacement curve such as 90,80 and 70 percent was set a the maximum of load cycle. Minimum level of loading was chosen so as to obtain a load ratio of 0.1 (R=0.1). Load frequency was set at 10 Hz by the belt pulley system of the machine. Testing machine is started. The average of the maximum and minimum loads applied on the sample was recorded by using a software program named Genie. The values of the strain that was from strain gauge were recorded the computer in a folder with 1 hour by using Lab-View program.

The three different loading that mentioned above, was tested until occurring the fracture of the specimen.
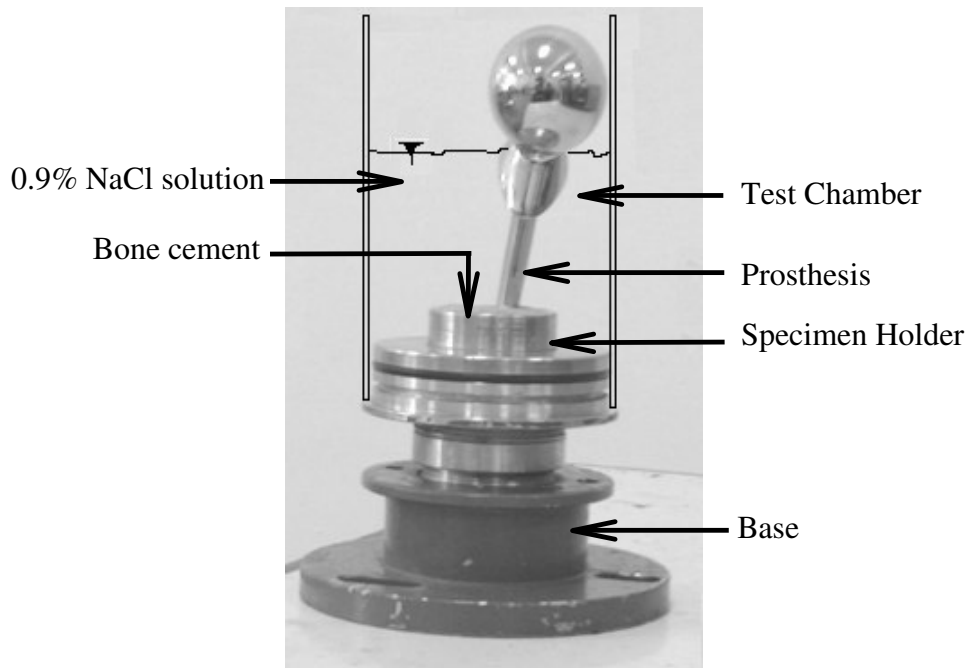
Figure 4.7. Specimen mounted on the

4.4. The Evaluation of the Test Results

The strain values obtained by rosette strain gauges were used to calculate the principle strains by the use of the following formulas (Vishay, 1970):

$$\varepsilon_{p\cdot q} = \frac{\varepsilon_1 + \varepsilon_3}{2} \pm \frac{1}{\sqrt{2}} \sqrt{(\varepsilon_1 - \varepsilon_2)^2 + (\varepsilon_2 - \varepsilon_3)^2} \tag{1}$$

$\varepsilon_1, \varepsilon_2, \varepsilon_3 =$ strains measured along the corresponding axes of the rosette elements, in/in (cm/cm)

$\varepsilon_{p\cdot q} =$ algebraically maximum and minimum principal strains, respectively, in/in (cm/cm)

The maximum and minimum stresses, σ_p and σ_q, were calculated by substituting ε_p, ε_q, υ, and E in equation (2a) and (2b).

$$\sigma_p = \frac{E}{1-\upsilon^2}\left(\varepsilon_p + \upsilon\varepsilon_q\right) \tag{2a}$$

$$\sigma_q = \frac{E}{1-\upsilon^2}\left(\varepsilon_q + \upsilon\varepsilon_p\right) \tag{2b}$$

$\sigma_{p,q}$ = algebraically maximum and minimum principal stresses, respectively, psi (Pa or N/m^2)

υ = Poisson's ratio

E = modulus of elasticity, psi (Pa or N/m^2)

Changes in maximum and minimum principal strains and stresses as a function of time are exemplified in Figure 4.8 and 4.9 respectively.
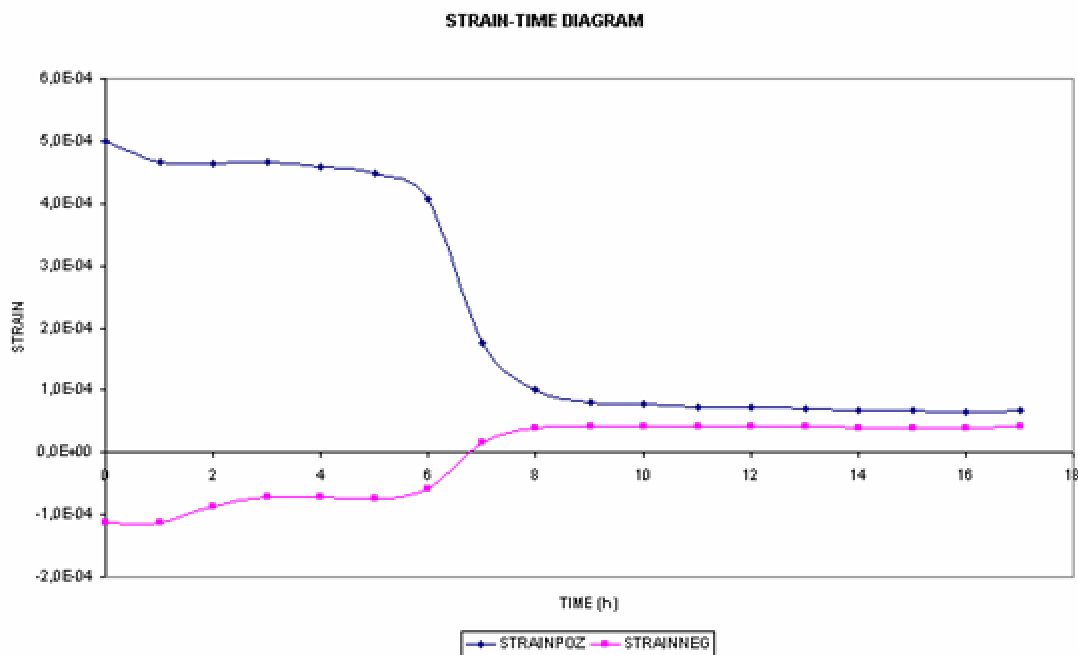
Figure 4.8. Change of Strains as a function of time.
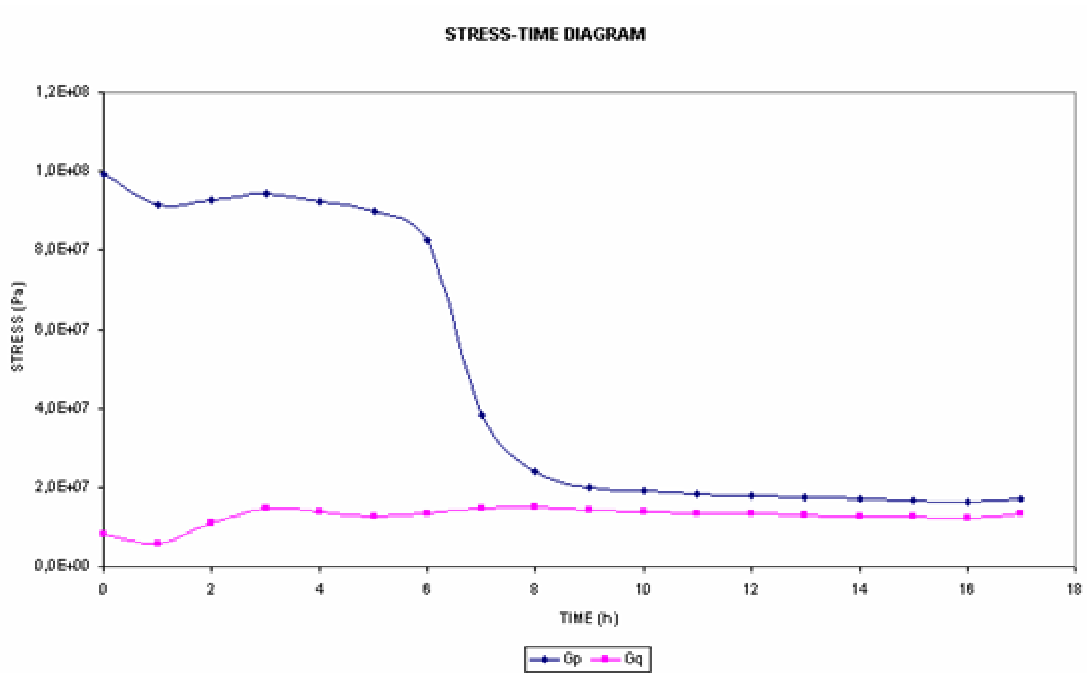
Figure 4.9. Change of Stress as a function of

Sudden changes both in strains and stresses indicated the failure of the prosthesis. The changes in maximum tensile strains, and stresses in particular, became evident upon the failure. The minimum strain remained in compression until failure took place then changed into tensile form thereafter both maximum and minimum strains converged to more or less same, smaller values. Similar changes also took place in stress values. Maximum and minimum stresses, which were both tensile, approached to somewhat same values upon the failure and remained more or less constant until the test was terminated.

CHAPTER FIVE
RESULTS AND DISCUSSION

Thompson Hip prosthesis fixed in the test rig as a whole (called as system hereafter) was compression tested with a constant crosshead speed of 0.1 mm/min by Shimadzu tensile test machine as described in Chapter four and load-displacement curves were obtained. The results of the compression test obtained for three systems are given in Figure 5.1, 5.2, and 5.3.

LOAD-DISPLACEMENT CURVE
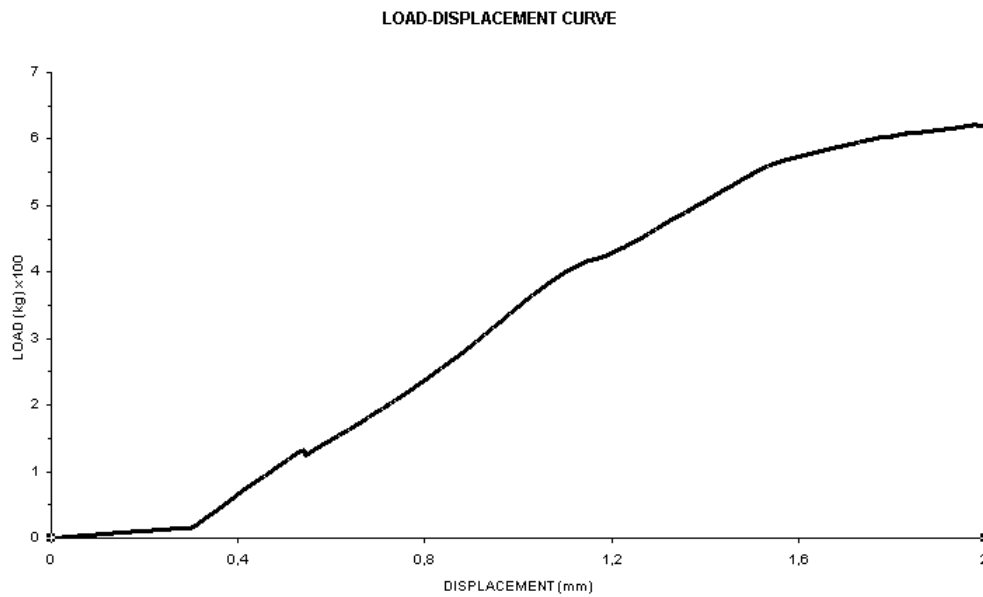
Figure 5.1 Change of the load as a function of displacement for the System1.

LOAD-DISPLACEMENT CURVE
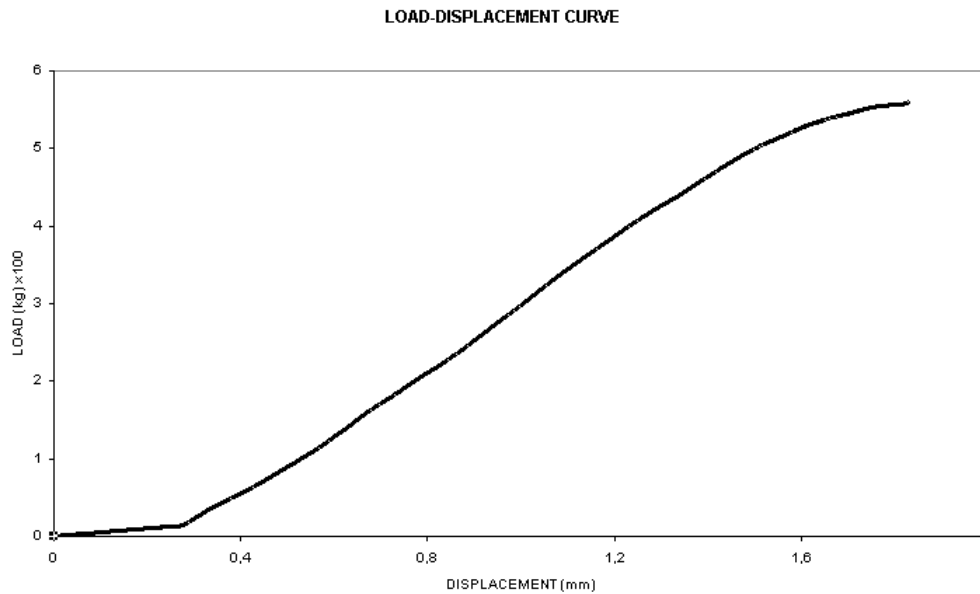
Figure 5.2. Change of the load as a function of displacement for the System2.

Figure 5.3. Change of the load as a function of displacement for the System3.

The loading conditions, namely loading range and true stresses measured by two strain gauges (σ_p) at the beginning of three tests are given in Table 5.1. The theoretical stresses calculated at various load levels by FEM modeling implementing I-DEAS program are also given in Figur 5.4 (Azem 2002). The ratios of the true stresses measured by strain gauges to the theoretical ones are given in the same table.

Table 5.1. Comparison made between measured and calculated stresses at the loading range used in this study.

Number of Test	Loading Range (kg)	Theoretical Stresses, N/mm²			True Stresses, N/mm²				Stress Ratio ($\sigma_{p\text{-gauge}}$) / $\sigma_{theo.}$	
		σ_{Max}	σ_{Below}	σ_{Above}	Gauge 1(G1) (Below)		Gauge 2(G2) (Above)		Gauge 1 (Below)	Gauge 2 (Above)
					σ_p	σ_q	σ_p	σ_q		
1	50-500	-	-	-	110	70	-	-	-	-
2	48-480	59	340	595	100	8	110	-2	0.29	0.19
3	32-320	39	210	396	78	29	74	34	0.37	0.19
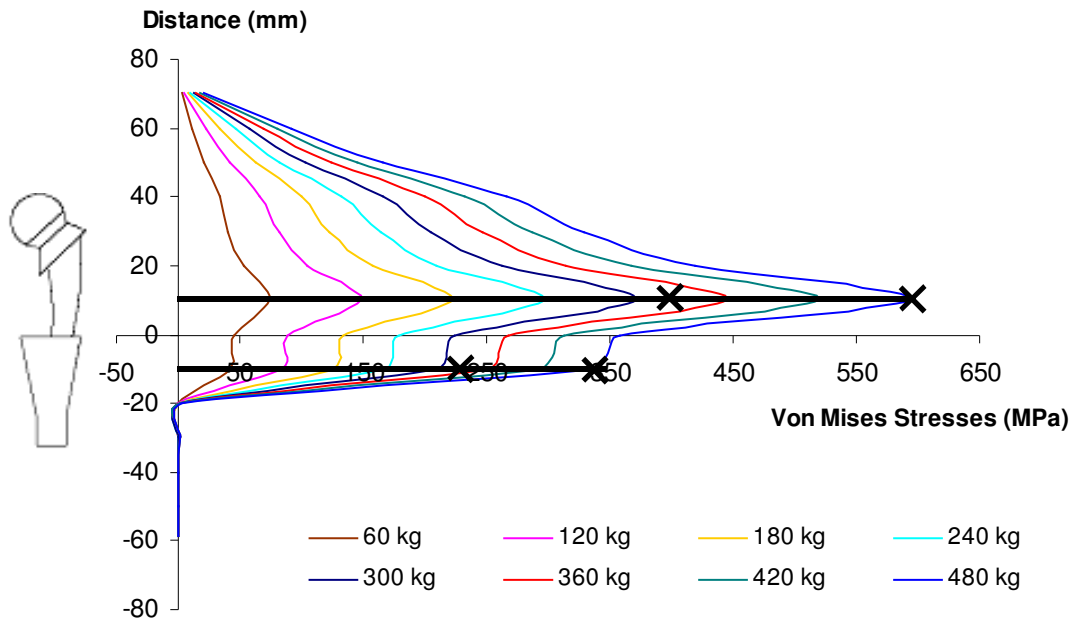
Figure 5.4. Stress distribution along the stem estimated by FEM modelling at various load levels (Azem,2002).

The true stresses measured by gauge 1 approximate to ~30% of the theoretical ones, while the same ratio for gauge 2 corresponds to ~20% for the loading range used in this study.

Figure 5.5 shows load variation with time of the system for Test 1. For test 1, strains gauge below the level of the bone cement was in good working conditions while the one above the bone cement was out of service. Therefore Stresses above the cement could not be evaluated. The changes in strains and corresponding stresses as a function of time are given in Figure 5.6 and Figure 5.7 correspondingly. It is noteworthy to indicate the changes in strains and stresses just as the failure commences. Maximum and minimum Stresses increased to a peak and then decreased to converge to almost same value of approximately 15 N/mm^2. Failure has taken place in 2 hours for this test.
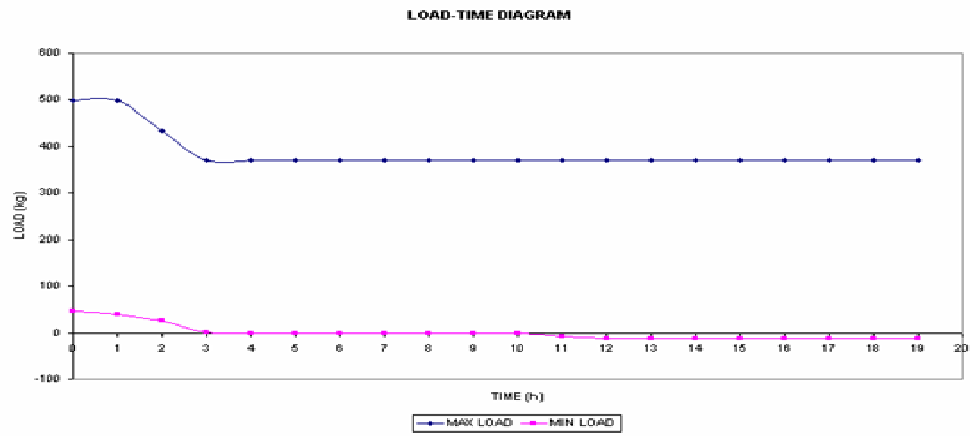
Figure 5.5. The load-time diagram of the system 1.
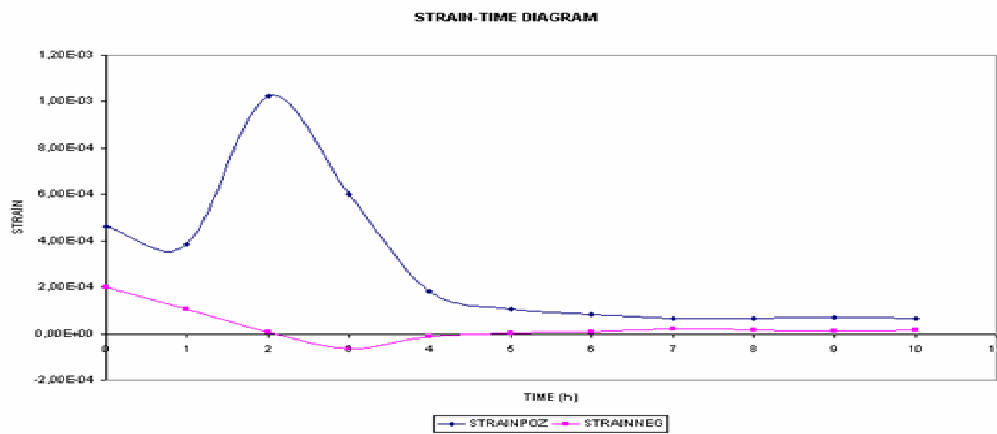
Figure 5.6. The strain-time diagram of the system1.
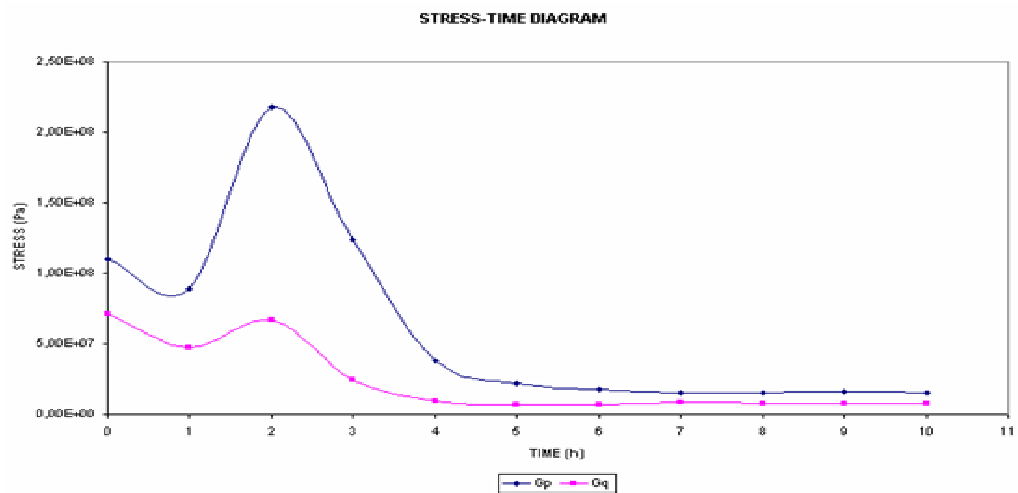
Figure 5.7. The stress-time diagram of the system 1.

Figure 5.8 gives load variation with time of the system for Test 2. Here both gauges were functional throughout the test. The changes in strains measured by two gauges as a function of time are given in Figures 5.9 and 5.10 for gauge 1 and gauge 2 respectively. Figures 5.11 and 5.12 show the corresponding changes in stresses versus time. Abrupt changes in stresses took also here in this test conducted at a loading range between 48 - 480 kg. Stresses measured by gauge 1 tend to converge to, same as the principle strains, while the stresses above the cement (gauge 2) fall apart and remained parted following the occurrence of the failure in six hours.
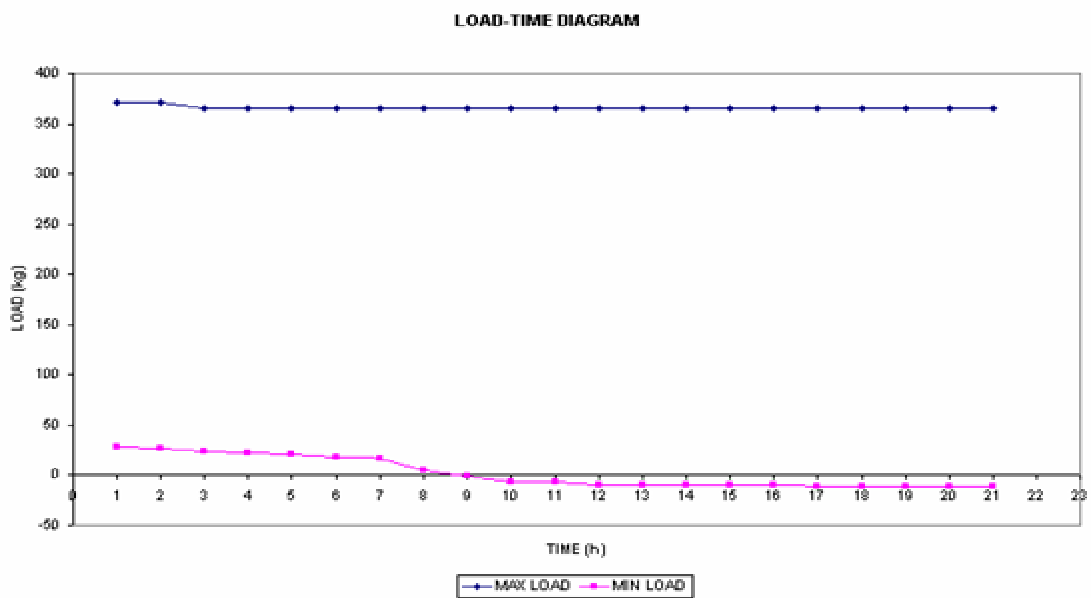
Figure.5.8. The load-time diagram of the system2.
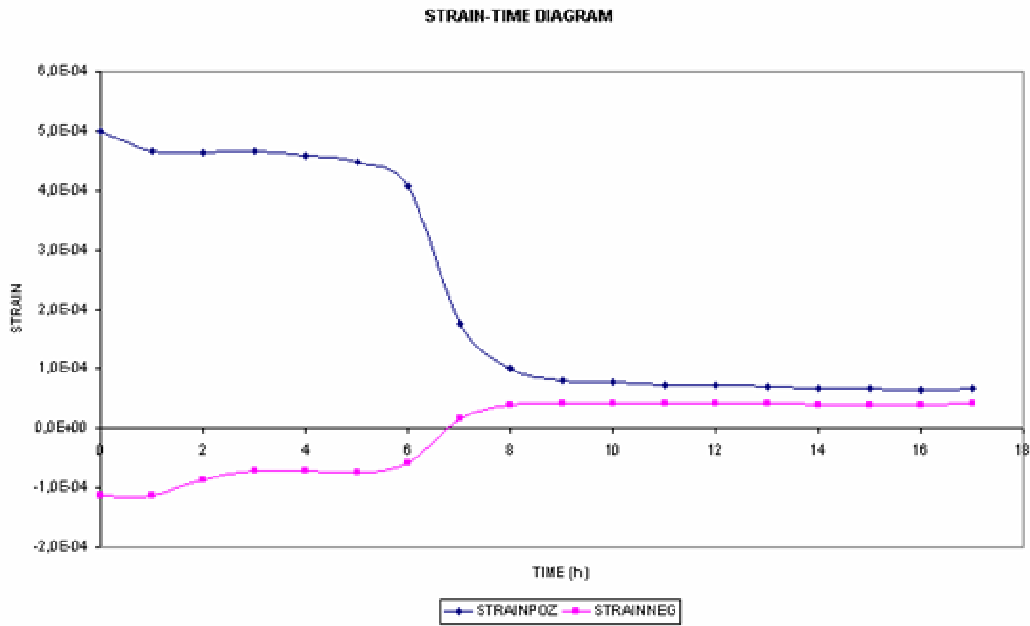
Figure 5.9. The strain-time diagram (below level of the bone cement) of the system2.
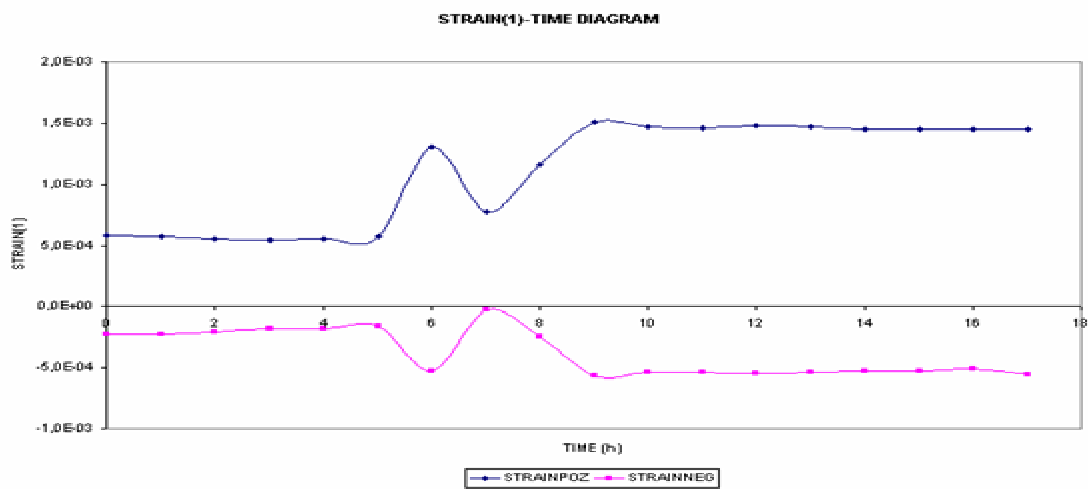
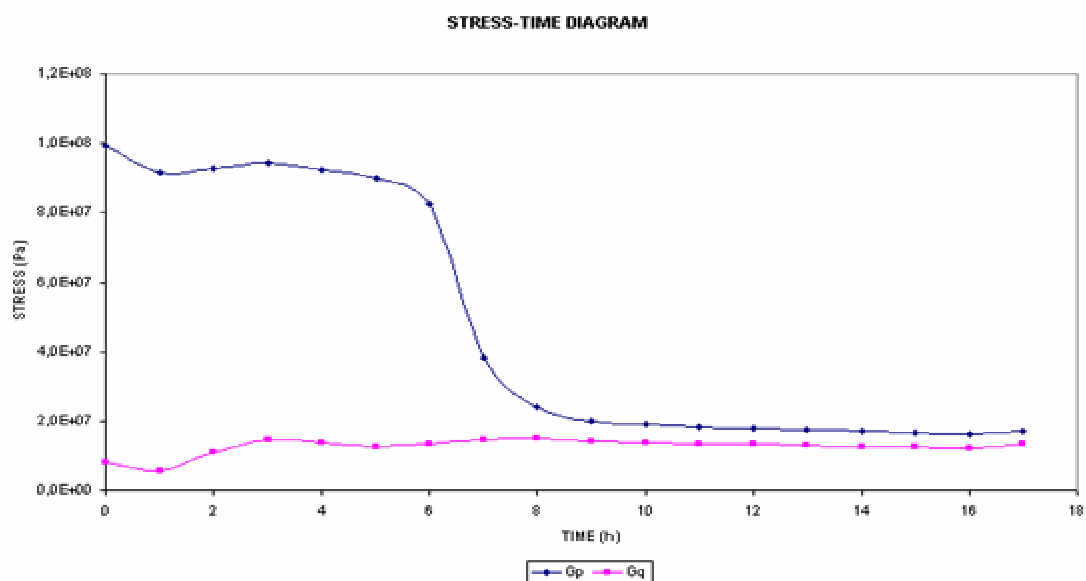Figure 5.10. The strain-time diagram (above level of the bone cement) of the system2.

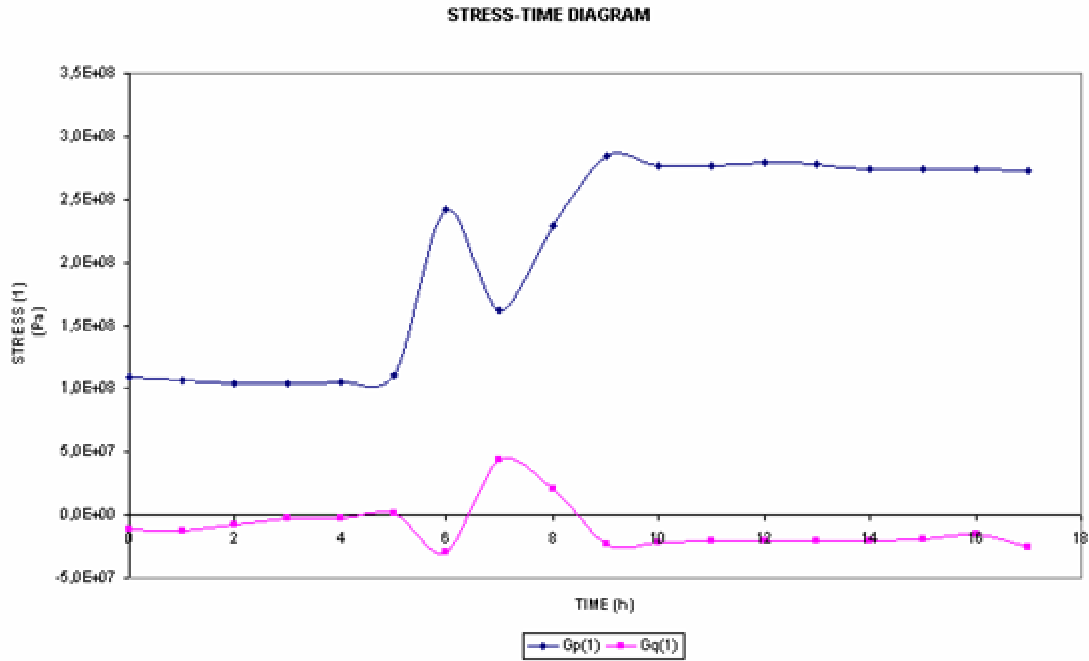Figure 5.11. The stress-time diagram (below level of the bone cement) of the system 2.

Figure 5.12. The stress-time diagram (above level of the bone cement) of the system

Figure 5.13 gives load variation with time of the system for Test 3. Strains measured by both gauges were recorded throughout the test (Figures 5.14 and 5.15) and used to calculate the corresponding principle stresses as shown in Figures 5.16 and 5.17.
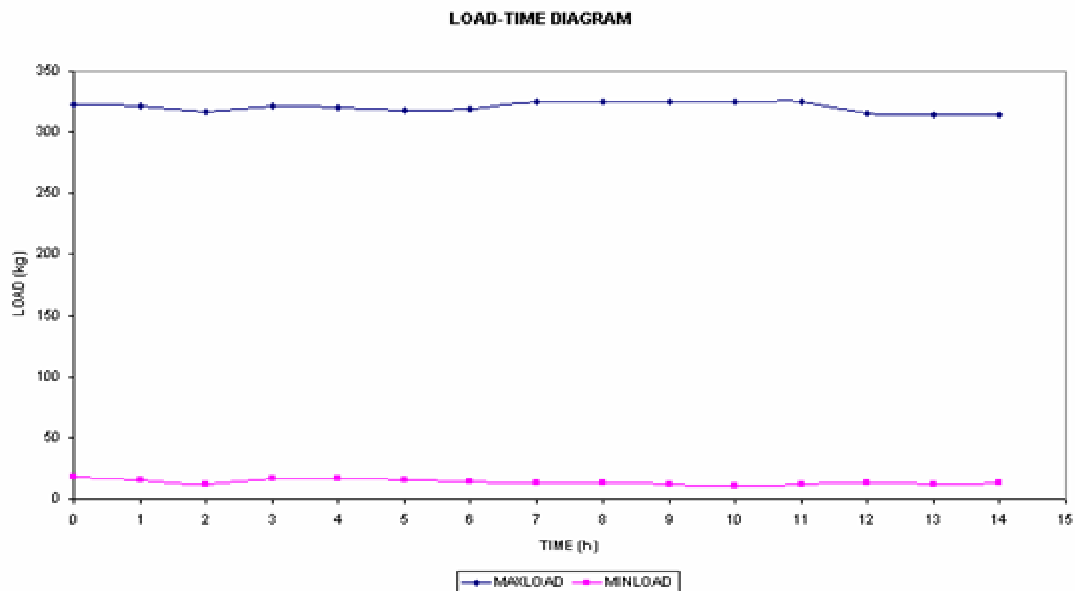

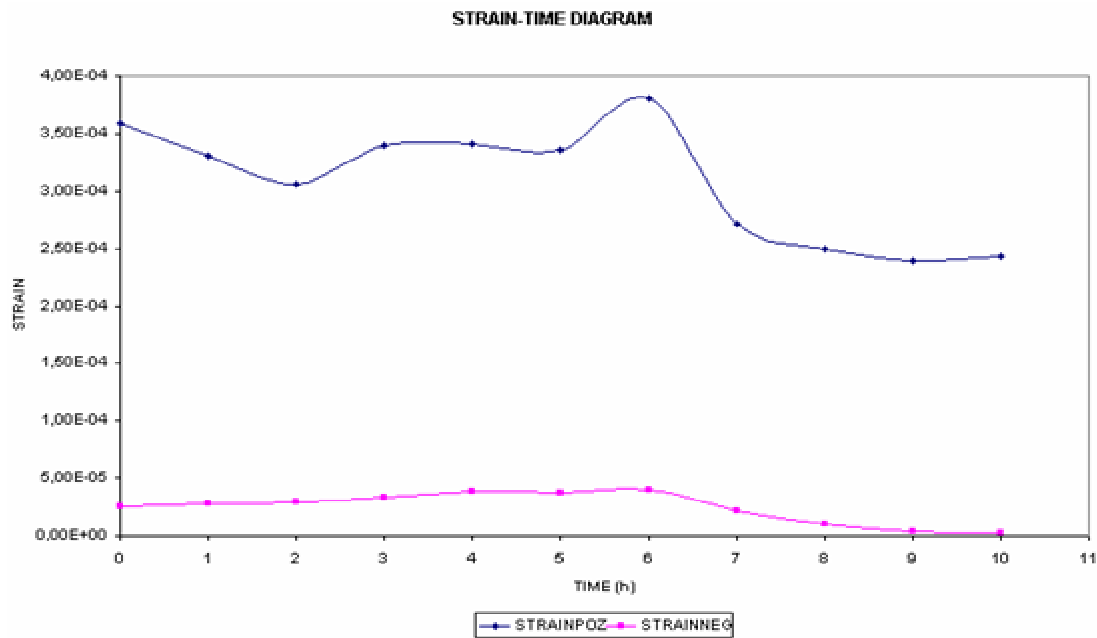Figure 5.13. The load-time diagram of the system 3.

Figure 5.14. The strain-time diagram (below level of the bone cement) of the system 3.
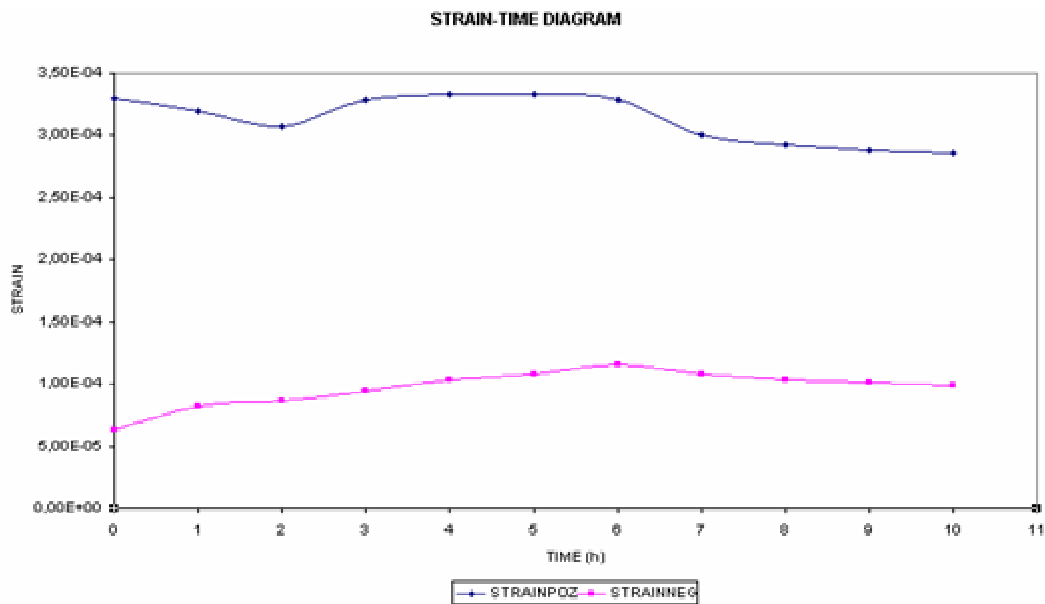

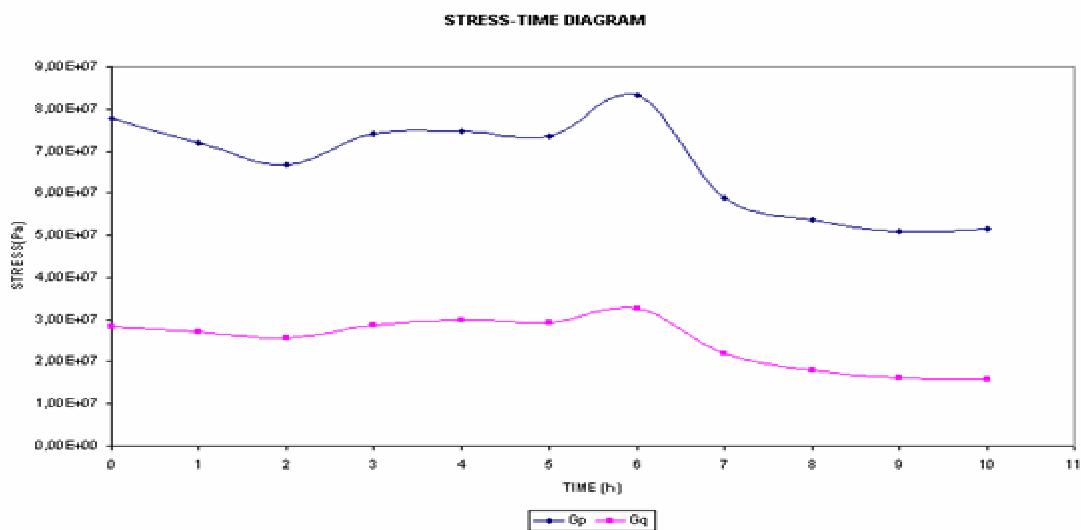Figure 5.15. The strain-time diagram (above level of the bone cement) of the system 3.

Figure 5.16. The stress-time diagram (below level of the bone cement) of the
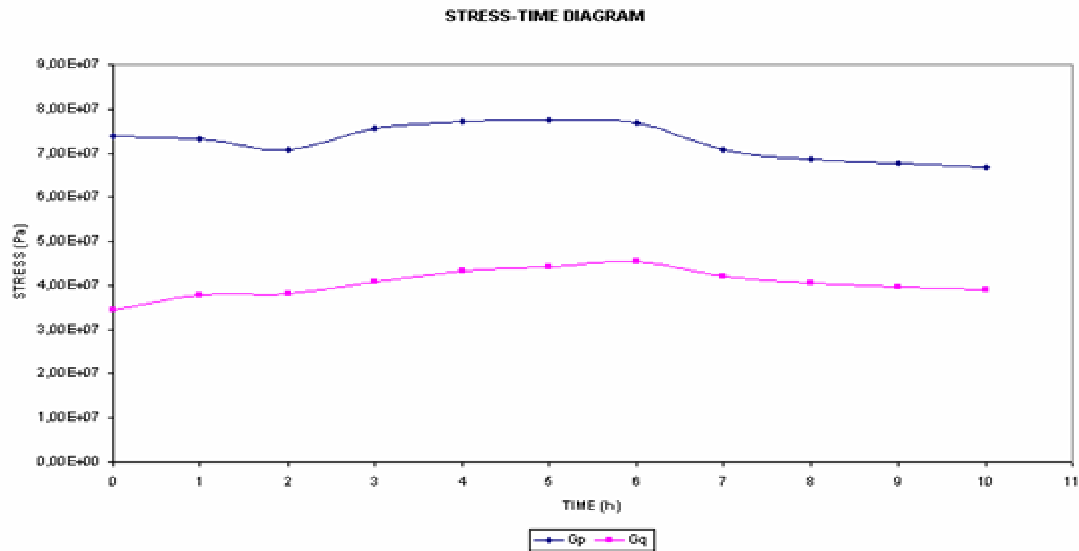
Figure 5.17. The stress-time diagram (above level of the bone cement) of the system 3.

5.1. Microstructural Examination

Microstructure of the 316L stainless steel taken from the hip prosthesis tested was studied and the following micrograph observed by image analyzer (Figure 5.18). The surface area of the impurities, as observed on the micrograph, approximates to 0.4% of the total surface investigated.

Figure 5.18. Micro structure of the 316L Stainless Steel used for the Hip prosthesis.

EDS analysis of the two distinct type of impurities observed on the surface are given in Figure 5.19 and Figure 5.20 with the corresponding micrographs. Aluminium and Titanium though are very small in amount, call attention among other elements that are expected from the chemical composition of the material tested. These may be actively involved in forming impurities which act as point of initiation for fatigue cracks when located at or near the surface as indicated in Figure 5.21.
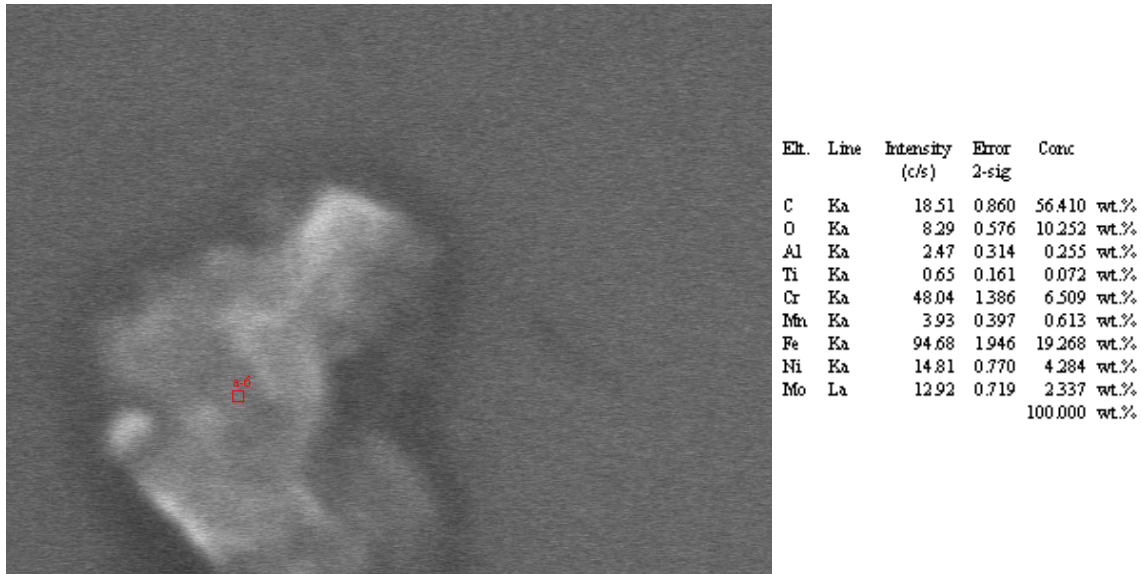

Elt.	Line	Intensity (c/s)	Error 2-sig	Conc	
C	Kα	18.51	0.860	56.410	wt.%
O	Kα	8.29	0.576	10.252	wt.%
Al	Kα	2.47	0.314	0.255	wt.%
Ti	Kα	0.65	0.161	0.072	wt.%
Cr	Kα	48.04	1.386	6.509	wt.%
Mn	Kα	3.93	0.397	0.613	wt.%
Fe	Kα	94.68	1.946	19.268	wt.%
Ni	Kα	14.81	0.770	4.284	wt.%
Mo	Lα	12.92	0.719	2.337	wt.%
				100.000	wt.%

Figure 5.19. The one of the dominant points and chemical composition of it.

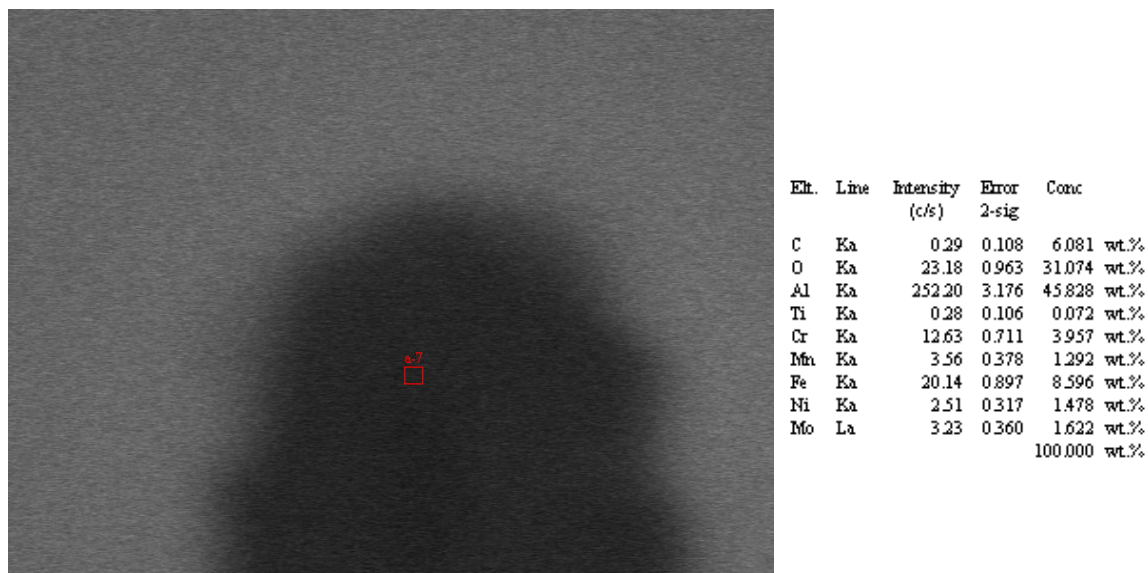| Elt.	Line	Intensity (c/s)	Error 2-sig	Conc	
C	Kα	0.29	0.108	6.081	wt.%
O	Kα	23.18	0.963	31.074	wt.%
Al	Kα	252.20	3.176	45.828	wt.%
Ti	Kα	0.28	0.106	0.072	wt.%
Cr	Kα	12.63	0.711	3.957	wt.%
Mn	Kα	3.56	0.378	1.292	wt.%
Fe	Kα	20.14	0.897	8.596	wt.%
Ni	Kα	2.51	0.317	1.478	wt.%
Mo	Lα	3.23	0.360	1.622	wt.%
				100.000	wt.%

Figure 5.20. The other of the dominant points and chemical composition of it.

The fracture surfaces of the stem of the prosthesis were investigated by using scanning electron microscope (JEOL JSM-6060, Japan). Micrographs taken from the fracture surfaces of the samples of the Test 1 are shown in Figures 5.21- 5.24. Arrows on the micrographs indicate the direction of the crack growth of the corrosion fatigue. It is worth noting that the faceted fracture surfaces were highly corroded due to elongated time of exposure to the corrosive medium as indicated in Figure 5.23.
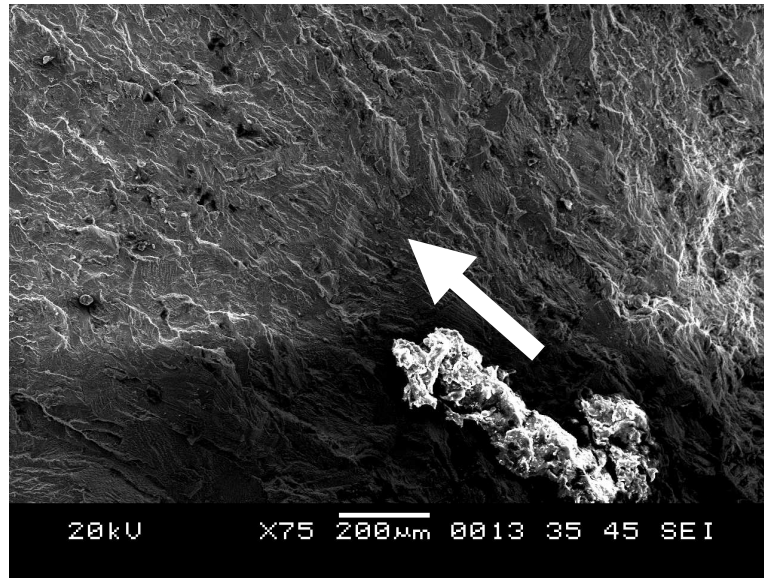

Figure 5.21. The fracture surfaces of the sample of Test 1.
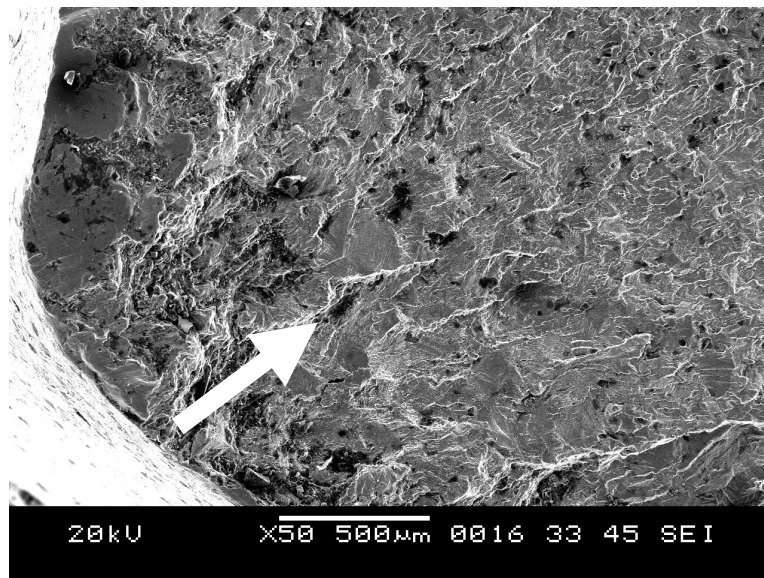

Figure 5.22. The one view of the samples of the Test 1.
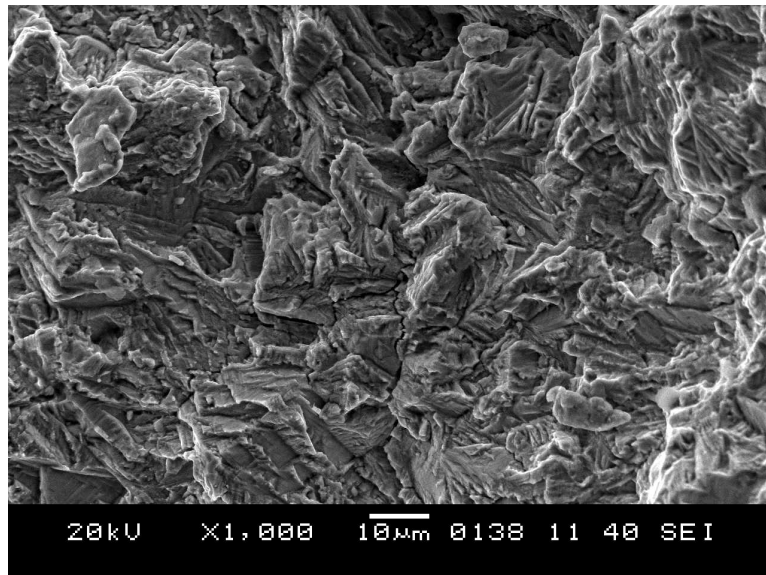
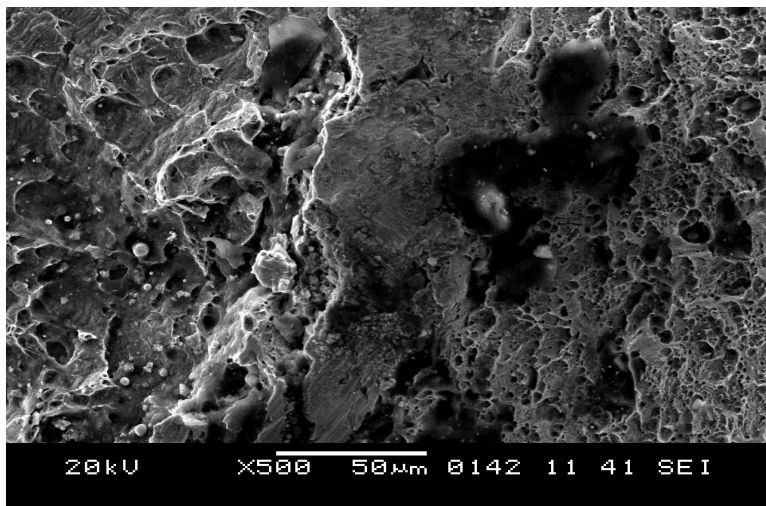Figure 5.23. The grain boundary of the samples of the Test 1.

Figure 5.24. The transition from the corrosion fatigued region to mechanically dimpled fracture created by the final separation of the fracture surfaces of the Test 1.

Figures 5.25 and 5.26 show micrographs of the fracture surface of the samples of the Test 2 taken by SEM. Area of the fracture surface created at early stage of failure become smoothened due to crack yawning and rubbing as shown in Figures 5.22 and 5.25. Striation lines, a typical feature of the fatigued surface, are indicated in Figure 5.26.
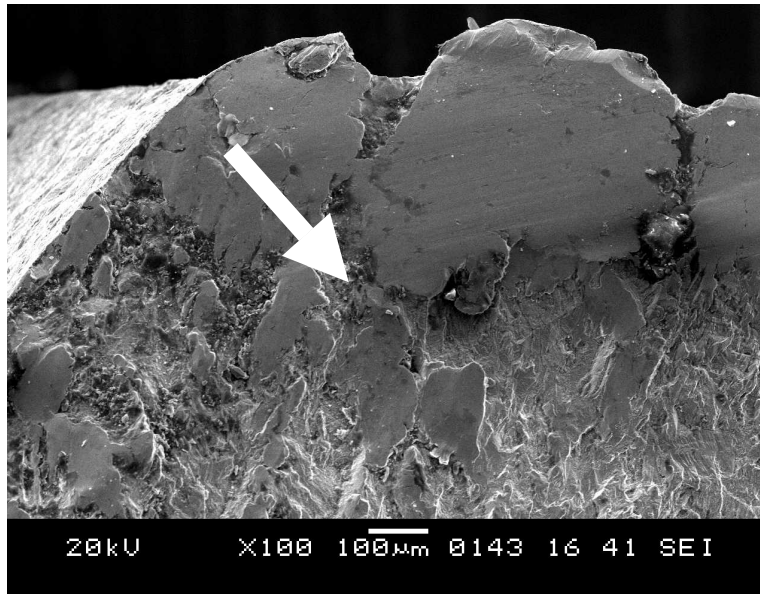
Figure 5.25. Smoothened area of fracture surface indicating the region of crack initiation. for the Test 2.
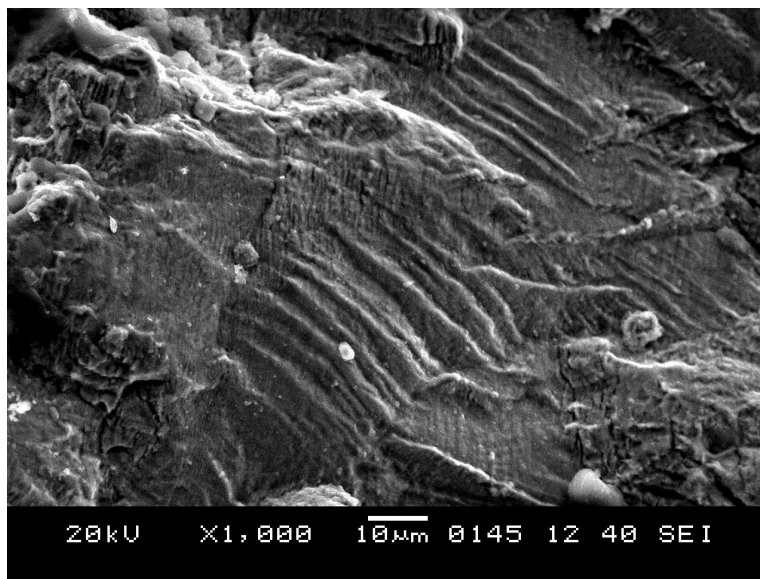

Figure 5.26. Striation lines indicating fatigue failure of the the test sample of the test 2.

CHAPTER SIX
CONCLUSION

Fatigue properties of 316L stainless steel hip prostheses were investigated in 0,9% saline solution at 37±1 ^{o}C at different load levels with the aim to follow the changes in stresses in situ, hence observe the initiation and propagation stages of the failure as it proceeds. It was also intended to compare the real stresses exerted upon dynamic loading and measured by strain gauges with the theoretical ones obtained by FEM method. The following conclusions were drowned from the experimental works carried out in this study:

1. As a result of cyclic loading of prosthesis according to ISO 7206/4 by means of double cantilever beams bending fatigue machine, maximum stresses were obtained experimentally by means of strain-gauge measurement system and these were compared with the theoretical stress values that were calculated by FEM method implemented using I-DEAS. As a result, the true stresses measured by gauge 1 approximate to ~30% of the theoretical ones, while the same ratio for gauge 2 corresponds to ~20% for the loading range used in this study.

2. 316L stainless steel Thompson hip stem was cyclic loaded with a stress rate of R=0.1. Specimen loaded at an ultimate load of 50-500 kg failed at a stress cycles of 40.000, while the other with an ultimate load of 48-480 kg lasted for 225.000 cycles. No fatigue crack was initiated in 500.000 cycles when a load range of 32-320 kg was applied.

For further study, more fatigue tests should be carried out to obtain a true S/N curve.

REFERENCES

Azem, N. F. (2002). Detrmination and evaluation of S/N curves for TiN and ZrN coated 316L hip stems. *M. Sc. Thesis.*

Azem, Z. (1999). Corrosion fatigue properties of 316L implant steel by double cantilever beams bending machine. *M. Sc. Thesis.*

Baleani (1999). Endurance testing of hip prostheses: a comparison between the load fixed in ISO 7206 standard and the physiological loads. *Clinical Biomechanics 14*, 339-345.

Baleani (2000). Endurance verification of custom-made hip prostheses. *International Journal of Fatigue 22*, 865-871.

Bauer, T. W. &ils, J. (1999). The pathology of total joint arthroplasty, II. Mechanism of implant failure. *Skeletal Radiology 28*, 483-497.

Bement, A. L. (1971). *Biomaterials: Bioengineering Applied To Materials for Hard and Soft Tissue Replacement*. London: University of Washington Press.

Bishop (1996). Porosity reduction in bone cement at the cement-stem interface. *Journal of Bone and Joint Surgery 78-B*, 1349-1356.

Boyer, H. E. (1986). *Atlas of Fatigue Curves*. Metals Park, Ohio: American Society for Metals.

Bronzino, J. D. (1995). The Biomedical Engineering Handbook. In J. B. Park *Biomaterials*.

Bronzino, J. D. (1995). The Biomedical Engineering Handbook. In K. R. Kaufmann & K. An (Eds.), *Joint-Articulating Surface Motion*. London: CRC Press.

Bronzino, J. D. (2000). The Biomedical Engineering Handbook. In J. B. Park & Y. Kon Kim (Eds.), *Metallic Biomaterials*. London: CRC Press.

Bronzino, J. D. (2000). The Biomedical Engineering Handbook. In J. B. Park, *Hip Joint Prosthesis Fixation-Problems and Possible Solutions.* London: CRC Press.

Christel (1988). Role of stem design and material an stress distributions in cemented total hip replacement. *Journal of Biomedical Engineering 10*, 57-63.

Colange, V. J. & Heiser, F. A. (1987). *Analysis of Metallurgical Failures (2nd Edition)*. New York: John Wiley & Sons, Inc.

Cowin, C. S. (2001). Bone Mechanics Handbook. In Prendergast P. J., *Bone Prosthesesand Implants*. London: CRC Press.

Crowninshield, R. (1988). An overview of prosthetic materials for fixation. *Clinical Orthopaedics and Related Research 235*, 166-172.

Desmond (1993). Fracture and loosening of charnley femoral stems. *Journal of Bone and Joint Surgery 75-B*, 259-265.

Dieter, E. G. (1988). *Mechanical Metallurgy*. London: Mc-Graw-Hill Book Company.

Disegi, J. A. & Eschbach, L. (2000). Stainless steel in bone surgery. *Injury 31*, S-D2-6.

Dowson, D. (1992). *Friction and Wear of Medical Implants and Prosthetic Devices*. ASM Handbook, vol. 18. Gereland: Materials Park,OH: ASM International, 656-664.

Ducheyne (1983). Fatigue properties of implant materials in hip prosthesis form: A standardized test. *Journal of Biomedical Materials Research 17*, 45-57.

Ducheyne, P. & Hastings, G. W. (Eds.) (1984). *Metal and Ceramic Biomaterials, Volume II: Strength and Surface*. Florida: CRC Press.

Edmonson, A. S. & Crensham, A. H. (19899. *Campbell's Operative Orthopaedics (6th Ed.).* U.S.A., Lea & Febiger.

Eftekhar, H. S. (1990). *Total Hip Arthroplasty.* New York: Columbia University Press.

Friedmann (1993). Current concepts in orthopaedic biomaterials and implant fixation. *The Journal of Bone And Joint Surgery 75-A*, 1086-1109.

Frost, N. E., Marsh, K. J. & Pook, L. P. (Eds.)(1974). *Metal Fatigue.* Northern Ireland: Oxford University Press.

Fuchs, H. O. (1980). *Metal Fatigue in Engineering.* New York: John Wiley & Sons, Inc.

Greco, R. S. (1994). *Implantation Biology: The Host Response and Biomedical Devices.* London: CRC Press.

Gross, S. & Abel, E. W. (2001). A finite element analysis of hollow stemmed hip prostheses as a means of reducing stress shielding of the femur. *Journal of Biomechanics 34*, 995-1003.

Gruen, A. T. (1979). Modes of failure of cemented stem type femoral components. A radiographic analysis of loosening. *Clinical Orthopaedics and Related Research 141*, 17-29.

Hall, R. M. & Unsworth, A. (1997). Review: Friction in hip prostheses. *Biomaterials 18*, 1017-1026.

Higo, Y. & Tomita, Y. (1994). Biomaterials Mechanical Properties, ASTM STP 1173. Kambic, H. E & Yokobori, A. T. (Eds.). *Evaluation of Mechanical Properties of Metallic Biomaterials.* Philadelphia: American Society for Testing Materials.

Huiskes (1983). A survey of finite element analysis in orthopaedic biomechanics: The first decade. *Journal of Biomechanics 16*, 385-409.

Huiskes (1998). Migration, stem shape and surface finish in cemented total hip arthroplasty. *Clinical Orthopaedics and Related Research 355*, 103-112.

Humphreys (1990). Testing of total hip replacements: endurance tests and stress measurements PartI: endurance tests. *Proceedings of the Instıtute of Mechanical Engineers 204*, 29-34.

Humphreys (1991). An investigation into the fixation of hip replacements. *Proceedings of the Instıtute of Mechanical Engineers 205*, 145-153.

Hübler (2001). Wear and corrosion of 316L femoral implant by deposition of thin films. *Surface and Coatings Technology 142-144*, 1078-1083.

Ikeda (2002). Effect of nitrogen plasma-based ion implantation on joint prosthetic material. *Surface and Coatings Technology 156*, 301-305.

ISO 7206/4 (1984). International Standard. *Implants for surgery-Partial and total hip joint prostheses – Part 4: Determination of endurance properties of stemmed femoral components with application of torsion*. Switzerland.

Jones (1992). Bending and fracture of the femoral component in cemented total hip replacement. *Journal of Biomedical Engineering 14*, 9-15.

Kuo, D. & Huang, K. (2001). Kinetics and microstructure of TiN coatings by CVD. *Surface and Coatings Technology 135*, 150-157.

Lewis, G. (1997). Properties of acrylic bone cement: state of the art review. *Journal of Biomedical Materials Research 38*, 155-182.

Ling (1992). The use of a collar and precoating on cemented femoral stems is unnecessary and detrimental. *Clinical Orthopaedics and Related Research 285*, 73-83.

Long, M & Rack, H. J. (1998). Titanium alloys in total joint replacement – a materials science perspective. *Biomaterials 19*, 1621-1639.

Macionczyk (2001). Repassivating tantalum/tantalum oxide surface modification on stainless steel implants. *Surface and Coatings technology 142-144*, 1084-1087.

Mann (1995). Coulomb frictional interfaces in modling cemented total hip replacements: a more realistic model. *Journal of Biomechanics 28*, 1067-1078.

McCormack (1998). A statistical analysis of microcrack accumulation in PMMA under fatigue loading: applications to orthopaedic implant fixation. *International Journal of Fatigue 20*, 581-593.

McCormack (1999). Fatigue of cemented hip replacements under torsional loads. *Fatigue and Fracture of Engineering Materials 22*, 33-40.

McGee (2000). Implant retrieval studies of the wear and loosening of prosthetic joints: a review. *Wear 241*, 158-165.

Papakyriacou (2000). Effects of surface treatments on high cycle corrosion fatigue of metallic implant materials. *International Journal of Fatigue 22*, 873-886.

Park, J. B. (1984). *Biomaterials Science and Engineering*. New York: Plenum Press.

Pohler, O. E. M. (2000). Unalloyed titanium for implants in bone surgery. *Injury 31*, S-D7-13.

Prendergast, P. J. (2001). The functional performance of orthopaedic bone cement. *Key Engineering Materials 198-199*, 291-300.

Raimondi, M. T. & Pietrabissa, R. (1999). Modelling evaluation of the testing condition influence on the maximum stress induced in a hip prosthesis during ISO 7206 fatigue testing. *Medical Engineering & Physics 21*, 353-359.

Raimondi, M.T. & Pietrabissa, R. (2000). The in-vivo wear performance of prosthetic femoral heads with titanium nitride coating. *Biomaterials 21*, 907-913.

Ramakrishna (2001). Biomedical applications of polymer-composite materials: a review. *Composites Science and Technology 61*, 1189-1224.

Ratner, B. D. (1996). *Biomatreials Science: An Introductionto Materials in Medicine*. San Diego: Academic Press.

Rieu (1991). Ion implantation effects on friction and wear of joint prosthesis materials. *Biomaterials 12*, 139-143.

Schmalzried, T. P & Callaghan, J. J. (1999). Current concepts review: Wear in total hip and knee replacements. *Journal of Bone and Joint Surgery 81-A*, 115-137.

Sedriks, A. J. (1996). *Corrosion of Stainlees Steels*. New York: John Wiley & Sons, Inc.

Sivakumar (1995). Failures in stainlees steel orthopaedic implant devices: A survey. *Journal of Materials Science Letters 14*, 351-354.

Sivakumar (1995). Investigation of failures in stainlees steel orthopaedic implant devices: pit-induced fatigue cracks. *Journal of Materials cience Letters 14*, 148-151.

Sivakumar, M. & Rajeswari, S. (1992). Investigation of failures in stainlees steel orthopaedic implant devices: pit-induced stress corrosion cracking. *Journal of Materials Science Letters 11*, 1039-1042.

Sloten (1998). Materials selection and design for orthopaedic implant with improved long-term performance. *Biomaterials 19*, 1455-1459.

Teoh, S. H. (2000). Fatigue of biomaterials: a review. *International Journal of Fatigue 22*, 825-837.

Tiainen, V. (2001). Amorphous carbon as a bio-mechanical coating-mechanical properties and biological applications. *Diamond and Related Materials 10*, 153-160.

Uhlig, H. H. (1955). *The Corrosion Handbook* (5th Ed.). new York: John Wiley & Sons, Inc.

Vishay Experiment In Mechanics (1970). *Strain Gage Series*. Malvern, Pennsylvania: Vishay Research & Education, a division of Vishay Intertechnology, Inc.

Walczak (1998). In vivo corrosion of 316L stainless steel hip implants: morphology and elemental compositions of corrosion products. *Biomaterials 19*, 229-237.

Williams, D. F. (1994). Titanium: epitome of biocompatibility or cause for concern. *The Journal of Bone and Joint Surgery 76-B*, 348-349.